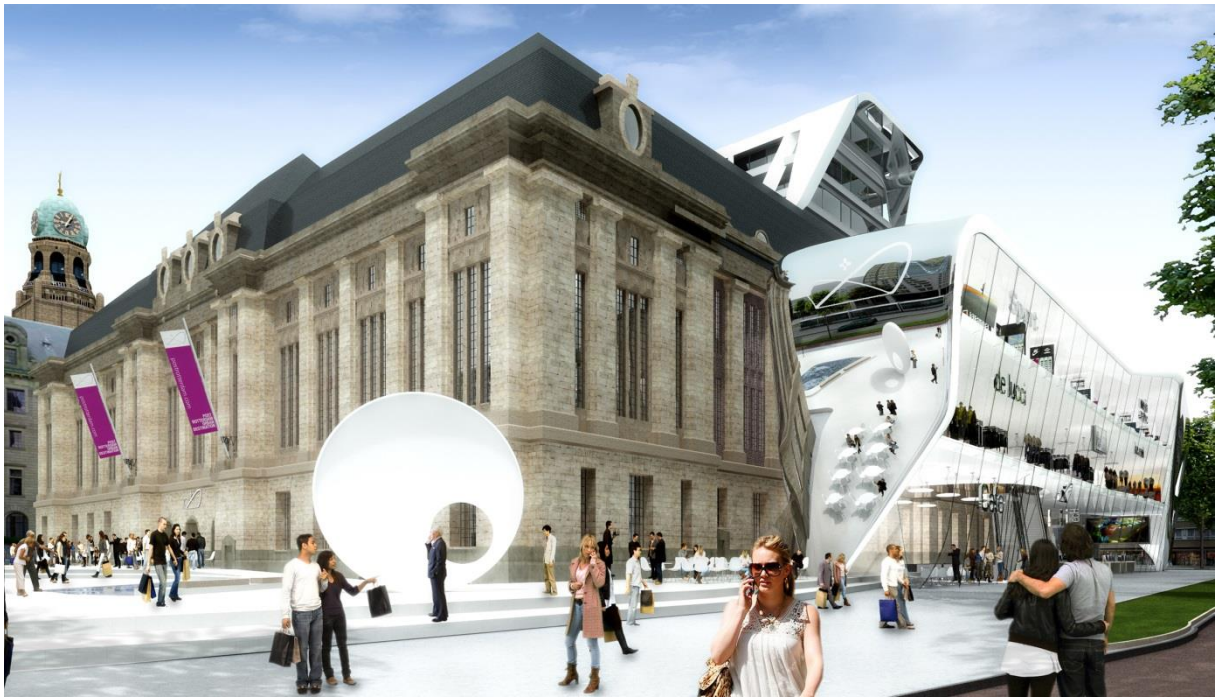


MSc Thesis

Performance-based form-finding and material distribution of free form roof structures

Implementation in the Post Rotterdam Case Study



Stavroula Schoina

St.N. 4324420

January 2016

Cover photo: Render from the design of UNStudio for the redevelopment of Post Rotterdam.

Reference: <http://www.designscene.net/2009/12/post-rotterdam-by-unstudio.html>

Performance-based form-finding and material distribution of free form roof structures

Implementation in the Post Rotterdam Case Study

by

Stavroula Schoina

In partial fulfilment of the requirements for the degree of

Master of Science

in Civil Engineering

at the Delft University of Technology

January 2016

An electronic version of this thesis is available at

<http://repository.tudelft.nl/>

Personal Details

Name: Stavroula Schoina
Student no: 4324420
MSc: Building Engineering
Specialization: Structural Design
Faculty: Civil Engineering and Geosciences
e-mail: sschoina@gmail.com
Tel.: (+31) (0) 62 62 33083

Committee Members

Chair:

Prof. Ir. R. Nijse
Delft University of Technology
E: R.Nijse@tudelft.nl
T: (+31) (0) 15 27 85488

Supervisors:

dr. ir. J.L. Coenders
White Lioness technologies
Delft University of Technology
BEMNext Laboratory
E: J.L.Coenders@tudelft.nl
E: jeroencoenders@white-lioness.com

ir. S. Pasterkamp
Delft University of Technology
E: S.Pasterkamp@tudelft.nl
T: (+31) (0)15 2784982

ir. R.M.J Doomen
Pieters Bouwtechniek B.V.
E: r.doomen@pbt-delft.nl
T: (+31) (0) 15 219 0300

Preface

This Master's thesis was written as part of the curriculum of the Msc in Building Engineering with a specialisation in Structural Design. Building Engineering is a Master track of Civil Engineering at the Delft University of Technology. The research was carried out in collaboration with the Faculty of Civil Engineering and Geosciences, the BEMNext lab and the engineering company 'Pieters Bouwtechniek'.

Firstly, I would like to thank my graduation committee as a whole for assisting and guiding me through this process. Without their fruitful comments and advice during the committee meetings, the outcome of the thesis wouldn't be the same.

In particular, I would like to express my sincere gratitude towards dr. Ir. Jeroen Coenders, my daily supervisor at Delft University of Technology, for his guidance and help throughout the whole graduation period. His advice and remarks, especially during the periods where decisions had to be made, were vital and very much appreciated.

Furthermore, my gratitude goes to Ir. Rob Doomen, my supervisor at "Pieters Bouwtechniek" for giving me the opportunity to work on this very interesting project and through it to expand my knowledge in the fields of parametric modeling, finite element analysis and programming. By sharing his engineering experience with me, he helped me perceive the practical background of this research.

Moreover, I would like to thank Professor Rob Nijse for chairing my graduation committee and for organizing the productive discussion during our meetings. My gratitude goes also to Ir. Sander Pasterkamp for his crucial remarks and helpful comments.

I would sincerely like to thank the engineering company Pieters Bouwtechniek for providing me with a pleasant working environment and the required resources to conduct my Master's thesis. I would also like to thank my colleagues at Pieters Bouwtechniek for their interest in my graduation topic and for offering their help when needed.

Last but not least, I would like to thank my family for their unlimited support of any kind and my friends for being helpful and tolerant during this busy period.

Stavroula Schoina

Delft, January 2016

Abstract

The purpose of the current research project is to propose a design process, based on performance-based design, in order to optimise the shape and distribute the material of free form roof structures. The study was initiated due to a part of the redevelopment of the Post Rotterdam, which is designed by the architectural firm UNStudio. This old monumental building has been planned to be transformed into a shopping centre and a hotel. Not only is the existing building planned to be renovated, but also some new structures are designed to be attached to the monumental building. One of these additions is a vertical foyer that will be used as the new main entrance of the shopping mall. The vertical foyer has a special design and as a result, a special analysis method is required. The preliminary analysis of the proposed shape showed an excess of material usage, consequently a research on modification of the shape and material distribution in order to reduce the estimated required material is deemed necessary. This free form roof structure is used as the case study of the current graduation project.

The proposed design process has been translated into a design tool for the automated manipulation of geometry-material distribution based on finite element analysis. The base design tool consists of two steps combined in one integral process. With the help of the first optimisation loop, the geometry of the structure is manipulated and with the help of the second optimisation loop, the stress based material distribution in the structure is achieved. The software used for the development of the tool are: Rhino-Grasshopper for the parametric configuration of the geometry, Ansys for the performance of finite element analysis, Galapagos evolutionary algorithm for the optimisation of the geometry and GhPython for the scripted component that performs the connection between Grasshopper and Ansys as well as the material distribution in the structure. The tool is designed according to the requirements of the vertical foyer but it is also oriented for the analysis of other similar projects.

The desired construction material of the case study is steel, consequently the stiffened steel shell construction method has been chosen as an object of study, which is borrowed from the ship building industry. The structure is composed out of two steel plates placed in a distance and ribs and stiffeners connecting the two plates. It has been chosen not to model the full structure, but a simpler-equivalent one, that will show equivalent global structural behaviour as the original structure. The most adequate way of modeling is to model the roof structure as one surface and assign to it the stiffness properties of the real full structure. This simplification is required since in this research, the global behaviour of the structure is deemed very important. One fitness value has to be computed characterising the whole structure in order to be used as input of the optimisation algorithm, since many different shapes will be analysed in order to conclude which is the optimum one.

The validation of the functionality of the design tool is accomplished by implementing it for the analysis of the case study. The implementation revealed that special requirements of the specific project had to be taken into account and necessary additions to be included in the base methodology. A material distribution algorithm was necessary for ensuring that the deflection remains in the design limits. After modifying the base design tool and defining all relevant users' input, three analyses of the case study are performed with the help of the design tool, with each analysis having a different goal-fitness value. The set goals are to minimise the total weight, minimise the weight per unit area and minimise the mean Von Mises stress of the structure. A fourth analysis

is performed subsequently, in which the set-up of the problem is iterated by modifying the design space where the algorithm can search for defining the optimum geometry.

The development of the design tool as well as the implementation in the case study, revealed that the applicability of the design method is not restricted to a specific geometry, material or cross section type. On the contrary, it can be used as the basis for developing custom-made design tools for the analysis and optimisation of various projects. Furthermore, the findings of the different analyses show that the geometry plays a significant role in the performance of the structure and the set-up of the problem influences notably the result of the optimisation algorithm. It is also concluded, that the use of the design tool in the early design phase can lead to the estimation of less required material for a free form structure compared to a simplified analysis. Further expansion of the functionality of the design tool as well as further research on its usability is recommended.

Table of contents

| | |
|--|----|
| Abstract | ix |
| 1. Introduction..... | 1 |
| 1.1 Performance-based design..... | 3 |
| 1.2 Optimisation techniques | 4 |
| 1.3 Shell optimisation | 7 |
| 2. Methodology | 9 |
| 2.1 Research objective | 9 |
| 2.2 Methodology of the research..... | 9 |
| 3. Strategy of tool development | 11 |
| 4. Case study description..... | 15 |
| 5. Design tool development | 17 |
| 5.1 Parametric model | 17 |
| 5.2 Connection between the parametric model and the FE analysis..... | 23 |
| 5.2.1 Meshing of the surface | 23 |
| 5.2.2 Import mesh in Ansys | 25 |
| 5.3 Structural system..... | 26 |
| 5.4 FE analysis..... | 28 |
| 5.4.1 Stress recovery | 31 |
| 5.4.2 Validation of the equivalency | 33 |
| 5.4.3 Analysis types | 36 |
| 5.5 Thickness distribution..... | 38 |
| 5.5.1 Validation of the thickness distribution algorithm..... | 39 |
| 5.6 Fitness function | 46 |
| 5.7 Optimisation algorithm | 46 |
| 5.8 Visualisation of the results | 48 |
| 6. Case study..... | 49 |
| 6.1 User input required for the case study analysis..... | 49 |
| 6.1.1 Material properties..... | 49 |
| 6.1.2 Boundary conditions..... | 49 |
| 6.1.3 Loads..... | 50 |
| 6.1.4 Cross section list | 51 |
| 6.1.5 Mesh density | 52 |
| 6.1.6 Limits | 53 |

| | | |
|-------|---|----|
| 6.1.7 | Penalties | 54 |
| 6.2 | Additions to the base tool | 54 |
| 6.2.1 | Grouping | 56 |
| 6.2.2 | Deflection loop | 58 |
| 6.2.3 | Validation of the functionality of the tool | 60 |
| 6.3 | Validation of the analysis | 61 |
| 6.4 | Analyses and results | 63 |
| 6.4.1 | Analysis No 1 | 64 |
| 6.4.2 | Analysis No 2 | 65 |
| 6.4.3 | Analysis No 3 | 66 |
| 6.4.4 | Comparison between analyses | 67 |
| 6.4.5 | Analysis No 4 | 68 |
| 6.4.6 | Translating the FE model to a structure | 69 |
| 6.4.7 | Comparison between the design tool and the preliminary analysis | 71 |
| 7. | Discussion | 73 |
| 8. | Conclusions and recommendations | 75 |
| 8.1 | Conclusions | 75 |
| 8.2 | Recommendations | 76 |
| | Bibliography | 77 |
| | Appendix 1 - Loading | 1 |
| | Appendix 2 - Geometry transfer | 7 |
| | A) Import geometry in Ansys | 7 |
| | B) Create geometry in Ansys | 8 |
| | Appendix 3 - Equivalent structure | 13 |
| | Appendix 4 - Stress equivalency comparison | 17 |
| | Appendix 5 - Analyses results | 23 |
| | Appendix 6 - Tool manual | 33 |
| | Table of Figures | 38 |

1. Introduction

Structures that don't follow conventional or geometrically regular building forms are usually referred as free-form (Veltkamp, 2007) and they can generally be recognized by their smooth, flowing lines, distinctive and changing shape and absence of symmetry (Hambleton et al., 2009). The history of free form structures is long. Nowadays, architects tend to incline more and more to free forms in their design. However, current free form structures don't resemble the ones from the past. This is due to the existence of computerized design and calculating tools that has given them the freedom to explore the infinity of the design space. Furthermore, there is an intention to implement new building techniques in free form construction borrowed from other industries, such as the shipbuilding industry or the automotive industry. A constant effort for lighter structures and larger unsupported spans can be noticed.

Two recent examples of this tendency are the Arnhem station roof structure in the Netherlands (Figure 1) and the Porsche pavilion in Wolfsburg, Germany (Figure 2). In the first project a stiffened double curved steel skin has been used amongst others as the loadbearing roof structure (Van Dijk et al., 2015) while in the second two double curved stainless steel sheathing plates are connected by ribs and stiffeners (Pasternak and Krausche, 2013).



Figure 1. Arnhem station roof structure. Design by UNStudio (<http://www.unstudio.com/projects/arnhem-central-transfer-hall>)



Figure 2. Porsche pavilion in Wolfsburg, Germany. Design by HENN Architects
(<http://www.henn.com/de/projects/culture/porsche-pavilion>)

The mechanical behaviour of non-conventional curved surfaces is difficult to be described by deriving formulas. The reason is that very little analytical mathematical functions exist that are adequate to describe the structures that are proposed in free form architecture. A possible solution is to use computer programs based on the finite elements method for the calculation of the stresses and strains that are exerted on these irregular structures (Coenders, 2008).

The form of these surfaces is defined through form finding procedures. According to Coenders (2011; 2008) in order to perform form finding, two approaches can be followed:

- (a) Classical form finding, which includes the definition of structural shape (form), based on structural equilibrium for a given set of forces and topology. Some of the classical form finding techniques are: hanging chains or minimal energy shapes of soap films.
- (b) Modern form finding, which includes software aid in order to find an appropriate in the eyes of the designer shape which is not necessarily in structural equilibrium. In this approach many methods can be included, such as: NURBS definition, optimisation methods and generative methods.

As the name of each category reveals, the classical form-finding procedure was the first generation of form-finding to be adopted in order to define possible shapes of a free form structure. These methods are currently reviving with new computational techniques.

From the point that the form of the structure has been defined, with the help of a form finding technique, until the realisation of the structure the process is long. Vermeij (2006) mentions in his research that despite the fact that many free formed projects have come to life, an efficient integral design process for free form buildings does not exist. He spots the problem in the current education and experience, as well as available software and production techniques which are not well suited for an efficient free form design process.

The standard way of approaching a design problem is to design from crude to fine. In the case of free form structures it means that the approach is to start with simplified calculation models (orthogonal, etc.) and conclude to detailed models that the structure follows the form of the building. It would

probably be more efficient if from the early design stage a more appropriate calculation could be performed. The reason why more detailed calculations are postponed to a later design stage is the lack of time. It is true that the initial step of setting up the detailed problem in a parametric environment is time consuming.

A common design process is one directional (forward) and based on the trial and error approach. The data is sent from the design software to the calculation software, but then the data from the calculation software are not reused in an automatic way in order to make changes to the design. With the use of parametric models and optimisation algorithms the design process has changed.

Basically, “the parametric design approach describes a process of transferring intellectual decisions into computerized optimisation procedures and it is widening the field of potential designs and technical solutions. The parametric design approach can be seen as a design process which goal is to target the optimal combination of set parameters” (Scheible and Dimcic, 2011). An elaboration on the optimisation processes is presented in Section 1.2.

1.1 Performance-based design

In Figure 3 are presented the objectives in a building design according to Geyer and Rueckert (2005). Architects define the form of their design according to aesthetic and functional criteria as well as in a way that it follows the concept. They usually don't have an insight of the first and second group of objectives, which are achieved from the structural designer. As a consequence, it would be very interesting if architects could see directly the effect of their shape decisions on the structure and cost. That way, the structural and aesthetic design would be integrated, a fact that leads to many advantages.

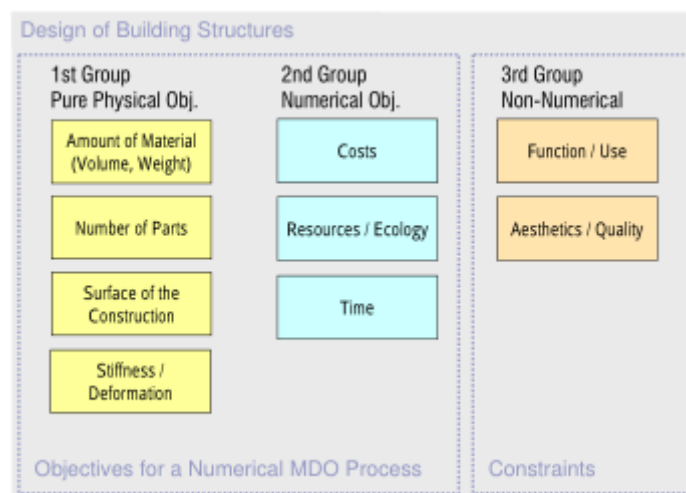


Figure 3. Objectives in building design (Geyer and Rueckert, 2005, p.2)

An effort towards this direction is the performance-based design. Its aim is to integrate the evaluation of the architectural performance in the early phase of conceptual design and form finding. During this early phase, the geometrical shapes are simplified and abstract attempts. However, when these shapes include performative information their complexity increases. It is very important to deal with this complexity, since the performance of the final project is highly dependent on the choices made in the early design phase (Buelow et al., 2010).

According to Woodbury and Burrow (2006), there are two important advantages when design alternatives are being explored: “*revelation*” and “*comparison*”. The first one implies that the design alternatives reveal things that couldn’t have been predicted from the beginning, as a consequence it opens up new ways of thinking and exploring. The latter implies that comparison is essential for understanding whether a design that satisfies the criteria set, is the optimum between those under consideration. It might be the case that many designs satisfy all the criteria set, as a consequence comparison between these designs has to be performed in order to conclude to the best one.

1.2 Optimisation techniques

The main categories of the optimisation problems are three (Christensen and Klarbring, 2009):

- Sizing optimisation: optimises the structural thickness or cross sectional areas
- Shape optimisation: optimises the form or contour of some part of the boundary of the structural domain
- Topology optimisation: optimises the geometry through changes in the topology of the structure.

A structural optimisation problem contains the following functions (Christensen and Klarbring, 2009):

- Objective function (f): A function used to classify designs. For every possible design, f returns a number which indicates the goodness of the design.
- Design variable (x): A function or vector that describes the design and which can be changed during optimisation.
- State variable (y): For a given structure, i.e., for a given design x , y is a function or vector that represents the response of the structure.

The general form of an optimisation problem is:

$$(SO) \quad \begin{cases} \text{minimize } f(x, y) \text{ with respect to } x \text{ and } y \\ \text{subject to } \begin{cases} \text{behavioral constraints on } y \\ \text{design constraints on } x \\ \text{equilibrium constraint.} \end{cases} \end{cases} \quad (1.1)$$

According to each specific problem and goals, many optimisation algorithms can be employed. A few of them are (Arora, 2012):

Global-Local optimisation methods: The Global optimisation methods are used in order to find the global optimum, which is the best solution of all the search space. On the other hand local optimisation methods are concluding to an optimum solution in a small neighbourhood of designs. This optimum is a local optimum but can at the same time be a global optimum. The starting state of the local optimisation algorithm plays a crucial role on the outcome.

Deterministic-Stochastic optimisation methods: Stochastic optimisation methods include randomness in the search of finding the optimum whereas deterministic methods present no randomness. They perform an exhaustive search of the design space.

Direct-Gradient optimisation methods: Direct optimisation methods do not use, calculate or approximate derivatives of the problem functions. On the other hand, gradient based methods are applicable in case of continuous differentiable functions and they perform faster than direct search methods.

As it becomes obvious, every optimisation problem has to be treated as unique. According to the nature of the problem different design variables, constraints and objectives have to be set. It is true that there is no optimisation technique that can fully optimise every aspect of one structure, since many objectives are usually contradictory. As a consequence, special attention has to be paid in the correct understanding of the problem in order to select the most appropriate algorithm, functions and processes.

The adequacy of the optimisation algorithm for the specific problem plays a crucial role in the concluded optimum result. Various researches have been conducted comparing the performance of algorithms such as the one of Fourie and Groenwold (2002). The chosen algorithm, though, if it is not scripted from the designer, depends also on the availability on the market.

In this research a genetic algorithm will be used, which lies in the category of global, stochastic and direct optimisation methods inspired by nature. Holland (1975/1992) is one of the first to develop the theoretical framework of genetic algorithms and test it in a range of applications. These algorithms mimic the processes of biological evolutions in order to solve problems (Mitchell, 1995). The application of these algorithms is suitable for a large variety of cases, since the problem functions are not required to be continuous or differentiable (Arora, 2012).

The algorithm starts by randomly generating an initial set of designs, the initial population, which will further evolve with the help of certain mechanisms in order to find the fittest solution. Every population contains a specific amount of genomes-individuals (designs to be analysed) and every genome includes a number of genes equal to the number of variables of the problem. Each individual is assigned a fitness value, which defines the relative importance of the design. The evolving mechanisms are used to create a new set of designs, a new population, based on the current one such that the average fitness of the population is improved (Arora, 2012).

Since randomness is included in the genetic algorithm, when the algorithm is executed at different times, can lead to a different sequence of designs and a different problem solution even with the same initial conditions (Arora, 2012).

The evolving mechanisms include (Arora, 2012; Rutten, 2010):

Reproduction: a set of designs from the current population is selected to be carried into the next population.

Cross over: the genomes are split at one or two points and by exchanging variables the offspring is generated.

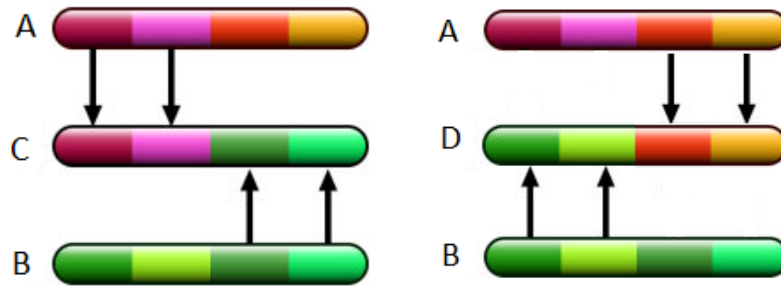


Figure 4. Cross over of two genomes with four genes each

Blending: the genomes are averaged in order to generate the offspring.

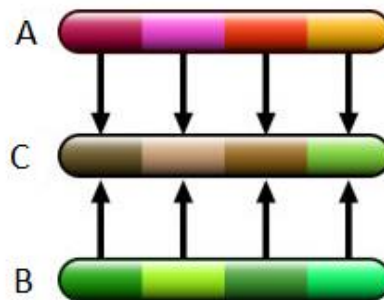


Figure 5. Blending of two genomes with four genes each

Blending is a mechanism that is not proposed in the original theory of genetic algorithms as presented by Holland (1975/1992), but can be found in current evolutionary algorithms available on the market.

Mutation: some genomes are selected and a randomly chosen variable of them is iterated.

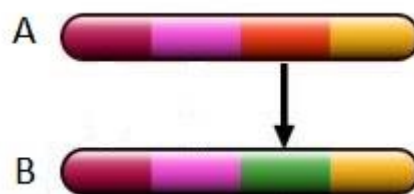


Figure 6. Mutation of a genome by iterating one gene

Only by performing mutation, it is not expected to improve the search for a solution, but it assures that no inflexible population will be developed incapable of further evolution (Holland, 1992).

The optimisation problem when genetic algorithm is used is formulated as (Arora, 2012):

$$\text{Minimise or maximise } f(x) \quad \text{for } x \in S \quad (1.2)$$

Where S is the constrained design space in which the algorithm can iterate to search the optimum solution.

1.3 Shell optimisation

The implementation of optimisation techniques in shell structures has been an interesting research topic for many years. Researchers have tried to tackle this problem following different approaches and setting various goals.

Ruben et al. (2002) combined shape and topology optimisation of shells having as a target to minimize the compliance of a shell structure under defined loading, with maximum stiffness design and a constraint on the volume of material used. Tomás and Martí (2010) researched the shape and size optimisation of concrete shells, with set goal the minimization of bending moments. Another research in the topic has been conducted by Della Puppa (2015) in which a new shape optimisation strategy for thin shell structures has been introduced, considering as objectives the strain energy, linear buckling load and imperfection sensitivity. Furthermore, Wu et al. (2015) proposed a hybrid optimisation method where the shape and thickness of free form shells is simultaneously optimized having as goal minimal strain energy.

The research has been extended further to the shape optimisation of stiffened shells either with beams where the optimisation variables contain the thickness of the shell, the cross section of the stiffeners and the density of the applied stiffeners (Lagaros et al., 2004) or truss stiffened having as variables the shell thickness, truss topology and truss elements cross section (Kegl and Brank, 2005).

In the current research an optimisation method will be applied in the form of a design tool for free form shell like structures. The main research objective and research questions are presented in the following chapter.

2. Methodology

2.1 Research objective

The main research objective of this graduation project is a design process, based on performance-based design, in order to optimise the shape and amount of material of free form roof structures.

The related research questions that will be attempted to be answered are:

What is the influence of the shape to the performance of a free form structure?

How the set-up of the problem influences the optimum result?

What is the influence in the prediction of the required amount of material when modeling a simplified structure that follows the exact free form shape?

2.2 Methodology of the research

The need for this research originates from the proposal of the Vertical Foyer of the redevelopment of Post Rotterdam. It is a unique free form roof structure that requires a special method to be analysed and constructed. The special method is translated in the current research in a design tool that will be developed and used for the analysis of this roof structure but will be also applicable to other similar projects. The structure of the study in order to complete this research is presented in the following:

Literature study

The first step of the research is to perform a literature study in order to gain adequate knowledge in the relevant fields. These fields include shell structures, form-finding, optimisation techniques-shell optimisation, performance based design.

Analysis of the building

In this part the special geometrical features of the case study building have to be analysed as well as the structural system to be used. This analysis will conclude to the requirements and limitations that have to be taken into account in the research.

Strategy development

When the requirements and limitations are defined, an adequate method for the analysis of the building has to be explored. Attention will be paid in the applicability of this method to other similar projects.

Implementation

The strategy is implemented by developing the design tool and using it for the analysis of the Post Rotterdam case study.

Validation

The accuracy of every step of the development of the design tool is important to be validated. This is performed through validation tests, which are elaborated in this report when the relevant step is presented.

Conclusions and recommendations

At this last part, the conclusions from the developed tool and the case study analysis are provided and recommendations for further development of the tool and investigation on the case study are given.

3. Strategy of tool development

The design process proposed in the research objective will be translated into a tool for the automated manipulation of geometry-thickness based on finite element analysis.

The strategy that will be used for the development of the base tool as well as the interfaces of each step are presented in Figure 7.

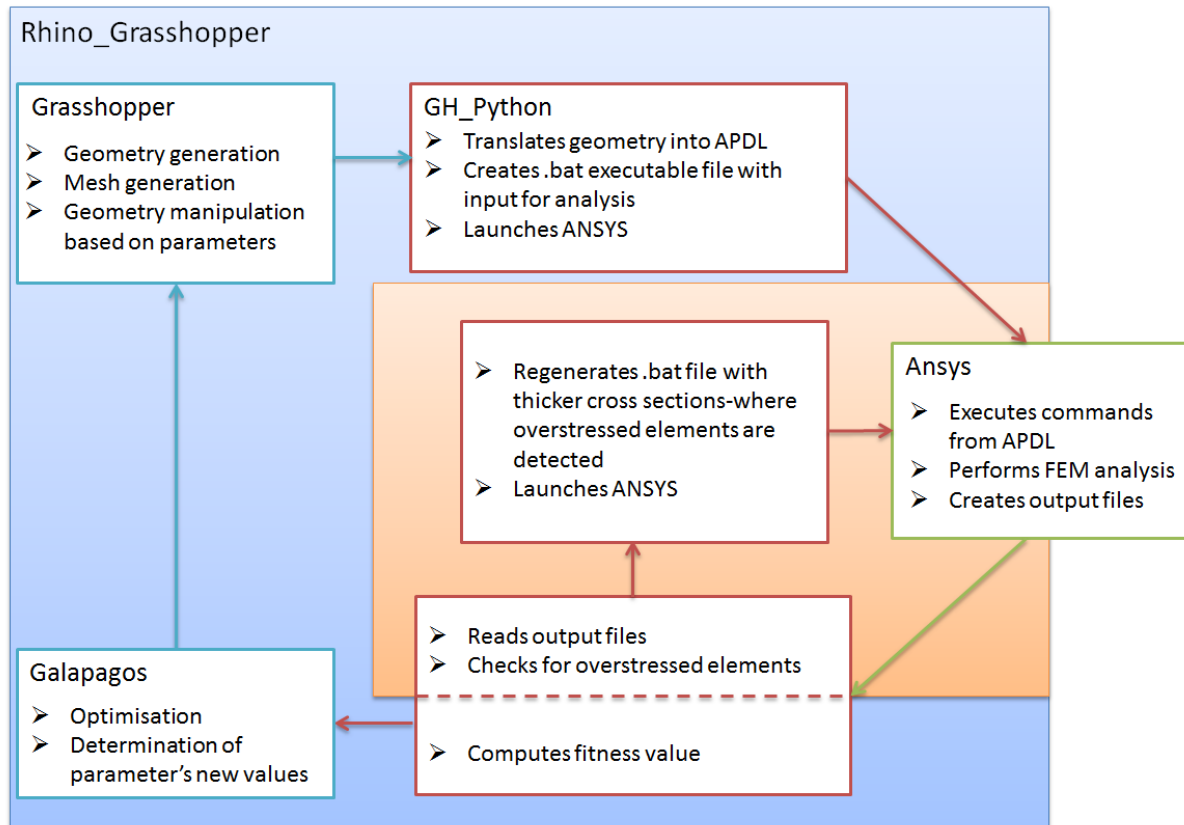


Figure 7. Strategy of the base tool

The base design tool consists of two loops combined in one integral process. With the help of the first loop (blue) the geometry of the structure is manipulated and with the help of the second loop (red) the material distribution in the structure is achieved.

The software packages that have been chosen for the creation of the tool are visible in Figure 7. A presentation of the capabilities of the software as well as the reason for choosing the specific software will be elaborated in this part.

For the generation of the parametric model, Rhino in combination with the parametric tool Grasshopper are being used. Rhino is a 3D modeling software that is adequate for creating free form shapes based on NURBS curves – surfaces. Grasshopper is a plug-in for Rhino that is used for creating parametric models visualised in Rhino and can be freely downloaded. The educational version of Rhinoceros 5.0 is used.

A parametric model created in Grasshopper consists of various objects placed on the canvas by the user, which are connected with wires in a specific order to form logic. Each object incorporates a specific functionality. The wider used objects are parameters and components. The parameters

contain data and the components actions. Each component requires an input and produces an output. As input of a component, a parameter can be applied or the output of other components as presented in Figure 8. A very useful parameter type is the number slider. The user can define the limits of the numeric domain as well as the accuracy of the number and the output of the slider will be a numeric value constrained to the limits (Akos and Parsons, 2014).

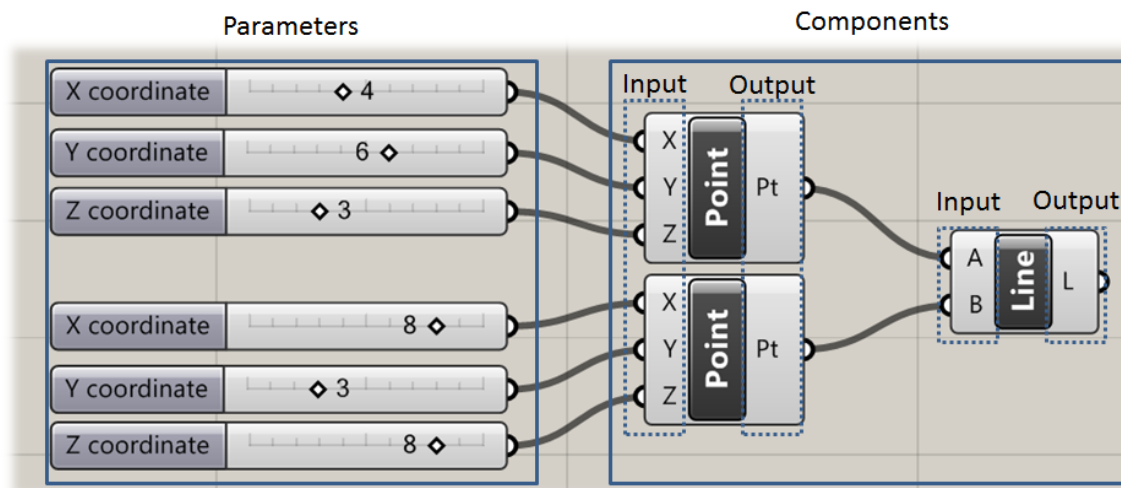


Figure 8. Grasshopper parametric model basics

For the finite element analysis the capabilities of two software packages have been explored. The first is Karamba, which is a plug-in for Grasshopper and the second is Ansys. Karamba is performing finite element analysis on various typologies of structures including shell surfaces. It is fully embedded in the parametric environment of Grasshopper and easy to use. A student licence of Karamba is available to be purchased. While there are many advantages for using Karamba as the finite element solver for this research, such as the fact that all the parts of the loops are located in one interface, it has been noted that the buckling analysis was failing to be performed for many of the possible shapes to be analysed and this was causing Rhino to crash. Consequently, another more stable software should be searched for this tool. Based on licence availability as well as capabilities of the software, Ansys Mechanical has been chosen. The academic teaching licence of this software is available at TU Delft.

For the realisation of the optimization loop a connection between the parametric model and the structural analysis is necessary. This can be achieved by scripting in many scripting languages, such as VB and C# which come integrated with the Grasshopper installation. Recently, there is the opportunity for more scripting languages to be used in the framework of Grasshopper. One addition is the plug-in GhPython which is a Python interpreter component for Grasshopper that allows executing dynamic scripts of any type. Python is a programming language that is particularly easy to be learned from users without prior programming experience because of its clean syntax and indentation structure (Python.org, 2015). For this reason, GhPython has been chosen for the automatic communication between Rhino-Grasshopper and Ansys.

The GhPython script does not include only the communication between the parametric model and the finite element software, but also the material distribution loop (red loop of Figure 7). The geometry manipulation, though, is achieved using an evolutionary solver. Galapagos evolutionary

solver has been chosen which is a free plug-in for Grasshopper developed by David Rutten (Galapagos, 2015).

As can become obvious, several executions of the finite element model will be required for the analysis of one geometry. Taking into account the large amount of geometries that have to be analysed before the evolutionary solver can conclude to an optimum design as well as the fact that the process is limited in the computation power of one computer, can be concluded that large computation time is expected to be required. In order to reduce the computation time the computing power of a cluster of computers can be used. This approach has not been incorporated in this research mainly due to the lack of multiple licence availability.

After the presentation of the software that is used for the development of the design tool, the design process will be further elaborated. It is divided in 6 steps as presented in Figure 7:

- 1) As a first step, the parametric model has to be generated. The parameters chosen for the shape generation as well as their boundaries have to be defined in this step. The result of the parametric model should be a surface or a boundary representation (Brep) in order to be able to be further meshed and analysed in the FE analysis software. The mesh of this surface is performed as the last part of this step.
- 2) The mesh generated in the first step will be used in the second step for transferring the geometry from grasshopper to Ansys with the help of the GhPython script. The script creates the .txt file which contains not only the geometry but also the listing of commands in the Ansys Parametric Design Language (APDL) for the analysis to be performed. When the APDL listing file is generated, the .bat executable file is created that contains the input for the analysis. Lastly, Ansys is launched in batch mode.
- 3) Ansys is executing all the commands from the APDL file performing a finite element analysis. The output files are generated which contain information such as the deflection of the structure. The generation of the files is achieved in the form of commands executed in Ansys.
- 4) The output files are read from the Python script and useful information is further processed either for a recalculation of the structure or for the final output of the script which is the fitness value necessary for the Galapagos optimisation.
- 5) In case some elements of the structure are overstressed, a thicker cross section is assigned to them. A new APDL file is generated and Ansys is again launched in Batch mode. Following, step 3 has to be performed.
- 6) In the last step, the fitness value is used as input for the genetic algorithm and based on that the determination of the new values of the parameters is accomplished.

The methodology presented in this chapter is the basis methodology proposed for the analysis of free form surface structures. It has to be noted that each project to be analysed presents special requirements that might lead to necessary additions to this methodology. The application of the basis methodology for the development of a design tool has been accomplished and will be elaborated in Chapter 4. An implementation of the design tool in the Post Rotterdam case study has been carried out, during which special requirements were identified and modification of the tool was deemed necessary. The applied modifications are elaborated in Chapter 5.

4. Case study description

For the validation of the proposed design process, a case study will be used. This is the redevelopment of Post Rotterdam. The main post office of Rotterdam was built in 1923 and is located in the center of Rotterdam at the Coolsingel.



Figure 9. Post Rotterdam building before redevelopment (<http://www.skyscrapercity.com/>)

In 2007, the main post office was decommissioned and the old monumental building has been planned to be transformed into a shopping centre and a hotel. The architectural firm UN Studio is the designer of the redevelopment. Not only is the existing building planned to be renovated, but also some new structures to be attached to the monumental building. One of these additions is a vertical foyer that will be used as a new main entrance of the shopping mall. This structure has a special distinctive shape and around 65m span.

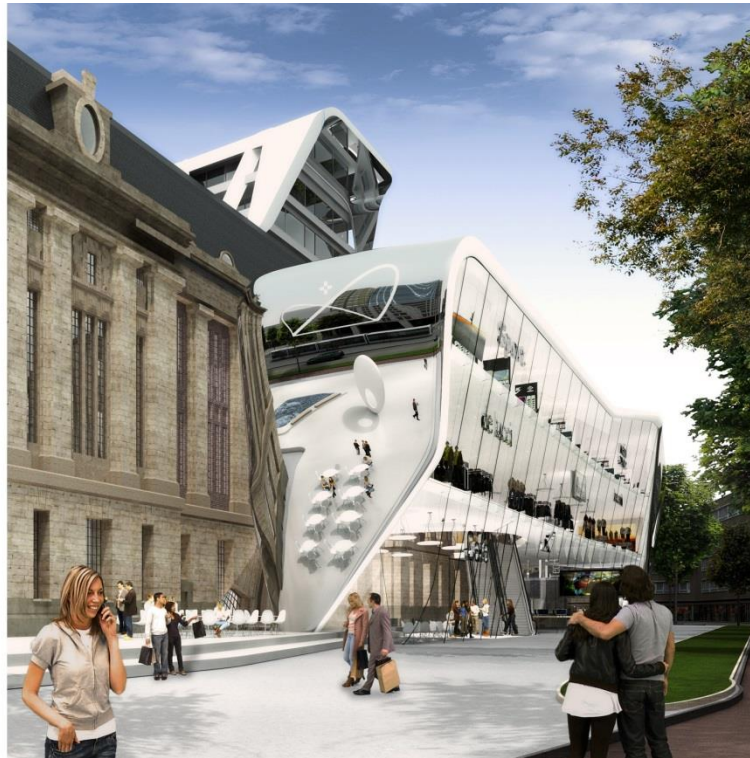


Figure 10. Design of the redevelopment of Post Rotterdam. Design by UNStudio (<http://www.unstudio.com/projects/post-rotterdam>)

From the preliminary structural analysis that was performed by the engineering company Pieters Bouwtechniek, has been concluded that the material required for the realisation of this design was more than the desired. The excess of material in combination with the difficult production technique, leads to an expensive structure. As a consequence, optimisation in the form of the roof had to be performed in order to minimize the material needed and therefore the total cost.

The special features of the vertical foyer will be analysed in Chapter 5 where the parametric model of this shape will be generated.

5. Design tool development

In this chapter the implementation of the steps for the development of the design tool will be presented as well as the necessary validation of the accuracy of some steps.

5.1 Parametric model

The first step of the design tool is to create a parametric model for the shape definition in Grasshopper platform. The parameters of the model are unique for every project and are chosen according to the requirements of the project and the desire of the architect. In this research, the parametric model will be created according to the special features of the vertical foyer.

The original design of the vertical foyer (Figure 11) will be used as a starting shape in order to select the parameters that define the form and will be included in the parametric model. The main characteristics of the shape are the inclined sides, the triangular covers in the 2 opposite corners, the double curvature in the angles that connect the roof, the sides and the covers as well as the downward inclination of the roof part.

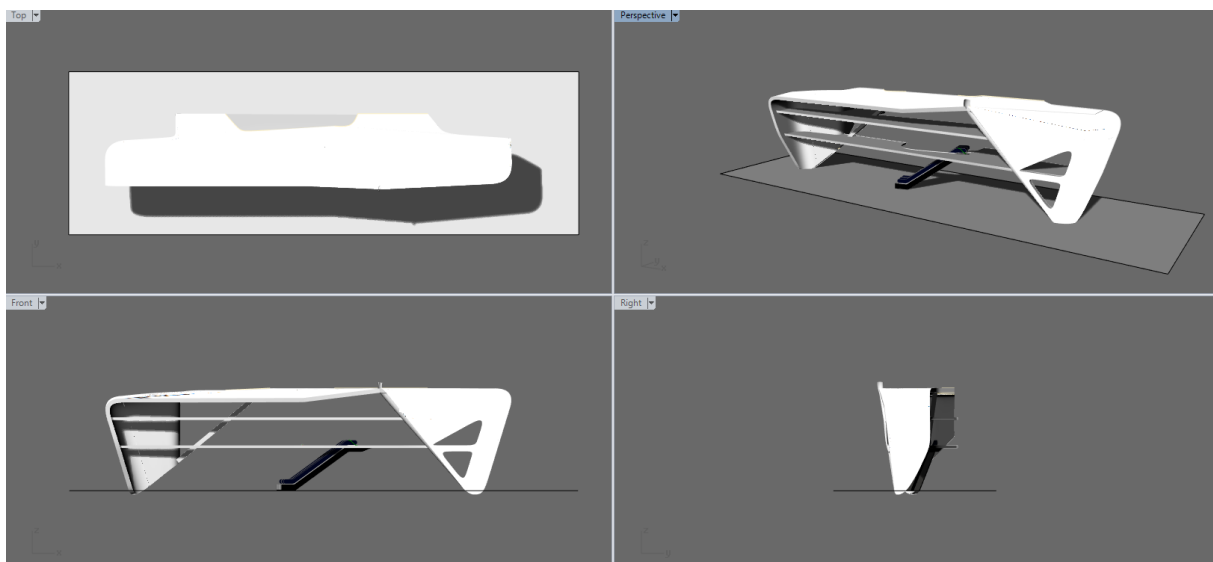


Figure 11. Original design of the vertical foyer from UNStudio

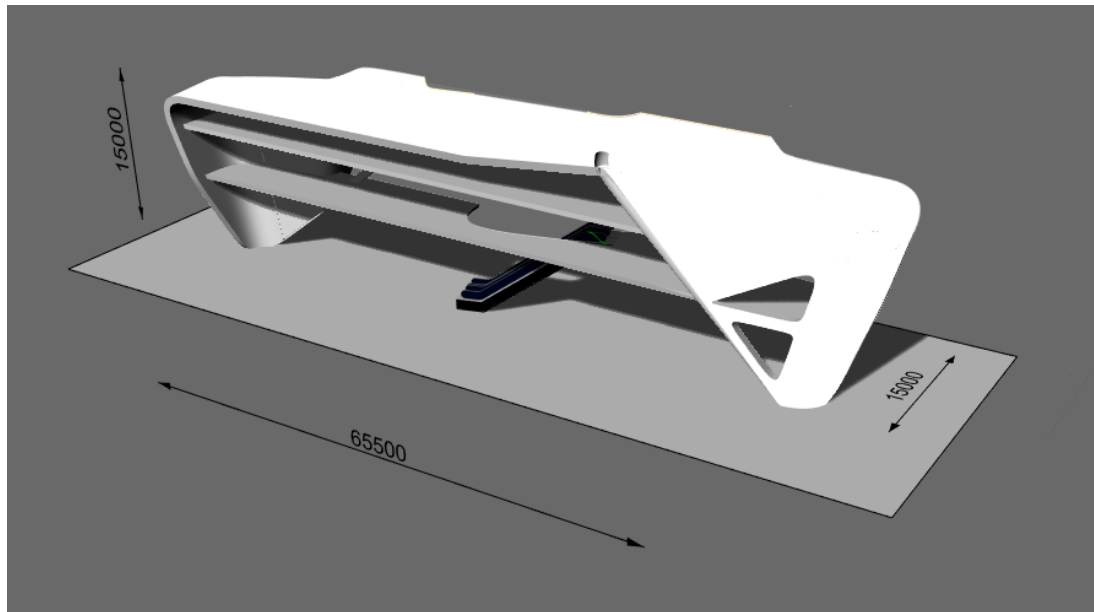


Figure 12. Dimensions (in mm) of the original design from UNStudio

These characteristics will influence the way the parametric model will be set up. Each parameter has a range of values assigned by the user. These value ranges define the possible shapes that can be formulated by the parametric model and as a consequence the shapes that will be further analysed in the optimisation process. They define, consequently, the space that can be explored from the optimisation algorithm in order to conclude to the optimum design.

As can become obvious, the selection of the parameters as well as the value ranges, play a major role in influencing the optimised design that will be the output of the optimisation process. The input has to be very well considered in order to get an optimised design that is desired from the user.

Since the design tool is focusing on analysing shell-like structures, the output of the parametric model should be a surface or a boundary representation (Brep) so that it can be further analysed by the finite element software.

From the original model can be noticed that the shape of the vertical foyer is irregular. Single or double curvature exists in the roof structure but non-curved parts are also present, which are not likely to be found in free-form architecture. Since the design tool is oriented on analysing free-form shell like structures, it has been decided to transform the shape of the vertical foyer into a smooth free-form shape. As a consequence, the representation of the original model will not be exact. It is desired to achieve a starting shape that is as close to the original as possible by making use of NURBS curves.

NURBS (Non-Uniform Rational B-Splines) are mathematical representations of 3D geometry. They are widely used, since they can accurately describe any shape from a simple 2D line, circle, or curve to the most complex 3D organic free-form surface or solid. For the formulation of a NURBS curve the degree has to be defined as well as its control points. Most free form curves are degree 3 or 5. The control points define the shape of the free form curve and the minimum number of control points to be defined is one higher than the degree. Furthermore, when moving the control points, the shape of the NURBS curve changes (Rhino, 2015).

The steps that have been followed for the creation of the parametric model are presented in Figure 13 to Figure 21. For the modeling of the free-form roof, two NURBS curves are created. Each of them is determined by 9 control points. Their coordinates are variables that define the span, height and curvature of the roof.

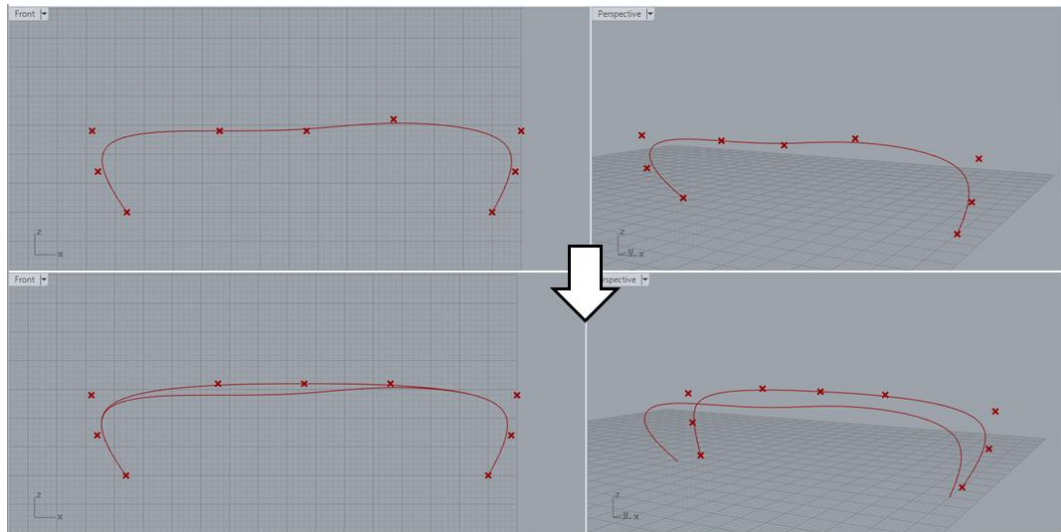


Figure 13. Modeling of the roof structure with two NURBS curves of 9 control points each

Following, the base lines as well as the diagonal lines of the triangular like covers are created. The angle of the triangular cover depends on the location of the base point as well as the selection of the upper point from the available control points of the NURBS curve.

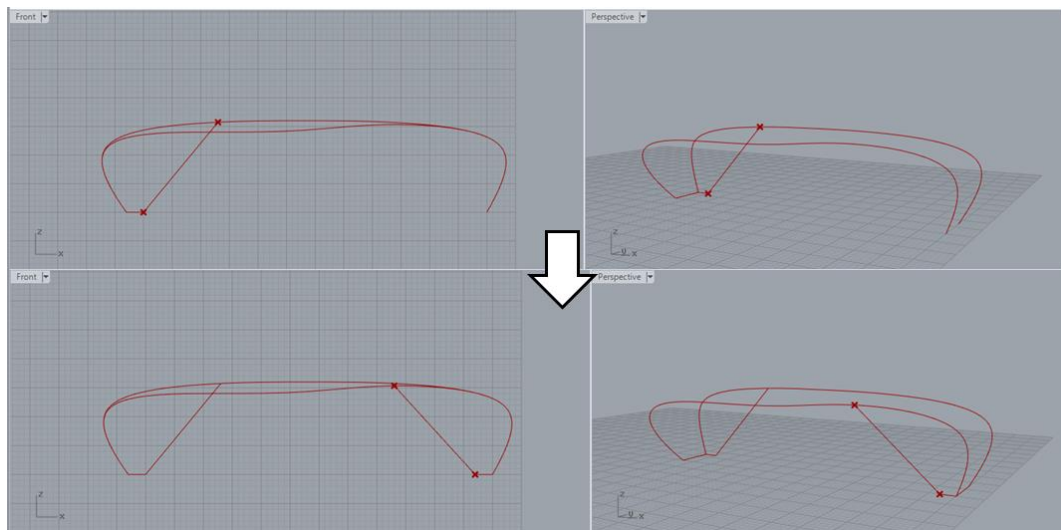


Figure 14. Modeling of the base and the triangular covers

The next step is to model the double curvature that is present in the connection of the roof, sides and cover. In order to achieve that, parts of the two NURBS curves are divided in 10 equal segments and the division points are projected on the diagonal line. As a following step of this process, the points that are generated on the two NURBS curves and the diagonal line are connected with the help of horizontal lines as shown in Figure 15.

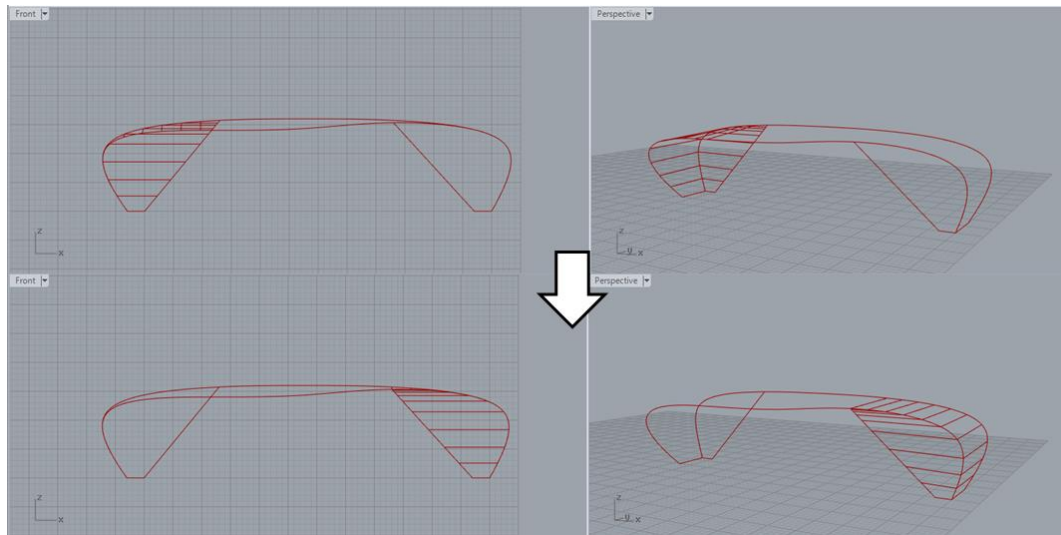


Figure 15. Modeling of horizontal lines connecting the 2 Nurbs curves and the triangular cover

These horizontal lines are filleted in order to model the double curvature. The radius of the fillet is a variable for the optimisation.

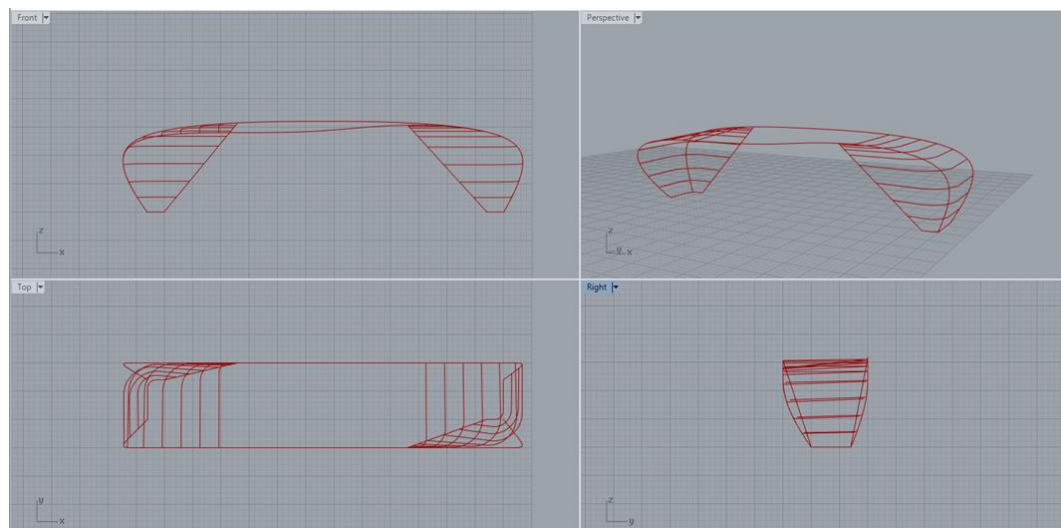


Figure 16. Fillet of the horizontal lines

For accommodating the modeling of the surface, additional lines are generated in the remaining roof part.

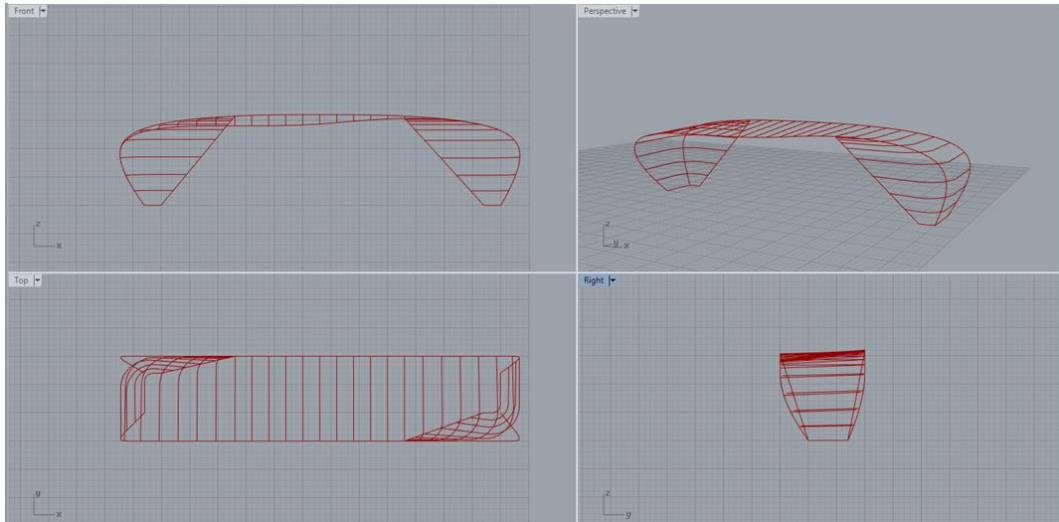


Figure 17. Curves-lines defining the shape of the vertical foyer

At this point, the shape of the roof structure is defined from various curves and lines. The target is to define the shape with a surface or a Brep. Grasshopper offers many different ways to model free form surfaces as can be seen in Figure 18.

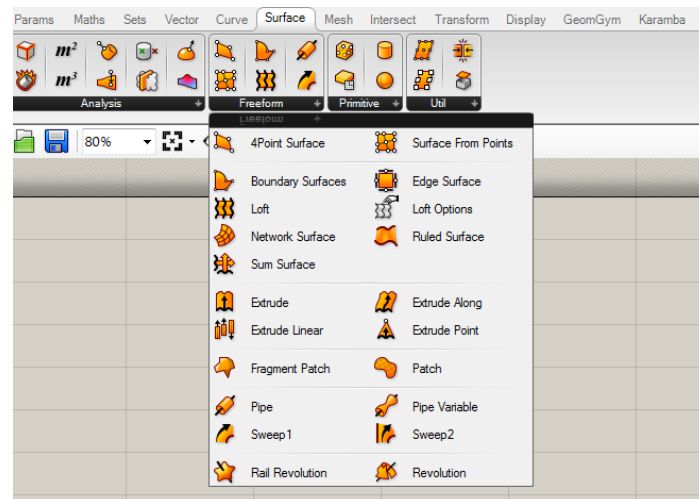


Figure 18. Options for modeling a free form surface in Grasshopper

In this specific case, none of the options is capable of modeling one surface/brep out of these curves-lines. It would be expected that the loft command is adequate for generating this surface since by its definition it creates a lofted surface through a set of section curves (Akos and Parsons, 2014). The part that causes the failure of the loft algorithm is the transition from the filleted curve to the line. Consequently, the generation of the roof surface is divided in 5 loft commands and these surface parts are merged in order to conclude to one open Brep (Figure 19 to Figure 21). It has to be noted that the merged Brep does not present the same characteristics as if there was the possibility the geometry to be generated by one surface. The characteristics of each part surface remain, as well as any discontinuities in the connection of the adjacent surfaces.

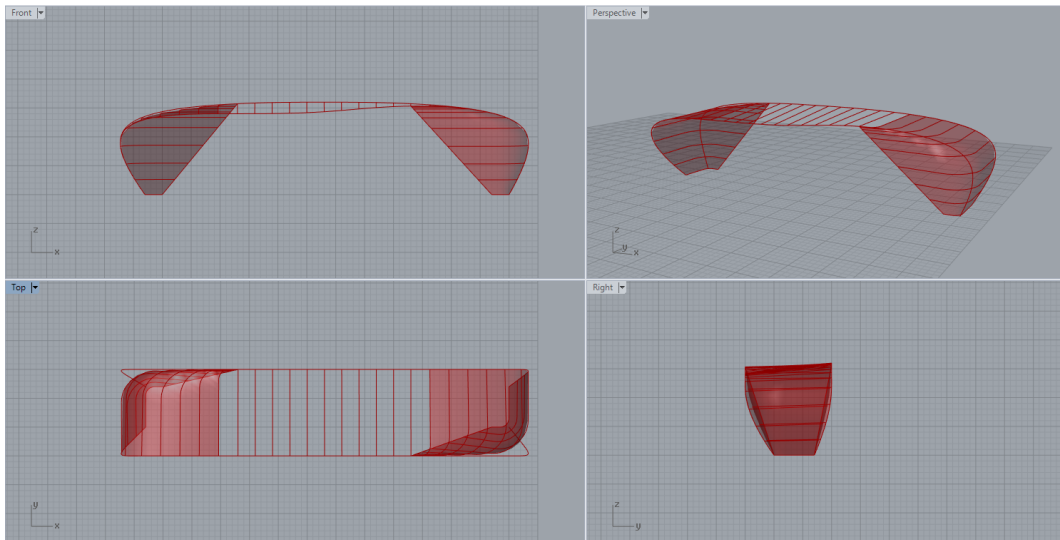


Figure 19. Left and right part of surface

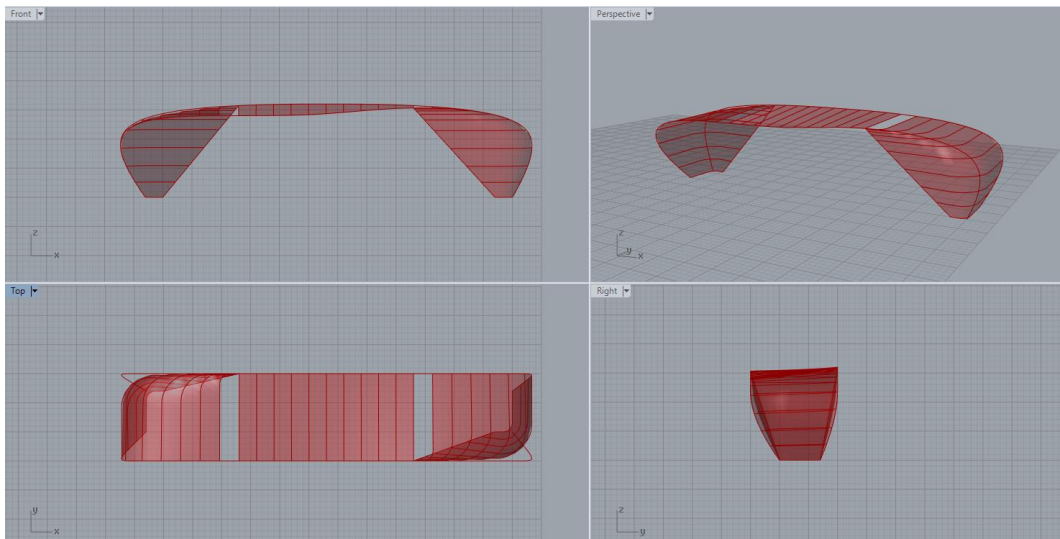


Figure 20. Left, right and top part of surface

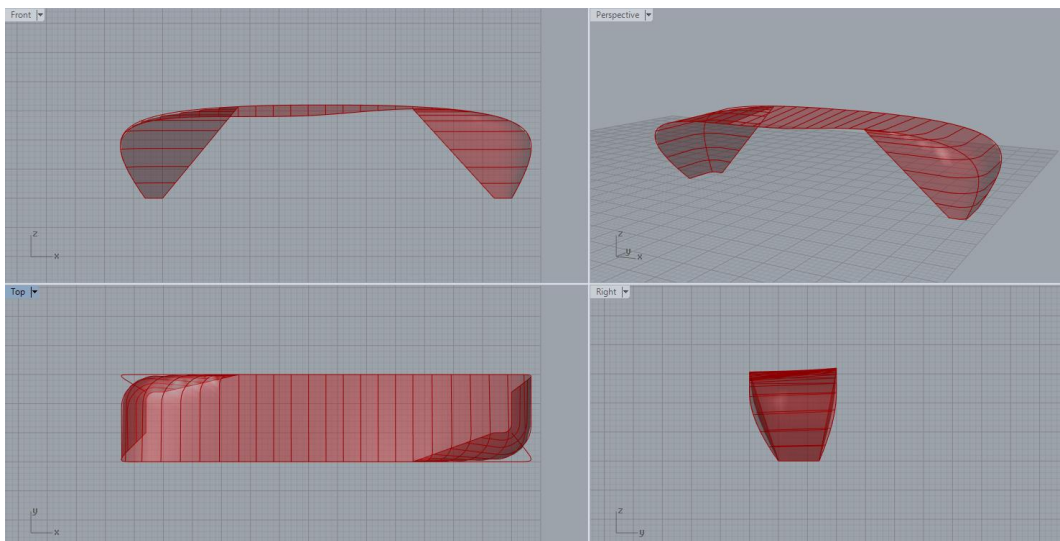


Figure 21. Merged surface defining the shape of the vertical foyer

5.2 Connection between the parametric model and the FE analysis

When the parametric generation of the geometry in Rhino-Grasshopper is achieved, the structural analysis of the geometry has to be performed by using the FEA software Ansys. Consequently, the geometry has to be transferred/generated into Ansys. Different methods to transfer/generate the surface structure in Ansys have been explored. The most adequate method for this tool is considered to be to transfer the geometry through transferring the mesh of the FEA model. The other methods that have been explored as well as the reasons why they are deemed to be unsuitable solutions can be found in Appendix 2 - Geometry transfer.

5.2.1 Meshing of the surface

As has already been mentioned, the step after the parametric generation of the geometry is the meshing of the open Brep. For achieving this, various meshing tools exist. Additionally to the already installed meshing tools in Grasshopper, there are various meshing plug-ins as well as user-scripted components available to be downloaded. Before deciding which meshing component is going to be used for the design tool, its desirable characteristics have to be set.

A target of the design tool is to analyse many different shapes in order to conclude on which is the optimum one based on the specified goal. As a consequence, the meshing component should be able to adjust to the changing shape of the structure without the need of external stimulation. Furthermore, plug-ins exist which iteratively improve the mesh before converging to one that fulfills the set goals such as the target edge size of the mesh. In this case, the FE analysis has to be initiated after the convergence of the mesh component. Consequently, when this kind of meshing algorithm is chosen, a way of informing the design tool about the convergence of the mesh has to be explored.

Additionally, a desired application of the tool is to be able to analyse not only a roof structure but also other parts that will be connected to it, such as floors and balconies. This is introducing an additional requirement for the meshing algorithm since the connection of the elements has to be achieved through the mesh. The connection is succeeded when the edges of the mesh elements are shared between the elements of the different parts to be connected, as presented in Figure 22 and Figure 23.

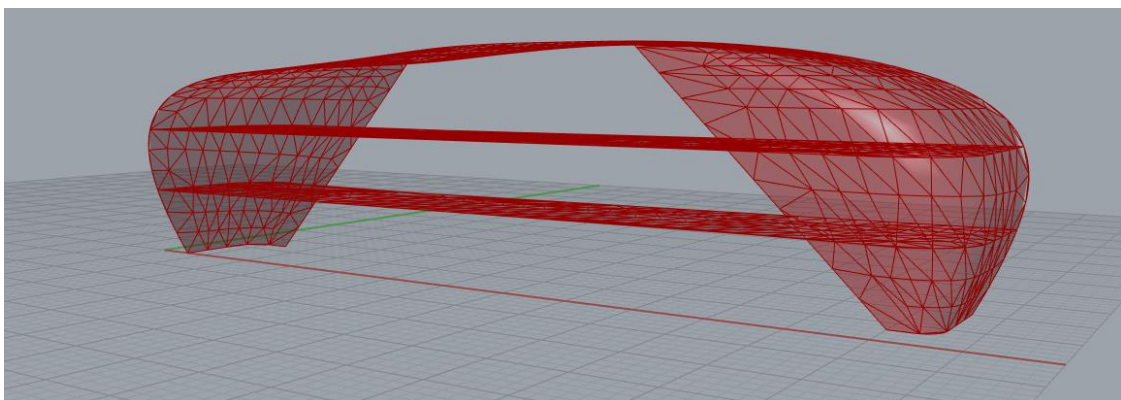


Figure 22. Floors are connected to the roof structure through the mesh

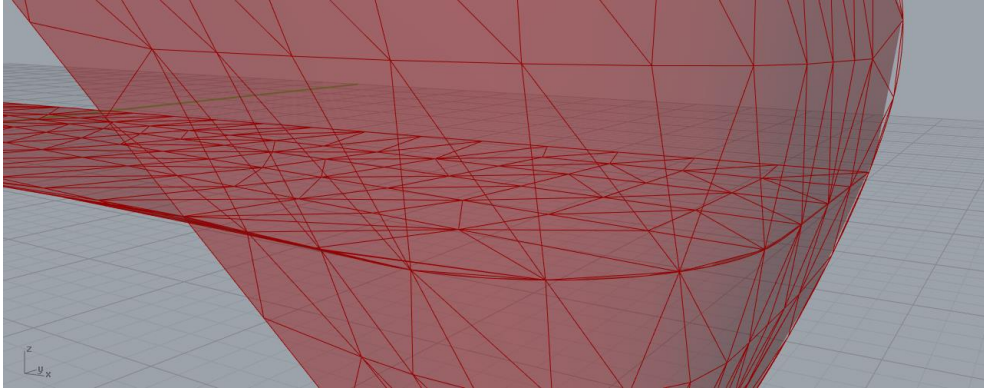


Figure 23. Detail of the connection between the floor and the roof structure

Based on the presented requirements, a comparison between the meshing components has been conducted and is visible in Figure 24.

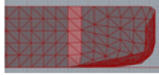
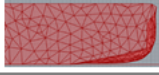
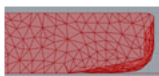
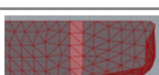

| Component | Mesh | Connect additional elements | Timer-Reset not needed | Response in changing shape |
|-----------------------------|---|-----------------------------|------------------------|----------------------------|
| MeshBreps (Karamba) |  | ✓ | ✓ | ✓ |
| C# (Daniel Piker) |  | ✗ | ✗ | ✗ |
| Extended C# (Stefan Spreng) |  | ✓ | ✗ | ✗ |
| ReMesh (Kangaroo) |  | ✗ | ✗ | ✗ |
| MeshMachine (Kangaroo) |  | ✓ | ✗ | ✗ |

Figure 24. Comparison of meshing components

The comparison presented in Figure 24 shows that the MeshBreps component of Karamba plug-in fulfills all the requirements of the meshing algorithm, consequently it is considered to be the most adequate for the design tool. The algorithm of this component is developed to be used for the Karamba analysis. Since Karamba is using a triangular TRIC element (Argyris et al., 2000) for executing finite element analysis of surfaces, the meshing is achieved with triangular elements. The preferred meshing in Ansys FE analysis, though, is with quadratic elements. Triangular elements might show a stiffer behaviour than in reality that is not desirable. This effect is known as shear locking. In order to avoid the problem of transverse shear locking, the analysed mesh should be structured with regular element shapes (Bletzinger et al., 2000). The aspect ratio of the elements should not exceed a certain limit. When this limit is exceeded, Ansys produces a warning regarding the shape of the element. Furthermore, when higher order isoparametric elements are used in combination with the use of reduced integration techniques, the results are “reasonably acceptable” as Kabir (1992) is stating. In this particular case, the MeshBreps meshing algorithm is producing a structured mesh with regular element shapes since no warning regarding the element aspect ratio is produced in Ansys software.

Additionally, a higher order shell element exists in Ansys that is adequate for triangular formed elements.

5.2.2 Import mesh in Ansys

In order to import the mesh in Ansys there are two options considered. The first is to define each element of the mesh by the coordinates of its nodes and the second is to transfer each mesh face as area that will be further meshed in Ansys. The information for building up the mesh in Ansys is extracted from Grasshopper and more specifically from the mesh deconstruction component. The output of this component is the coordinates of the mesh vertices, the index of the three mesh vertices that constitute a mesh face as well as the mesh normal (Figure 25). Since the coordinates of the mid-nodes of the elements are not a direct output of the mesh deconstruction in Grasshopper but are necessary for the mesh element definition, the second option is considered to be more suitable.

Consequently, the topology of the mesh, namely the vertices and the faces, is translated into keypoints and areas of the Ansys model with the help of the Python script. At first the topology of the mesh is written in .txt files, which are further processed in order to be translated into the adequate format of the APDL command listing. In this method each area that is generated can be used as one mesh face for the FE analysis (Figure 27) or further be divided in smaller segments-mesh faces (Figure 28). It can be noted that each mesh face is planar. The double curvature is more precisely represented when denser mesh is chosen.

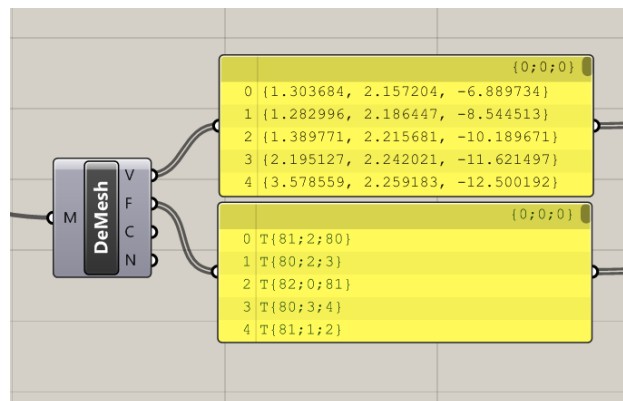


Figure 25. Topology extraction of the mesh



Figure 26. Meshing of the surface in Grasshopper

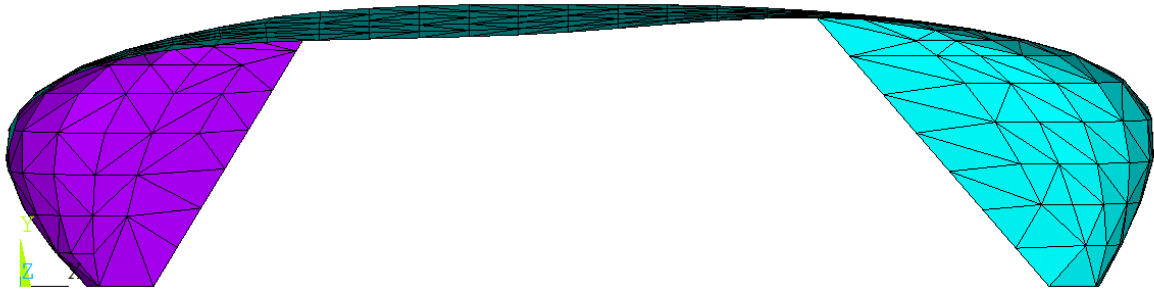


Figure 27. Geometry generation in Ansys based on the mesh of the parametric model

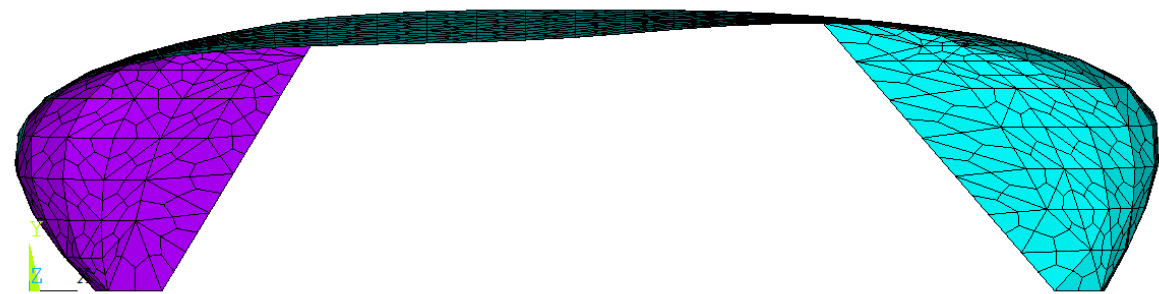


Figure 28. Meshing of the geometry in Ansys by dividing each line in 2

5.3 Structural system

The desire of the architect for the covering of the vertical foyer is steel polished finishing. As a consequence the material of the structure has been chosen to be steel. The structure is composed by 2 plates placed in a distance and ribs and stiffeners connecting the 2 plates (Figure 31). This type of structure is very common in the ship and automotive industry. Lately an effort has been noticed of including these techniques in the building industry. An example is the Porsche pavilion in Wolfsburg, Germany, designed by HENN architects (Figure 29 & Figure 30).

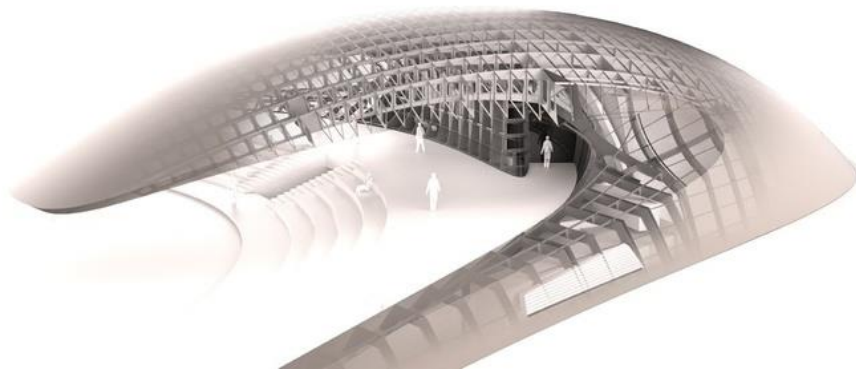


Figure 29. Structure of the Porsche pavilion [<http://www.archiscene.net/hospitality-retail/porsche-pavilion-henn-architekten>]



Figure 30. Details of the Porsche pavilion structure [<http://www.archiscene.net/hospitality-retail/porsche-pavilion-henn-architekten>]

The analysis of this type of structure in combination with the free form building shape can be performed by using finite element calculation. For the detailed analysis of this structure, modeling of every part of the structure (plates, ribs, stiffeners) is very important. In that way the local effects will be visible, such as local buckling or local excess of stress in the contact between the elements.

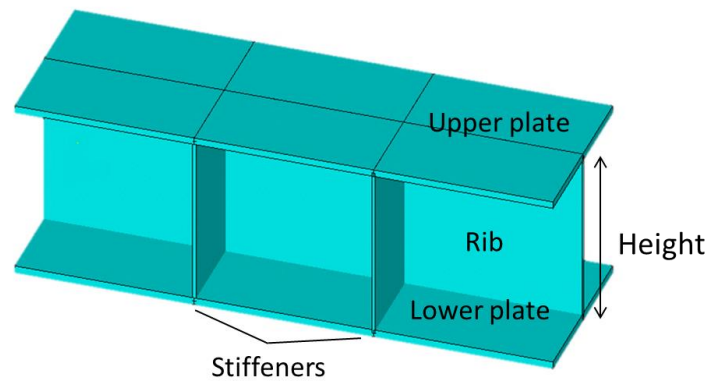


Figure 31. Parts of the structure of the vertical foyer

In this research, the global behaviour of the structure is deemed very important. One fitness value has to be computed characterising the whole structure, since many different shapes will be analysed in order to conclude which is the optimum one. When the desirable shape is discovered, detailed analysis can be performed in order to take into account local effects.

In case a detailed analysis has to be included in the optimisation process, the spacing between the ribs and the stiffeners as well as the thickness of every element has to be defined as variables for the optimisation process. The number of mesh elements in this analysis as well as the number of variables for the optimisation algorithm will increase significantly, which will cause the required time for convergence to increase significantly as well.

Furthermore, in order to take into account the option of analysing the detailed structure, a part of the parametric model that includes all the structural elements has been generated in Rhino-Grasshopper. An offset of the already generated surface has been performed for modeling the two plates. The ribs and stiffeners have been modeled as surfaces having as boundaries the two plates. It has been noted that when importing the surfaces in Ansys, the ribs and stiffeners are not connected properly with the plates. In Figure 32 a part of the imported structure is presented in which the

outside surface as well as the ribs are visible. As can be noted, the areas of the ribs, which are coloured different than green, deviate from their boundary surface. Manual work will be most probably required in order to achieve a fully working model that contains all the structural elements, which is not desirable for an optimisation process where the user cannot manually control every iteration.

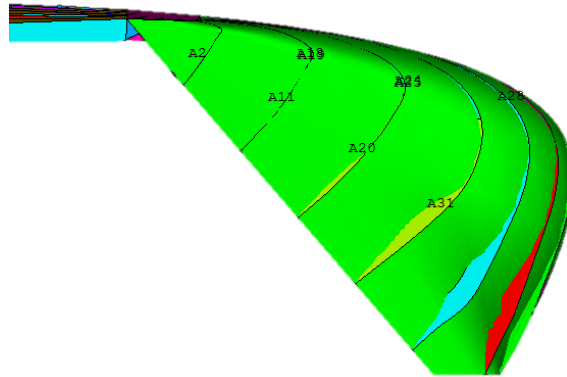


Figure 32. Deviations in the connections of the areas when ribs are modeled in Grasshopper and imported in Ansys

Consequently, it has been chosen not to model the full structure, but a simpler-equivalent one that will show equivalent global structural behaviour as the original structure. In order to achieve this many possibilities have been considered based on Ansys capabilities. The most adequate for this modeling is to model the roof structure as one surface and assign the stiffness properties of the real structure. In this way, the usability of the design tool is not restricted to a specific structural system or material. When different stiffness properties are assigned from the user to the surface, a different complex cross section can be modeled and analysed without further manipulation necessary. The process that has been carried out before concluding on the adequacy of the current approach is analysed in Appendix 3 - Equivalent structure.

5.4 FE analysis

For building up and testing the finite element model, the starting shape of the vertical foyer has been used. This shape is visible in Figure 27.

As has been mentioned in the previous section, the roof structure is modeled as one surface and is further meshed for the finite element analysis. There are many element types available in Ansys. Based on the field of application as well as the formulation of the element, the choice can be made. For this structure SHELL281 element has been chosen. It is an 8-node element with six degrees of freedom at each node: translations in the x, y and z axis and rotations about the x, y and z axis. The formulation of the element gives the freedom of choosing quad mesh or triangular mesh. In case a triangular mesh is chosen, three out of the 8 nodes are defined with the same node number, as shown in Figure 33.

The theory used for this element is the Mindlin-Reissner where shear deformation is taken into account (Ansys, 2015).

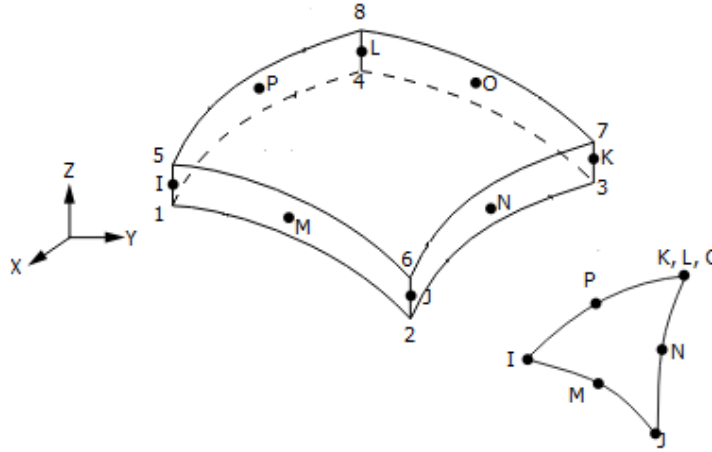


Figure 33. 8-node SHELL281 element (Ansys, 2015)

Since the structure modeled is one surface whereas the original structure to be constructed consists of more structural elements, the properties of the original structure have to be an input for the simplified model. In order to achieve this pre-integrated shell elements can be used.

The pre-integrated form of input allows the user to import homogeneous section-stiffness constants evaluated in other analyses. According to the theory behind Ansys software, defining pre-integrated section stiffnesses is common in analyses of layered composites, corrugated shells, or other complex section construction (Ansys, 2015)

This structure is a complex section construction, so homogenisation of the stiffness properties has to be performed and these to be assigned through a pre-integrated general shell section. It is assumed that the cross section presents an isotropic behaviour. This is actually not accurate, since the stiffeners will probably not be placed with the same spacing in both directions, since the transverse stiffeners will be mainly used to prevent the local buckling of the steel plates. The exact distribution of the ribs and stiffeners is not a part of this research. Consequently, a homogeneous stiffness is considered to be a good approximation for this stage of analysis.

The stiffness matrixes that are an input for the pre-integrated element are: membrane stiffness matrix [A], bending stiffness matrix [D], coupling between membrane and bending stiffness matrix [B] and transverse shear stiffness matrix [E].

The same formulas used in Ansys for computing the stiffness matrixes of SHELL281 element will be used, updated with the properties of the original structure. SHELL281 uses the formulas for plane stress analysis (Moaveni, 1999) for computing the membrane and bending stiffness matrix. It is assumed that there are no forces acting in the z-direction. Consequently, no stresses σ_{zz} , σ_{xz} or σ_{yz} are expected.

$$[v] = \frac{E}{1-\nu^2} \begin{bmatrix} 1 & \nu & 0 \\ \nu & 1 & 0 \\ 0 & 0 & \frac{1-\nu}{2} \end{bmatrix} \quad (5.1)$$

$$\text{Membrane matrix } [A] = [v] * A \quad (5.2)$$

$$\text{Bending matrix } [D] = [v] * I \quad (5.3)$$

$$\text{Shear stiffness matrix } [E] = \begin{bmatrix} GAs & 0 \\ 0 & GAs \end{bmatrix} \quad (5.4)$$

Where:

| | |
|-----------|--|
| E | Young's modulus |
| v | Poisson ratio |
| G | Shear modulus. It can be calculated as $G = E / (2 * (1 + v))$ |
| A | The area of the cross section |
| As | The area of the cross section that is taking up the shear forces |
| I | Moment of inertia |

Table 1. Symbols for stiffness matrixes

In order to validate the accuracy of results when using pre-integrated shell elements a test has been executed. A flat 10x1m clamped plate of 0.08m thickness is modelled with SHELL281 element. The stiffness matrixes of the plate are retrieved from Ansys and the internal forces are computed. The retrieved values of the membrane, bending and shear stiffness are now used for formulating the stiffness matrixes of a pre-integrated general shell section with the same dimensions and boundary conditions. The internal forces of the new way of modeling are computed once again. It has been noted that the axial, bending and shear forces of the two structures are identical but a small difference is presented in the torsion moment m_{xy} and shear Q_{yz} . This indicates that the lack of possibility to assign the torsion stiffness will lead to some inaccuracies when the torsion moment m_{xy} is computed.

For performing a static analysis of the structure, the loads as well as the boundary conditions of the structure have to be defined. Since these are unique for every structure, they are user inputs of the tool and the values used for the case study analysis will be presented in Chapter 6.

The application of the loads on the structure is achieved with a new element type that is necessary to be used. This is required because the available loading type of the already chosen element SHELL281 is only pressure normal to the surface. The structures that are intended to be analysed with the tool will most probably be loaded in different directions than only normal to the surface. In a common structural analysis, many loading types have to be applied at the same time, which have different direction. Consequently, an element type for load applications in 3D structural analysis has to be used. The chosen element is SURF154. This element can be overlaid onto the area face of the shell elements and many load effects can exist simultaneously (Ansys 2015). By choosing the appropriate keyoptions, the orientation of the load can be specified as well as the type of area of the applied load (projected/full area).

The unit type of the user input cannot be defined in Ansys. The user is responsible for setting consistent units of the input values. The units chosen to be used by the tool are based on the SI system of units. Consequently, the user input of the tool has to be in the following units:

Newton (N), meter (m), second (s), pascal (P), kilogram (kg), joule (J)

5.4.1 Stress recovery

When modeling with pre-integrated shell elements, the shell stresses are not available for output. This is expected since the stresses depend on the physical properties of the cross section which are not defined in this type of modeling. Consequently, the stresses have to be estimated based on the section forces computed in Ansys.

It has been assumed that the loadbearing parts of the cross section are the plates. Consequently, it is assumed that only the plates will be stressed. The approximated stress distributions in the y direction of the plates are presented in Figure 34. The highest value of stress is expected at the two most outer fibres of the cross section. Consequently, the calculation is performed for these parts.

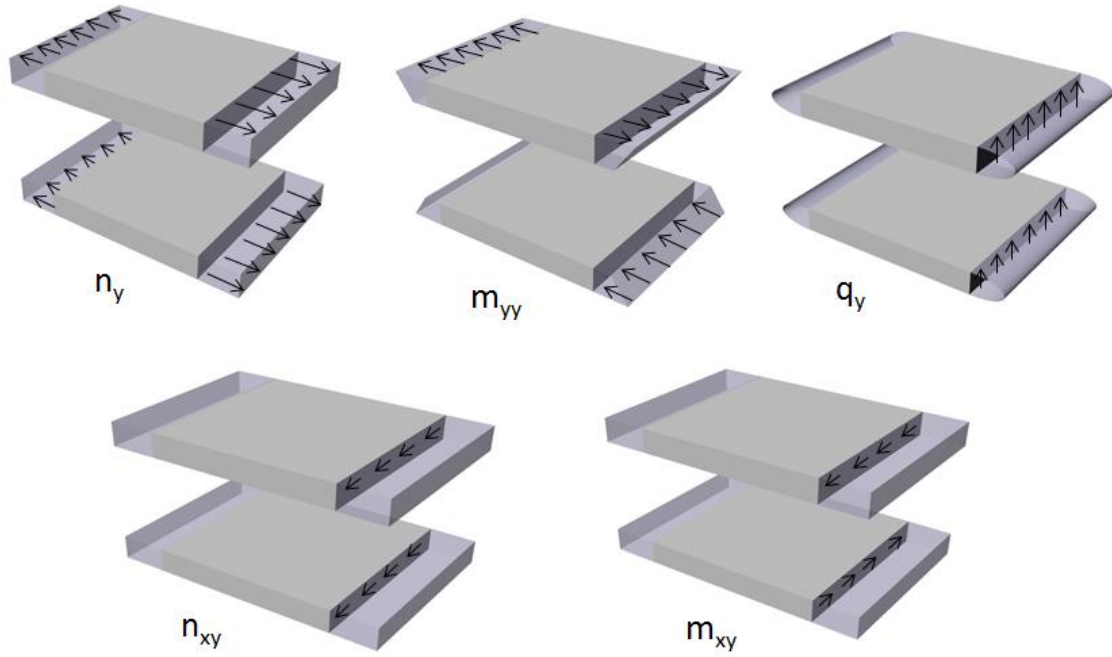


Figure 34. Approximated stress distributions of the presented section forces in the plates

From the formulas of the stress distributions the stress in the upper part of the top flange can be derived.

$$\sigma_{xx} = \frac{n_x}{A_x} + \frac{m_{xx} * y}{I_x} \quad (5.5)$$

$$\sigma_{yy} = \frac{n_y}{A_y} + \frac{m_{yy} * y}{I_y} \quad (5.6)$$

$$\sigma_{xy} = \frac{n_{xy}}{A_x} + \frac{m_{xy}}{\frac{A_x * h}{2}} \quad (5.7)$$

The behaviour of the real structure is orthotropic. The density with which the ribs and stiffeners will be placed is not necessarily the same. This is not taken into account in this stage of the analysis, since only the plates are analysed. Consequently, the behaviour is assumed to be isotropic with $A_x = A_y = A$ and $I_y = I_x = I$.

This assumption is necessary for this analysis, since the orientation of the section forces computed in Ansys are parallel to the element coordinate system. The coordinate system of each element is based on the location of the nodes I and J (Figure 33). The x axis is parallel to the line connecting nodes I and J and has the direction from I to J (Ansys 2015). Since the meshing is done in Ansys, the user has no influence on the determination of the element's coordinate system. It has been observed that adjacent triangular elements might have the x coordinate in the orientation of global-x or global-y axis. Consequently, this would create difficulty in computing the stresses if orthotropic behaviour was analysed.

The element forces that are computed in Ansys are interpolated in the central point of the element (Figure 35-Left). Consequently, these computed forces are assumed to be applied on the center of gravity of the original cross section. Since only the plates are considered and the assumed thickness of both plates is the same, the center of gravity is located in the mid distance between the 2 plates as presented in Figure 35-Right. The stress recovery process will lead to stresses at the central point of each plate element.

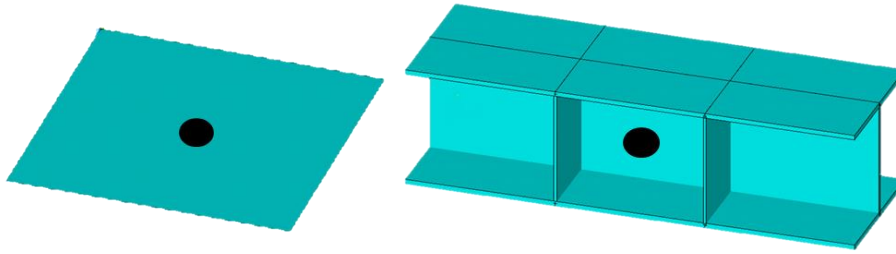


Figure 35. Left: Point that the element forces are computed in Ansys. Right: Assumed point of application of the forces in the original structure

The value that will be used for the control of the structure is the Von Mises stress of the elements. Since the structure under analysis is a steel structure, the equivalent stress according to Von Mises is important. If the Von Mises stress is higher than the yield stress, then the material will yield (Hoogenboom, 2015). From the Equation (5.8) which is used for computing the Von Mises stress, becomes obvious that the orientation of the computed stress σ_{xx} and σ_{yy} is not affecting the final value, since the difference between the two perpendicular stresses is part of the formula.

$$\sigma_{VM} = \sqrt{\frac{1}{2}((\sigma_{xx} - \sigma_{yy})^2 + (\sigma_{yy} - \sigma_{zz})^2 + (\sigma_{zz} - \sigma_{xx})^2) + 3(\sigma_{xy}^2 + \sigma_{xz}^2 + \sigma_{yz}^2)} \quad (5.8)$$

In the analysed case stresses exist at the x and y direction. The stresses at the z coordinate are zero. Consequently, the calculation of the von Mises stress is based on the simplified form of Equation 5.8.

$$\sigma_{VM} = \sqrt{\frac{1}{2}((\sigma_{xx} - \sigma_{yy})^2 + \sigma_{yy}^2 + \sigma_{xx}^2) + 3\sigma_{xy}^2} \quad (5.9)$$

The stress recovery approach that has been followed is similar to Hoogenboom (2005).

5.4.2 Validation of the equivalency

In order to check if the modeling of the stiffened structure with pre-integrated shell elements will lead to an accurate structural analysis, a part of the structure has to be modelled in both ways and checks need to be performed on the deflection of the structure and the Von Mises stress.

The local effects of the structure will not be taken into consideration in this research; consequently the part of the structure that will be chosen for the validation of the equivalency should have adequate dimensions, so that the local effects will not affect the global results of the model.

The length of the roof structure is around 65m. There is an upper part that does not show high curvature, the length of which is around 30m (Figure 36). It is considered a good approximation to model this part as a horizontal structure, in order to accommodate the modeling of the ribs and stiffeners. The boundary conditions of the horizontal structure have to be defined based on the behaviour of the real structure and the most appropriate support is considered to be the clamp. Consequently, a doubly clamped surface of 1mx30m has been used for the validation.

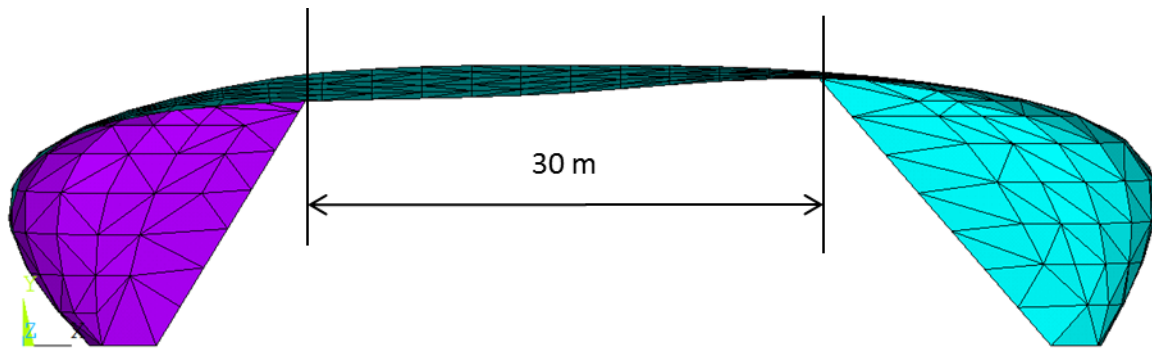


Figure 36. Part of the structure to be used for the equivalency validation

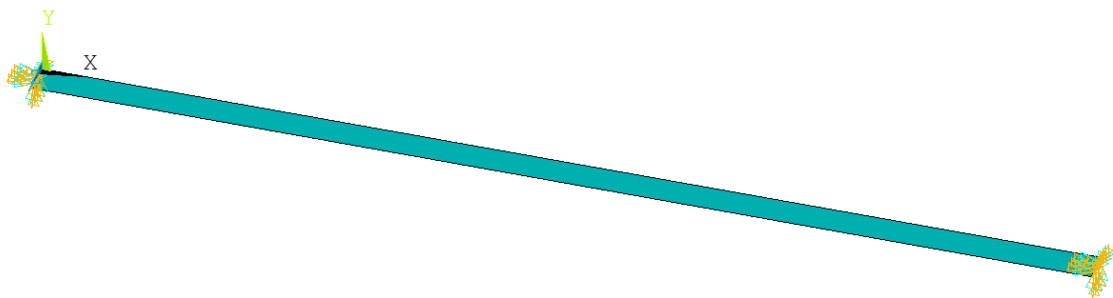


Figure 37. Double clamped surface for modeling the equivalent structure

The cross section used for the validation has a height of 1m, the thickness of the upper and lower flange is 40mm, the thickness of the ribs and stiffeners is 20mm and the distance between the adjacent ribs as well as stiffeners is 1m.

When modeling the original structure, the plates and the stiffeners are modeled as areas and are further meshed with SHELL281 elements. The thickness of each part of the structure is the thickness of the steel plates that will be constructed.

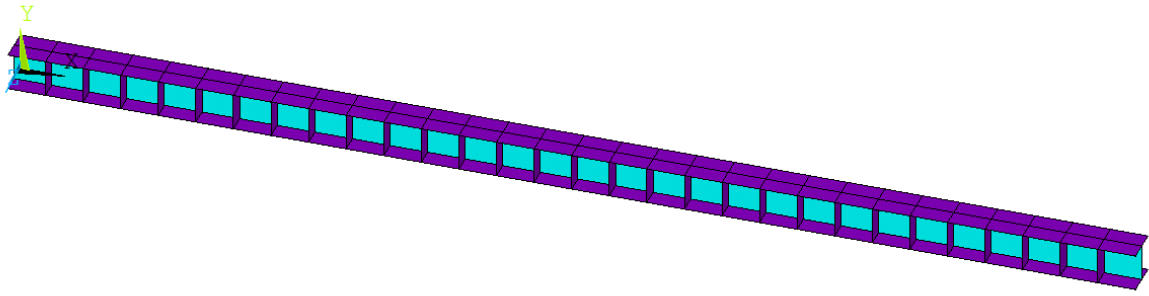


Figure 38. Modeling of the original structure

In the equivalent model, a single area of 1mx30m is modeled. Pre-integrated shell elements with assigned stiffness matrix are used.

The properties of the cross section are shown in the following table:

| Cross section properties | Symbol | Value | Units |
|---------------------------------|----------|----------|-------------------|
| plate width | s | 1.00 | m |
| height: distance between plates | h | 1.00 | m |
| thickness of the upper plate | t_{f1} | 0.04 | m |
| thickness of the lower plate | t_{f2} | 0.04 | m |
| thickness of the web | t_w | 0.02 | m |
| area | A | 0.099 | m ² |
| moment of inertia | I | 0.021 | m ⁴ |
| Material properties | | | |
| modulus of elasticity | E | 2.1E+11 | N/m ² |
| shear modulus | G | 8.75E+10 | N/m ² |
| density | γ | 7850 | Kg/m ³ |
| Poisson ratio | ν | 0.30 | - |
| Stiffness properties | | | |
| bending stiffness | EI | 4.51E+09 | N*m ² |
| shear stiffness | GA_s | 8.68E+09 | N |
| membrane stiffness | EA | 2.08E+10 | N |

Table 2. Properties of the original cross section

When importing these properties to Equations 5.1 to 5.4, the stiffness matrixes have the following values.

Membrane stiffness matrix:

$$A = \begin{vmatrix} 17500000000 & 3500000000 & 0 \\ 3500000000 & 17500000000 & 0 \\ 0 & 0 & 7000000000 \end{vmatrix}$$

Bending stiffness matrix:

$$D = \begin{vmatrix} 4699893333 & 939978667 & 0 \\ 939978667 & 4699893333 & 0 \\ 0 & 0 & 1879957333 \end{vmatrix}$$

Coupling membrane and bending stiffness matrix:

$$B = \begin{vmatrix} 0 & 0 & 0 \\ 0 & 0 & 0 \\ 0 & 0 & 0 \end{vmatrix}$$

Shear stiffness matrix:

$$E = \begin{vmatrix} 1750000000 & 0 \\ 0 & 1750000000 \end{vmatrix}$$

The load that is applied is the ULS2 combination of dead load and snow load (Appendix 1 - Loading). The load is a constant pressure of 13,6 kN/m² and the direction is parallel to the y-axis. In the original structure, the load is applied on the top flange.

The analytical formula for calculating the deflection of a clamped beam is shown in Figure 39. The analytical solution will be compared to the two ways of modeling the structure.

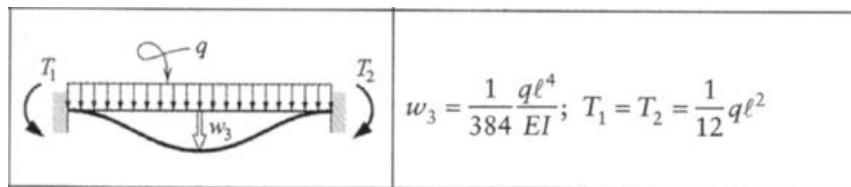


Figure 39. Deflection of a double clamped beam under distributed load

It is not expected to have the same deflection in the Ansys models and in the analytical solution, since the analytical solution is adequate for analysing a 2D beam, whereas the model in Ansys is a 3D structure where not only bending will be present. On the other hand, the analytical solution gives an indication of the magnitude of the deflection to be expected.

| | Analytical solution | Original model | Equivalent model | Difference original-equivalent | Difference with analytical |
|--------------------------------|---------------------|----------------|------------------|--------------------------------|----------------------------|
| Maximum deflection [mm] | 6.36 | 7.21 | 7.22 | 0% | -13% |

Table 3. Comparison of the maximum deflection of the models

As can be noted from Table 3, both models present the same maximum deflection when loaded under constant pressure. The analytical solution shows a stiffer behaviour of 13%.

Regarding the stress equivalency, the following process has been followed. Both structures have been analysed in Ansys. The element stress resultants of the equivalent model have been extracted. These forces are available only to the element centroid and are computed to the shell mid-plane. It has been assumed that these forces are applied in the centroid of the original cross section as presented in Figure 35. Based on these forces and the assumption made, the element stresses can be computed on the upper and lower flange with the process presented in Section 5.4.1. Since there is no difference in the thickness of the upper and lower flange and the centroid of the cross section is located in the mid part of it, the expected stresses on the upper and lower flange are equal. This is not the exact case in the original structure, since the forces are not applied on the centroid of the cross section. A difference of around 8-10% is noted between the Von Mises stresses of the upper and the lower flange.

Furthermore, the absence of torsion equivalency between the two structures is noticeable in the stress caused by the torsion moments (σ_{xy}). In the equivalent structure, the highest torsion moment is present at the clamps and is very quickly reducing to a very small value which is present to the biggest part of the structure, whereas in the original structure the stress caused by torsion is linearly reducing.

It can be noted that the difference between the computed stresses and the stresses of the original model is around 5-6% on the upper flange and 3-4% on the lower flange. These differences are derived mainly because of geometric reasons. A 3D structure modelled in Ansys will not have exactly the same behaviour as a 2D plane. In the 3D structure there are many elements the contact of which creates excess of stresses which are not possible to be modeled with the equivalent structure.

The absolute difference between the stresses is noted to be higher close to the clamps. These areas attract higher loads and consequently higher stresses. However, the clamps are not present in the real structure at this position; as a consequence the difference of stresses close to the boundaries of the structure should be ignored.

Furthermore, the difference of around 5-6% is considered relatively low based on the fact that the analysis is oriented to an early design phase, but still contains a higher accuracy than hand calculations or simple orthogonal modeling of the structure.

The tables and graphs of the equivalency analysis are presented in Appendix 4 - Stress equivalency comparison.

5.4.3 Analysis types

When analysing a shell-like structure two analyses are deemed important: a static analysis and a buckling analysis. Whether a linear or non-linear analysis will be chosen depends on the influence of non-linear effects to the structure. Furthermore, the required accuracy of the results as well as the acceptable computational time will influence the choice of analysis. For these non-regular structures, a non-linear analysis yields more accurate results. On the other hand, the computation time is a very important factor for the usability of the design tool. Consequently, linear static and linear buckling analyses have been incorporated in the tool.

At first a static linear analysis is performed. Based on the cross section forces computed in this analysis, the stresses are recovered. If the stresses are higher than the maximum allowable, then a bigger cross section is assigned to these elements and the static analysis is performed again. When this loop is finished, then an eigenvalue buckling analysis is computed based on the last static analysis. Eigenvalue buckling analysis generally yields un-conservative results (Ansys, 2015).

The load combinations that will be used for the buckling analysis have been chosen to be

$$\text{ULS2: } 1.20 G + 1.50 S \quad (5.10)$$

$$\text{ULS3: } 1.20 G + 1.50 W \quad (5.11)$$

These combinations are considered to cause higher instability than the other combinations that have been analysed.

For the calculation of the buckling load factors, all loads are scaled up to the point where instability is achieved. The eigenvalues calculated by the buckling analysis represent buckling load factors. If a unit load is specified, the load factors represent the buckling loads. In the tool has been decided to include load combinations, so that the control of the buckling load factors is straightforward. If a structure has a buckling load factor higher than one, then it yields that it can take up the applied loads without instability present. Since non-linear effects are ignored, the accurate limit load might be lower than the one computed by the linear buckling analysis. Consequently, a knock down factor should be used for ensuring a stable structure.

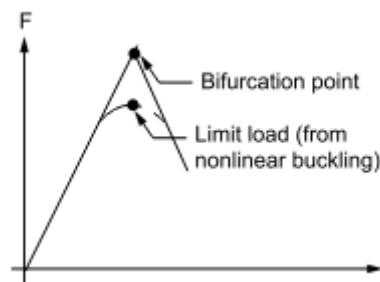


Figure 40. Linear (eigenvalue) buckling curve (Ansys, 2015)

Furthermore, knock down factors are used in the buckling analysis of shell structures in order to account for imperfection sensitivity. The structures that buckle due to bending are usually not susceptible to imperfections. This can be controlled by computing the first two buckling load factors and calculate the difference between them. If the difference is less than 2%, then the structure analysed is considered to be highly influenced by imperfections (Hoogenboom, 2015).

According to Hoogenboom (2015), the knock down factor can be experimentally defined and when little information is available a knock down factor of 6 can be used. The value of the knock down factor that is included in the tool is a user input. The value that has been used for the case study is presented in Chapter 6.

5.5 Thickness distribution

When a shell like structure is analysed, locations exist of higher stresses than others. Consequently, some areas of the structure will require more material than others. The target of the thickness distribution algorithm is to distribute the material in the structure in a way that no overstressed areas exist in it.

The algorithm requires as user input a list of cross sections through which can iterate in order to find the most suitable cross section of every finite element. The accuracy of the algorithm, as a consequence, depends highly on the user defined cross section list. The smaller the difference between the adjacent cross sections, the better the accuracy. On the other hand, a small difference leads to a longer cross section list and more iterations necessary for achieving the final result.

Two methods are available for a thickness distribution algorithm (Olsson, 2012):

The **direct sizing method** where the algorithm jumps to the fitted cross section and

The **incremental sizing method** where the algorithm in every iteration is scaling up or down the cross section of the element by a set number. In the approach followed in this research this would mean to move one position up or down in the cross section list for each element.

For some simple structures where not many load paths exist, both methods have equivalent results as validated by (Pruszkowski, 2015). According to Olsson (2012), the second method would not yield accurate results for a 3D space frame, due to the existence of many load paths. It is considered that in shell-like structures, the load paths are many and the jump of cross section might not lead to correct results. It is true though that the computation time of the direct sizing method is expected to be considerably lower, since less iterations will most probably be required.

Since the tool is oriented for analysing free form shell like structures, the gradual method is considered to be the most adequate approach. Consequently, this method is included in the tool. The first cross section of the list (the smaller) is assigned to the whole structure. The stresses are computed and a higher cross section is assigned to the overstressed elements. The process is repeated until no element needs modification, as presented in Figure 41.

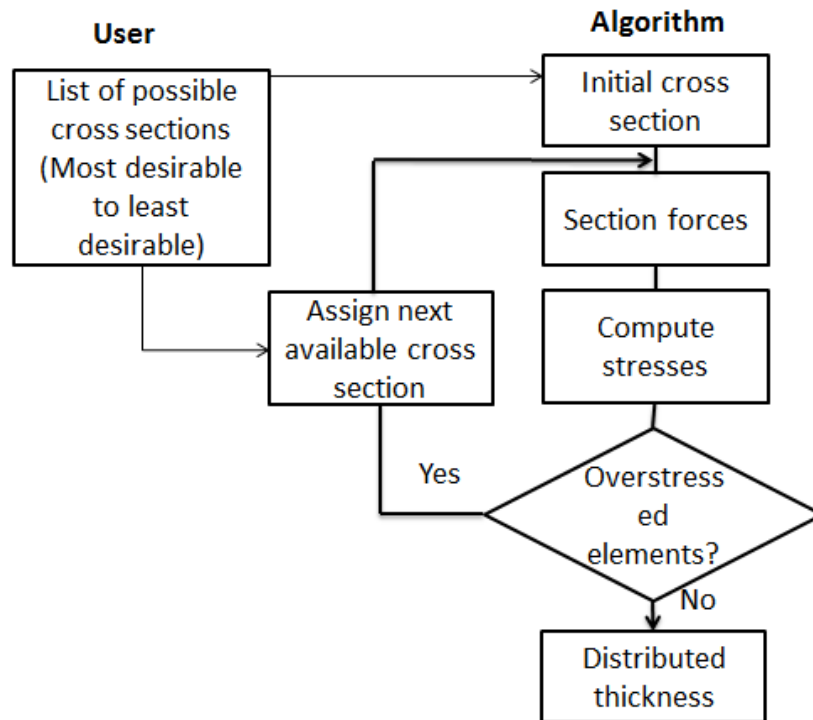


Figure 41. Thickness distribution algorithm

5.5.1 Validation of the thickness distribution algorithm

In order to test the thickness distribution algorithm a plate of 5x5m has been modelled. The force applied on the plate is a normal to the plate distributed load of 15KN/m^2 . The plate is clamped on one side.

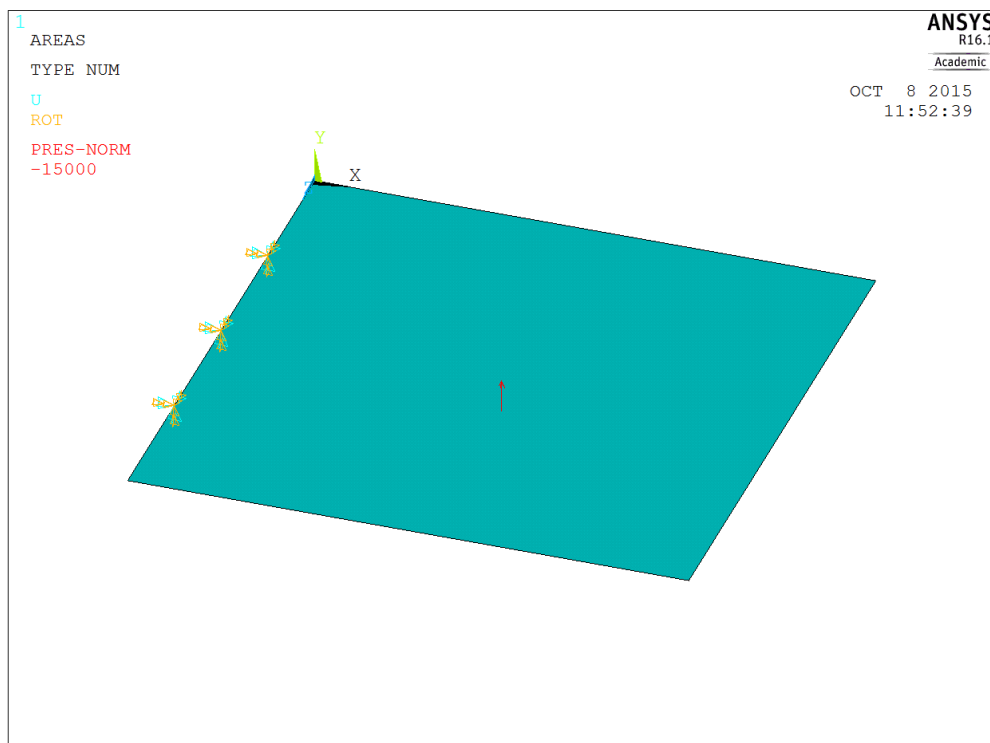


Figure 42. Plate modeled in Ansys, clamped boundary and pressure load

The meshing of the plate has been achieved by choosing the elements to have dimensions of 0.5x0.5m, consequently the mesh consists of 100 elements (Figure 43).

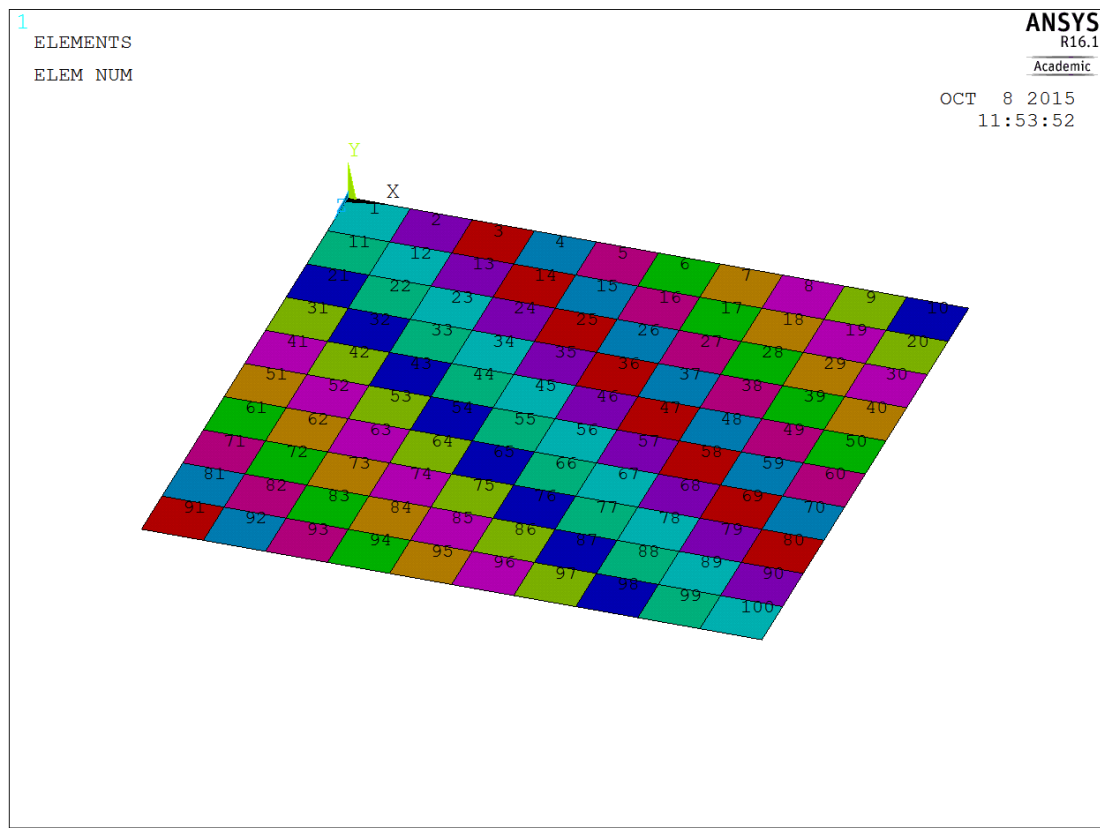


Figure 43. Meshing of the plate

The plate will take up the load in bending, as a result has been decided to keep the thickness of the upper and lower flange constant (20mm) and change the height between the plates. The available cross sections are imported as a list. A list of 10 cross sections has been created. The starting cross section (the smaller) has a distance between the plates of 500mm and the ending cross section a distance of 1500mm. The height difference between adjacent cross sections is 100mm.

Based on the Von Mises stresses that have been computed in the case that the whole plate is constructed out of the first cross section (500mm distance between the plates), has been decided to set a limit for the stresses of 8.5MPa.

It is expected to have a need of a bigger cross section close to the clamp, where the forces are higher and smaller cross section towards the free edge. Convergence has been achieved after 11 iterations. The output of the thickness optimisation algorithm in 4 out of the 11 steps is presented in Figure 44 to Figure 47.

Iteration number: 0

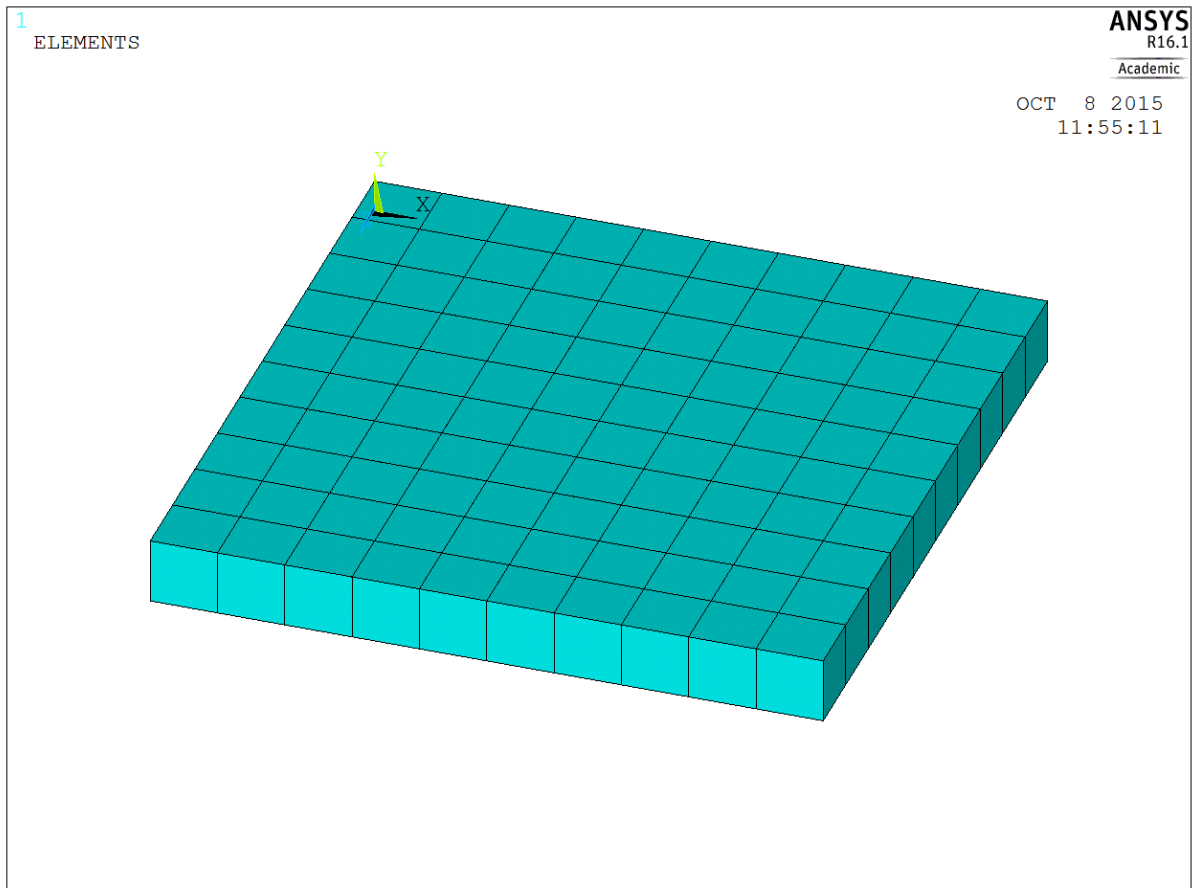
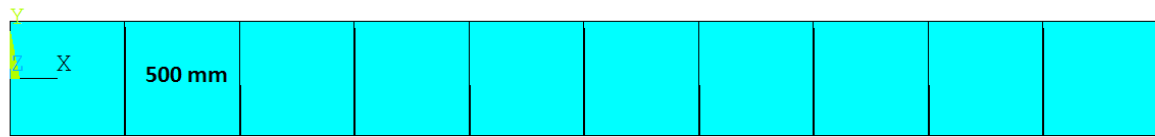


Figure 44. Starting cross section height-Iteration 0

Iteration number: 3

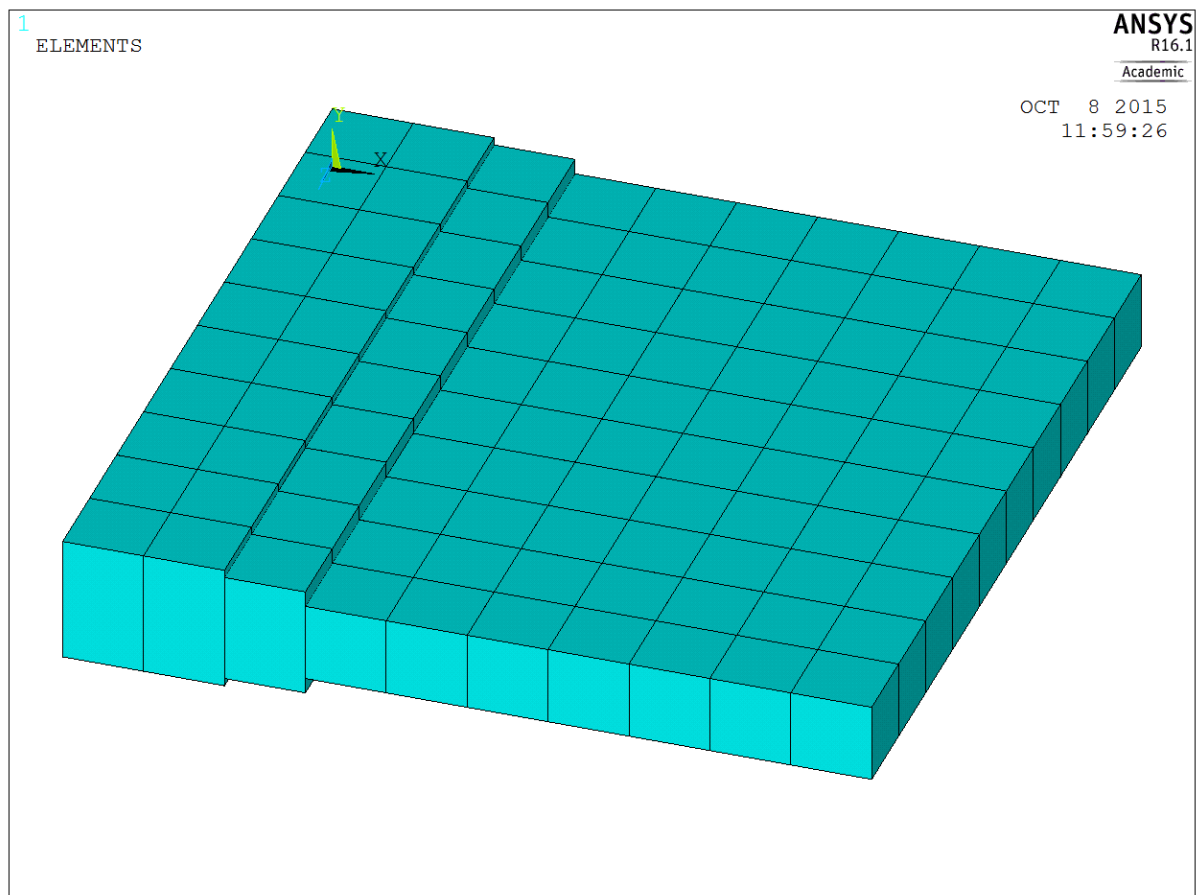
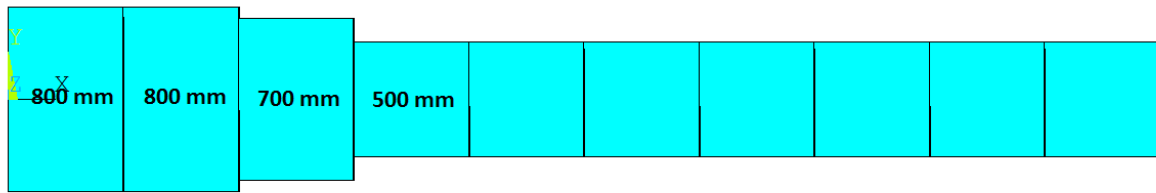


Figure 45. Element's cross section height-Iteration 3

Iteration number: 6

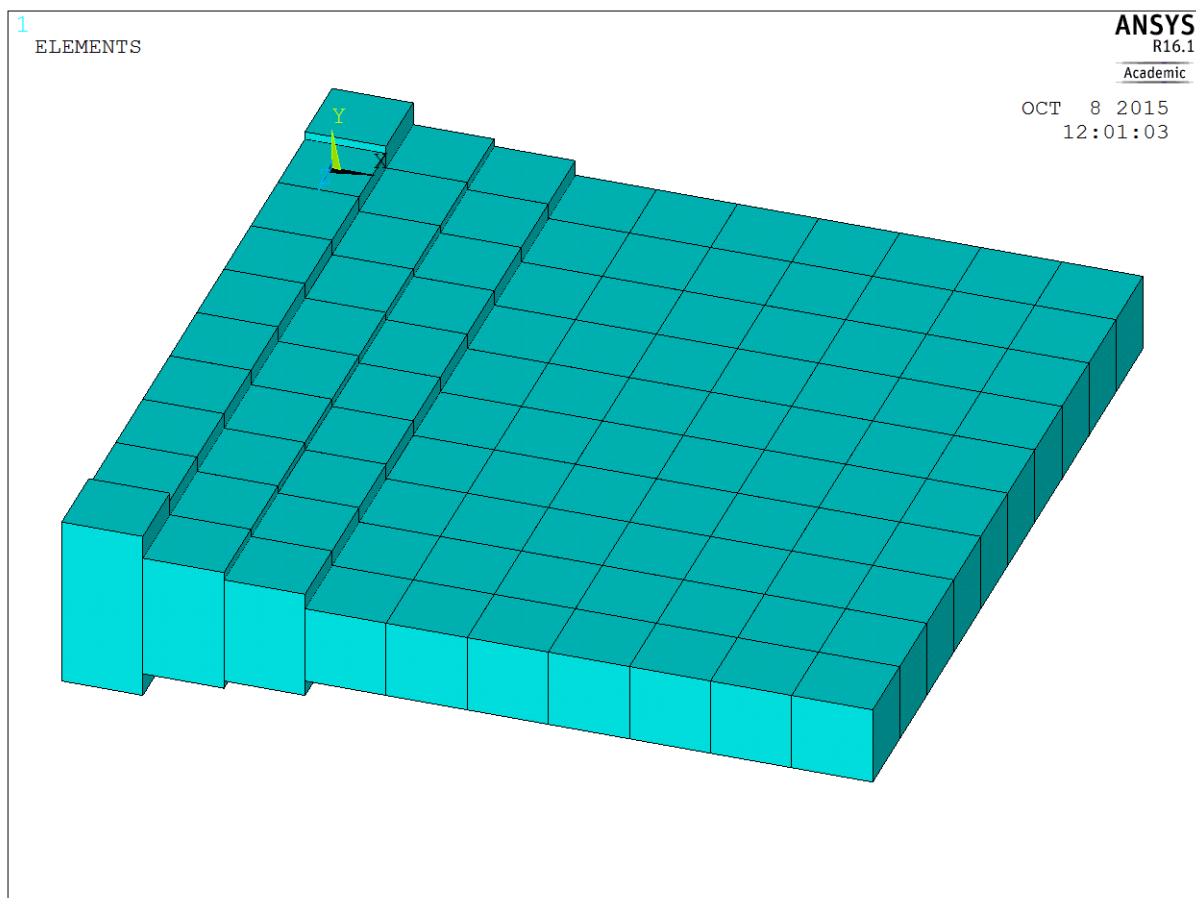
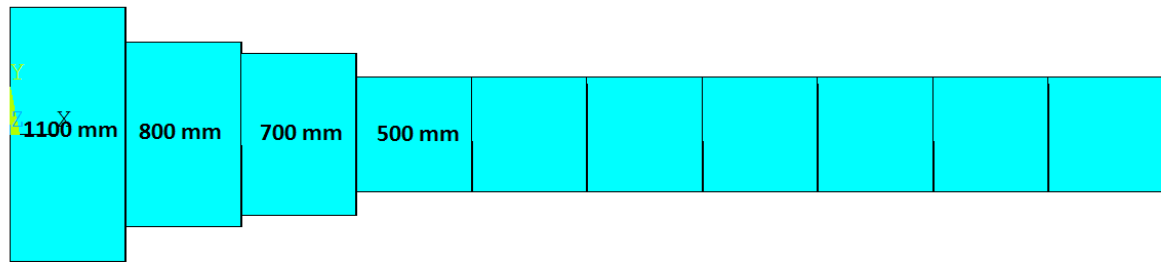


Figure 46. Element's cross section height-Iteration 6

Iteration number: 10

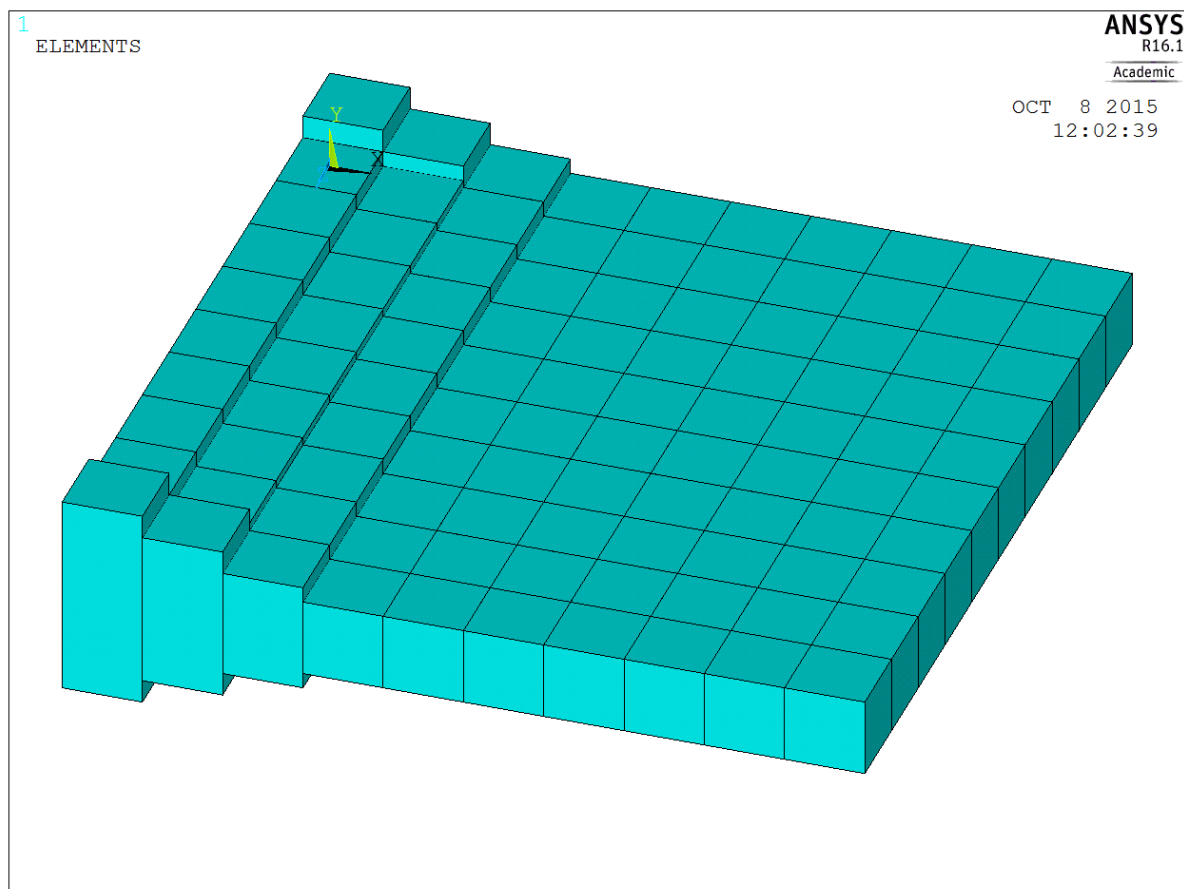
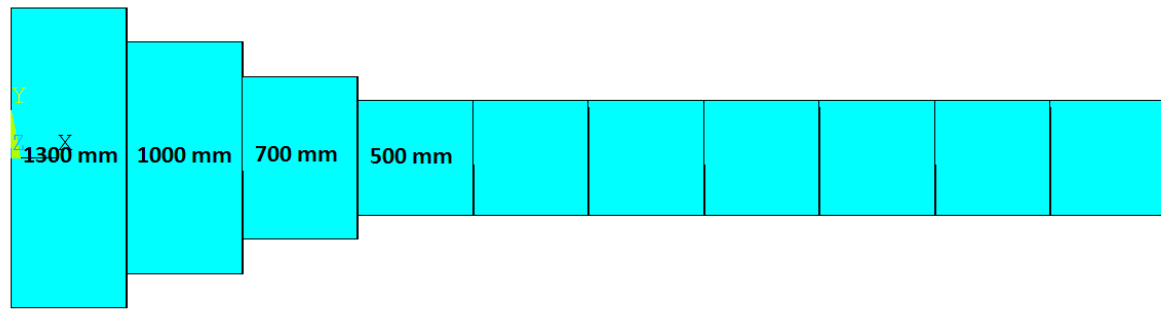


Figure 47. Element's cross section height at convergence-Iteration 10

As it can be observed, the bigger cross sections are needed towards the clamp and more precisely towards the free edges perpendicular to the clamp. The stresses of every iteration have been plotted on the free edge and are visible in Figure 49. Furthermore, the number of elements that needed modification in every iteration is presented in Figure 48.

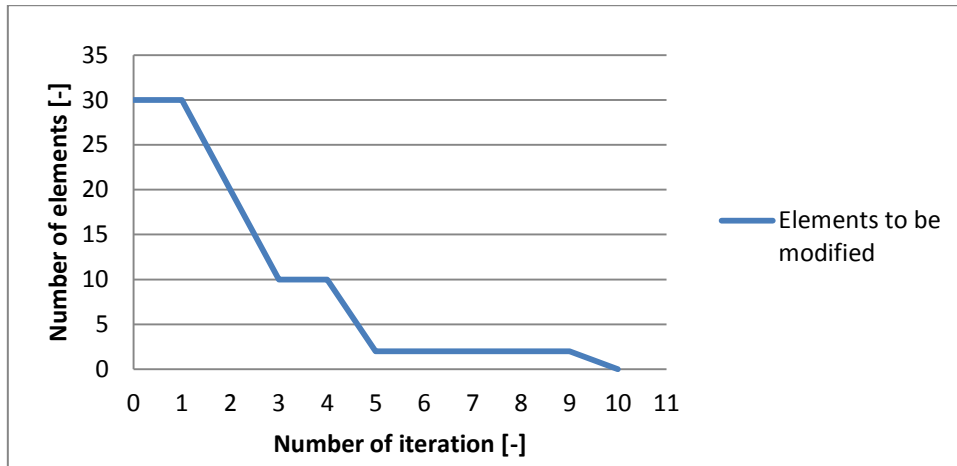


Figure 48. Number of elements that require cross section modification in every iteration

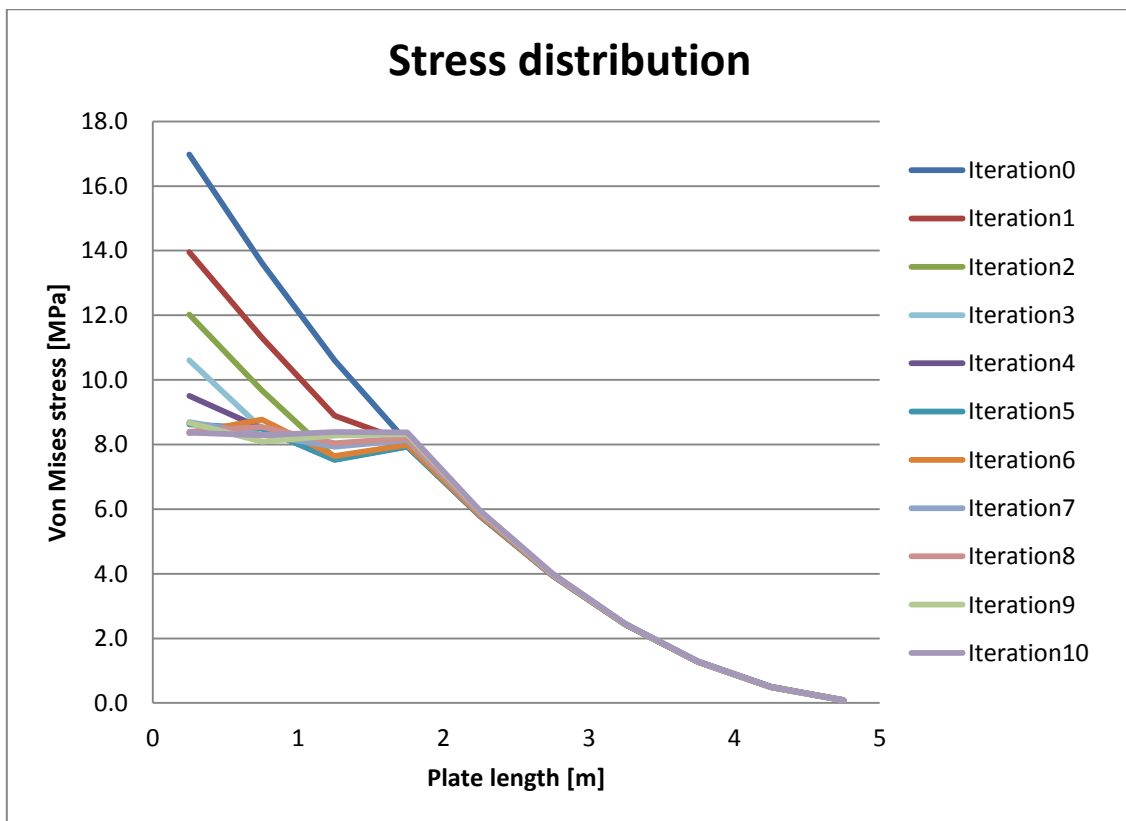


Figure 49. Stress distribution of a free edge of the plate in every iteration

It can be noted that the elements further than 2 meters away from the clamp present a stress lower than 8.5MPa even in the first iteration, consequently their cross section hasn't been modified. As far as the elements in the first 2 meters are concerned, a gradual reduction of the stresses is visible which leads to an almost equal stress distribution of 8.5Mpa in the converged result.

5.6 Fitness function

As output of the scripted component-design tool, a report with useful information for the user regarding the structural analysis is produced. Furthermore, single values representing the performance of the structure are available. These values concern the total weight and the mean stress of the structure and can be used as fitness value-input for the optimisation algorithm, since this is used to define the relative importance of a design. Possible fitness values are among others the total weight, the weight per unit area and the mean VM stress of the structure.

Every structure that is analysed should comply with specific design limits-constraints. If a structure violates these limits is considered as unfeasible. In order to prevent the optimisation algorithm from concluding in an unfeasible design, a common practice is to use penalty functions that manipulate the fitness value in proportion to the degree of constraint violation (Yeniay, 2005). A possible fitness function is:

$$\text{fitness} = \text{fitness value} + \text{penalty} \quad (5.12)$$

Since the stress in the structure is restrained in the acceptable limits due to the thickness distribution algorithm, there is no need for a penalty regarding excess of stress. The maximum deflection of the structure in the Serviceability Limit State as well as the critical buckling load factor in the Ultimate Limit State, are two possible restrains that can be introduced in the analysis as penalties.

The value of the penalty used in the fitness function is a user input and should be defined according to the choice of fitness value in order to make sure that the unfeasible structure will be considered as not adequate from the optimisation algorithm.

5.7 Optimisation algorithm

The geometry of the roof structure is iterated from the external optimisation loop so that the optimum solution can be discovered. For this loop a genetic algorithm has been decided to be used. The background behind genetic algorithms has been presented in Chapter 1. There are available Grasshopper plug-ins that include evolutionary algorithms and can be used in collaboration with the design tool such as Galapagos, Goat and Octopus. The user can decide which algorithm is adequate for each optimisation problem based on the number of objectives to be fulfilled or the necessity of finding a global or a local optimum.

In this research, Galapagos evolutionary solver has been deemed adequate to be used for the main optimisation algorithm. The external input required from the solver is the genes that form the genome and the fitness value. The possible assigned genes are floating point numbers that can accept all the values between two numerical boundaries (Galapagos, 2015).

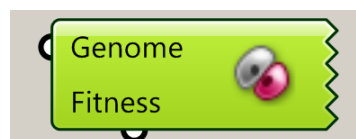


Figure 50. Galapagos component and the required input for the optimisation

In the Galapagos editor some further information from the user is necessary before the algorithm is executed. Firstly whether the fitness value should be minimised or maximised has to be defined. The number of designs that form a population as well as the multiplication factor of this number for the first population. Furthermore, the percentage of designs of a population that can be transferred in the next generation should be decided as well as the inbreeding percentage. The value of -100% is used for fully zoo-philic and the value of 100% for fully incestuous (Galapagos, 2015).

The algorithm terminates when the maximum assigned duration defined from the user is reached or when the number of consecutive generations without finding an improved solution exceeds the maximum stagnant limit.

The image shows a software dialog box titled 'Generic' and 'Evolutionary Solver'. The 'Generic' section includes a 'Fitness' dropdown set to 'Minimize', an empty 'Threshold' field, a 'Runtime Limit' checkbox that is unchecked, and a 'Max. Duration' field set to '3:0' (3 hours, 0 minutes). The 'Evolutionary Solver' section includes 'Max. Stagnant' (0:0:0:5:0), 'Population' (0:0:0:3:0), 'Initial Boost' (0:0:0:0:2), 'Maintain' (0:0:5 %), and 'Inbreeding' (+0:7:5 %).

| Parameter | Value | Unit/Label |
|---------------|---------------------------------|-----------------|
| Fitness | Minimize | |
| Threshold | | |
| Runtime Limit | <input type="checkbox"/> Enable | |
| Max. Duration | 3:0 | Hours / Minutes |
| Max. Stagnant | 0:0:0:5:0 | |
| Population | 0:0:0:3:0 | |
| Initial Boost | 0:0:0:0:2 | x |
| Maintain | 0:0:5 | % |
| Inbreeding | +0:7:5 | % |

Figure 51. Input used for the Galapagos evolutionary algorithm

The user input values for the Galapagos optimisation algorithm chosen in this research are presented in Figure 51. It has to be noted, that most of the values are the ones proposed from the developer of Galapagos.

As in every algorithm, Genetic algorithms present also drawbacks (Arora, 2012). In order to converge to a solution the algorithm requires a large amount of calculation even for reasonably sized problems. Furthermore, there is no guarantee that the converged design is the global optimum.

In order to overcome these drawbacks the computation power of many parallel computers can be used so that the computation time is reduced. As far as the optimum design is concerned, each problem can be set to run more than one times and the algorithm should be able to run for long time (Arora, 2012).

Consequently, it is not recommended to assign a maximum time limit for the algorithm when used in combination with the design tool. The maximum stagnant limit will define the termination of the algorithm.

Another option available is to use Goat. In this tool there are different algorithms integrated, either global optimisation algorithms or local. It is advised from the developer, to firstly use a global optimisation algorithm for a certain time and when this time is exceeded or the user considers a specific solution as good starting point, then to use a local optimisation algorithm starting from this solution in order to arrive to a local optimum, which might be at the same time the global optimum.

In this research, a local optimisation algorithm available in Goat plug-in has been used after the termination of Galapagos algorithm in order to control the optimality of the concluded Galapagos structure. It has been observed that no better solution could be detected from the local optimisation algorithm, which indicates that Galapagos is able to reach an optimum solution. Of course, there is no guarantee that this solution is the global optimum, but since the run time is not being restricted, the Galapagos result can be considered as the best possible.

5.8 Visualisation of the results

An important role in the usability of a design tool plays the visualisation of the results. The output of the design tool is a report with useful information regarding the structural analysis, as well as single values representing the performance of the structure. In order to improve the usability, visualisation of the material distribution on the structure and the computed Von Mises stresses is performed.

The material distribution is achieved by assigning adequate cross section to every mesh element. Each cross section has assigned a specific colour consequently all the elements that require the same cross section have the same colour as presented in Figure 52.

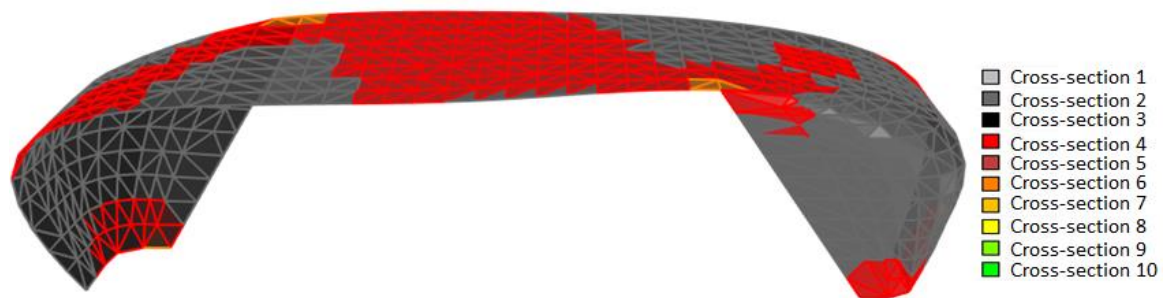


Figure 52. Material distribution visualisation

A better understanding of the structural performance of the free form structure can be achieved by visualising the Von Mises stress distribution on the structure. This is taking place by dividing the stress range in the desired by the user number of parts and by grouping all the mesh elements that show similar Von Mises stress. In Figure 53 the result of the VM stress visualisation is shown.



Figure 53. Von Mises stress visualisation

6. Case study

In Chapter 5 the strategy presented in Chapter 3 has been followed in order to develop the design tool. Already in this chapter became obvious that the tool has been designed according to the requirements of the vertical foyer of the Post Rotterdam case study, but it is oriented to be able to be used for the analysis of other similar structures. The fact that the shape of the cross section is introduced as a user input stiffness matrix, gives the option to analyse different cross section shapes and materials without the need of extensive manipulation of the tool. Consequently, the design process presented in the previous chapters is considered to be the base tool that is applicable to more than one case.

After the completion of the base tool, an implementation in the already mentioned case study has been performed. Some special requirements of the case study have been taken into account and modification of the base tool was deemed necessary.

6.1 User input required for the case study analysis

Every structure that will be attempted to be analysed with the help of the tool will have different requirements in terms of load values, material properties, boundary conditions. Consequently, these values should be user inputs of the tool in order to accommodate the analysis of various structures.

6.1.1 Material properties

The desire of the architect for the finishing of the vertical foyer is steel polished. Consequently, the structure has been decided to be constructed out of steel. The steel grade chosen is S355 with yield strength $f_y=355\text{N/mm}^2$ for a nominal thickness lower or equal to 40mm. The properties of steel required as an input for the analysis are presented in Table 4.

| | | | |
|------------------------------|-------|------------------|-----------------|
| Modulus of elasticity | E | $210 \cdot 10^9$ | N/m^2 |
| Shear modulus | G | $81 \cdot 10^9$ | N/m^2 |
| Poisson's ratio | ν | 0.3 | - |
| Density | d | 7850 | Kg/m^3 |

Table 4. Steel properties based on Eurocode 3 (EN 1993-1-1, Design of steel structures)

6.1.2 Boundary conditions

The roof structure is designed as a special entrance of the Post Rotterdam building. Consequently, it will be placed very close to the existing monumental building. This gives the option of transferring a part of the loads of the roof structure to the Post Rotterdam. The connections between the new roof structure and the existing building are considered to be expensive and should be avoided where possible. As a result, it has been decided to analyse the vertical foyer as a self-standing structure and not model connections with the existing building.

The boundary conditions of the model are applied to the basis of the roof structure. The existence of a basement underneath the structure as well as a concrete floor at the ground level indicates that clamp boundary condition is a good approximation of the real situation. Consequently, displacement in x, y, z direction as well as rotation about x, y, z axis are constrained.

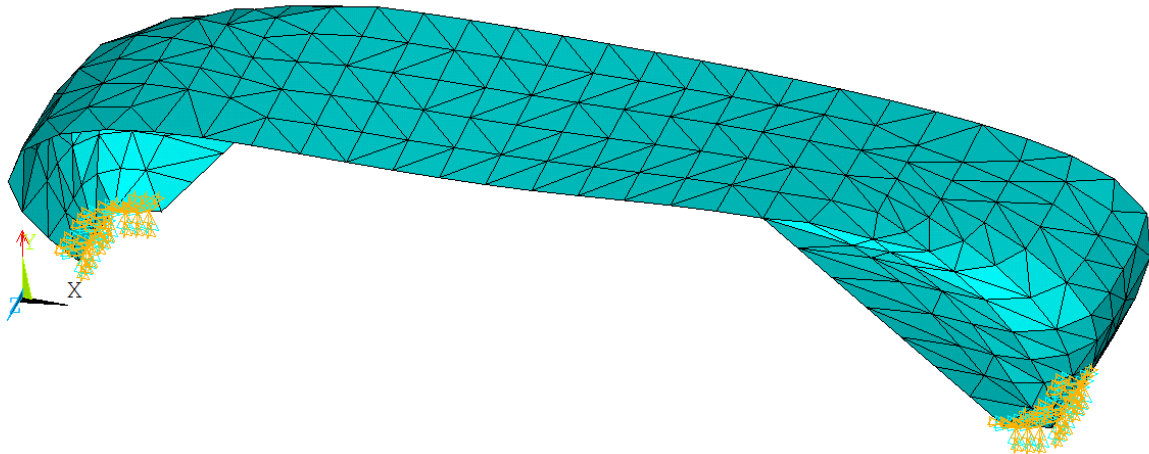


Figure 54. Applied boundary conditions to the model

6.1.3 Loads

The loads that will be taken into account for this analysis is the self-weight of the structure, dead load due to the ceiling, installations and pipelines, snow load and wind load. Because of the steel polishing, a temperature load is also applied on the structure, but this load is ignored in this analysis. The values of the considered loads as well as the way of application to the structure are shown in Table 5 and in Figure 55. The negative sign of loads is used to show that the direction of the loads is opposite to the positive axis orientation.

| Load type | Value [kN/m ²] | Area of application [m ²] | Orientation [-] |
|------------------------|-------------------------------|--|--------------------|
| Self-weight | calculated in Ansys | total area | global - y |
| Dead | -0.5 | total area | global - y |
| Snow | -1.68 | projected area | global - y |
| Wind left side | 0.56 | projected area | global - x |
| Wind right side | 0.24 | projected area | global - x |
| Wind up side | 0.008 | total area | global - x |

Table 5. Loads applied to the structure and way of application

The calculation of the loads as well as the load combinations that will be used for the static analysis of this structure are presented in detail in Appendix 1 - Loading.

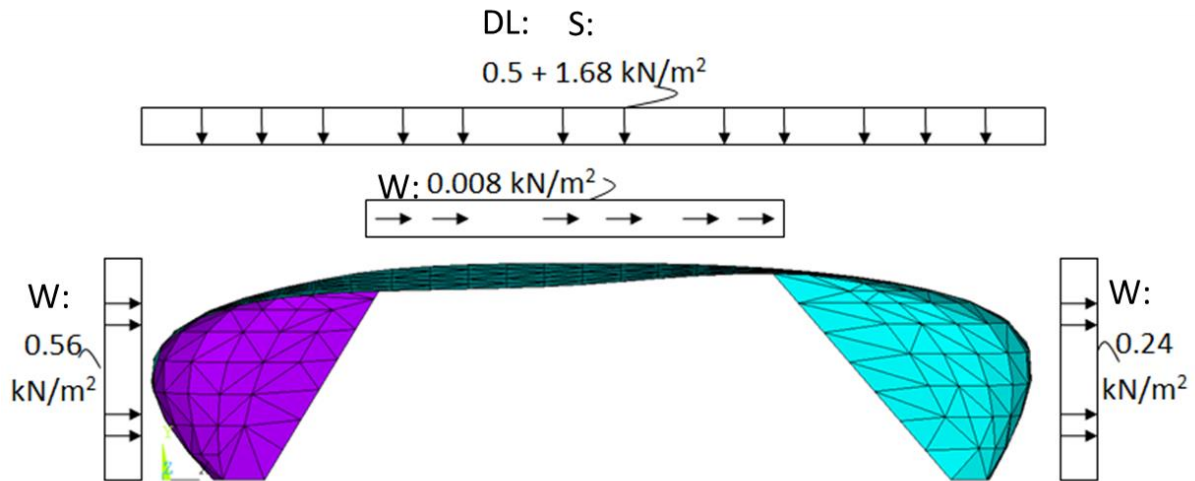


Figure 55. Loads that are applied on the structure

6.1.4 Cross section list

The list of cross sections through which the tool can iterate is an important user input. The information required for each cross section is the height difference between the two plates, the estimated density of the ribs and stiffeners and the thickness of the plates. It has been assumed that the thickness of the ribs and stiffeners is half the thickness of the plates; consequently it is not a user input.

In order to create the list of cross sections for the analysis of the case study, a minimum plate thickness of 8mm has been decided. Furthermore, the height difference between the plates defines the assembly method. If adequate space is available, the welding of the upper plate can be performed from the inside, as it is visible in Figure 30. If the distance is small, the welding has to be performed from the outside of the cross section, which is a more expensive assembly method. It has to be taken into account, also, the fact that higher height difference will lead to additional weight due to the higher dimensions of the ribs.

The cross section list that has been used for the analysis of the Vertical Foyer is presented in Table 6.

| Cross section number | | 1 | 2 | 3 | 4 | 5 | 6 | 7 | 8 | 9 | 10 | 11 |
|----------------------|-----|-------|-------|------|------|-------|-------|-------|-------|-------|-------|-------|
| Height difference | [m] | 0.2 | 0.3 | 0.4 | 0.5 | 0.6 | 0.7 | 0.8 | 0.9 | 1.0 | 1.1 | 1.2 |
| Rib density | [m] | 1.0 | 1.0 | 1.0 | 1.0 | 1.0 | 1.0 | 1.0 | 1.0 | 1.0 | 1.0 | 1.0 |
| Plate thickness | [m] | 0.008 | 0.008 | 0.01 | 0.01 | 0.012 | 0.012 | 0.015 | 0.015 | 0.020 | 0.020 | 0.020 |

Table 6. Cross section list of the analysis of the Vertical Foyer

6.1.5 Mesh density

A user input is not only the choice of the component for creating the mesh of the surface, but also the target mesh size. The irregular shape of the vertical foyer will not let the meshing algorithm achieve everywhere uniform mesh size, but a high percentage of the mesh elements will have a size close to the one set from the user. The smaller the mesh size the more accurate the results of the finite element analysis. On the other hand, the denser the mesh the more elements present for the analysis and consequently the more computing time required. A range of different mesh sizes has been tested. The convergence of the deflection and the stress has been taken into account as well as the computing time in order to decide which mesh density will be chosen for the analysis of the case study. The deflection checked is the maximum deflection present in the structure, whereas the Von Mises stress, has been checked at the element in the connection between the roof and the triangular cover as presented in Figure 56 (red mesh element).

| Mesh resolution | N° of elements | Max deflection | Difference | Stress | Difference | Elapsed time |
|-----------------|----------------|----------------|------------|--------|------------|--------------|
| [m] | [-] | [m] | [-] | [MPa] | [-] | [sec] |
| 3 | 379 | 0.258 | 1.9% | 149.2 | 20% | 7 |
| 2.5 | 569 | 0.263 | 1.5% | 185.7 | 9% | 9 |
| 2 | 932 | 0.267 | 0.0% | 203.4 | 5% | 13 |
| 1.5 | 1676 | 0.267 | 0.7% | 214.4 | 2% | 17 |
| 1 | 3751 | 0.269 | - | 219.0 | - | 28 |

Table 7. Deflection and stress convergence when the mesh density changes compared to the elapsed time

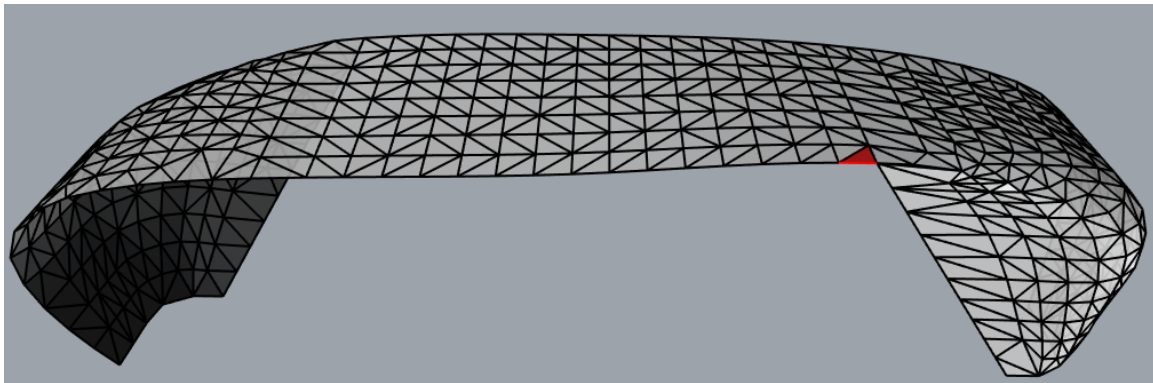


Figure 56. Element checked for stress convergence

It has to be noted that the denser the mesh the smoother the shape of the structure as can be seen in Figure 57. Furthermore, since the shape is transferred to the FE software through the mesh generated in Grasshopper, the area of the surface is not fixed. Consequently, the loads applied on the structure vary slightly, as they depend on the area of the surface. As can become obvious, perfect convergence is difficult to be achieved since the mesh density is not the only variable of the analysis. It has been considered adequate target mesh size to be 2m. With this mesh size, a balance between the accuracy of the results and the computing time is achieved.

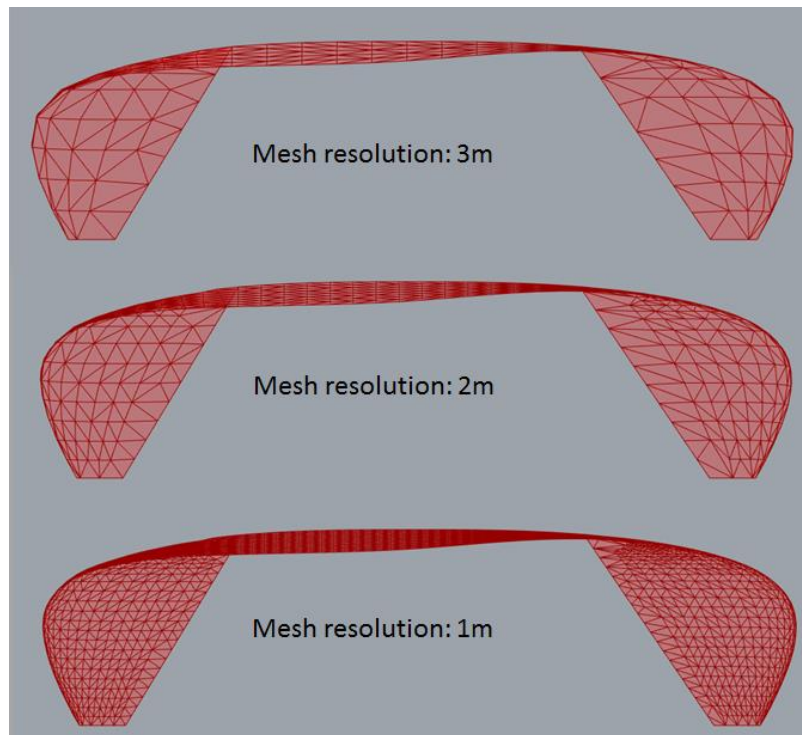


Figure 57. Shape of the structure based on the mesh density

6.1.6 Limits

In order to ensure the stability of the structure, certain design limits have to be set. Firstly, no part of the structure should show a Von Mises stress higher than the yield strength of the material used. Furthermore, the structure should be prevented from buckling and the maximum deflection of the structure in the Serviceability limit state has to be limited.

As has been presented in Section 6.1.1 the material used is steel S355. Since the thickness of the plates in the cross section list is not higher than 40mm, then the yield strength limit of the steel to be used is 355MPa.

The buckling of the structure is prevented when the critical buckling load factor is higher than the knock down factor. In Section 5.4.3 has been analysed in which cases a knock down factor is necessary. The structure of the case study is not expected to present sensitivity to imperfections due to the fact that the difference between the values of the first and second critical BLFs is more than 2%, but since non-linear effects are not taken into account a knock down factor is deemed necessary. The critical buckling load factor has been chosen to be acceptable when it has a value higher than 6.

The maximum allowed deflection in the serviceability limit state for roof structures is calculated according to the Dutch code (NEN 6702: Loadings and deformations, TGB 1990) as:

$$w_3=0.004x_l \quad (6.1)$$

Where:

w_3 is the maximum allowed deflection and

l is the length of the roof structure.

In this case, the length is around 60m, consequently the allowed deflection is:

$$w_3 = 0.004 \times 60 = 0.24 \text{ m.}$$

The design limits for the analysis of the Vertical Foyer are summarized in Table 8.

| | Design limit | Units |
|----------------------|--------------|-------|
| Von Mises stress | 355 | MPa |
| Deflection | 0.24 | m |
| Buckling load factor | 6 | - |

Table 8. Values of the design limits for the case study

6.1.7 Penalties

When the limits presented in Table 8 are violated, penalties should be assigned to the fitness function as presented in Section 5.6.

The thickness distribution algorithm assures that all the elements of the surface structure will present a Von Mises stress lower than the design limit. As far as the deflection and the buckling load factor is concerned, a preliminary analysis presented in Chapter 6.2 has shown that instability due to buckling is not likely to be created in the case study design. On the other hand, the maximum accepted deflection in the structure is violated when slender cross sections are assigned. Consequently, it has been deemed more adequate to incorporate a method for minimising the deflection so that an unfeasible structure will not be likely to be analysed, than penalise every structure that deflects more than accepted. The method is elaborated in Section 6.2.2.

Consequently, a penalty is necessary to be used only in the case that a structure with buckling load factor smaller than the design limit is analysed in order to prevent the genetic algorithm from concluding to an unfeasible design. In this research, a constant value of penalty has been decided to be incorporated, since the designs are not expected to violate the design limits and consequently the penalisation in respect to the degree of the violation is considered unnecessary.

The penalty value has to be present in the output of the Grasshopper component, which includes the total weight of the structure and the mean Von Mises stress, since these values will be used as fitness values for the Galapagos optimisation. For the total weight of the structure a penalty of 1000000Kg has been implemented, whereas in the mean Von Mises stress an additional stress of 100MPa.

6.2 Additions to the base tool

The influence of the assigned cross section to the structural response of the vertical foyer has been explored. A list of possible cross sections has been chosen and each of them has been applied to the entire roof structure. The maximum deflection present, the maximum stress present as well as the critical buckling load factor of the structure has been computed and studied. The range of heights of

the cross sections analysed is from 0.20m till 0.60m and the flange thickness is 0.001 and 0.002 m for every cross section. The results of the analysis are presented in Figure 58 to Figure 60.

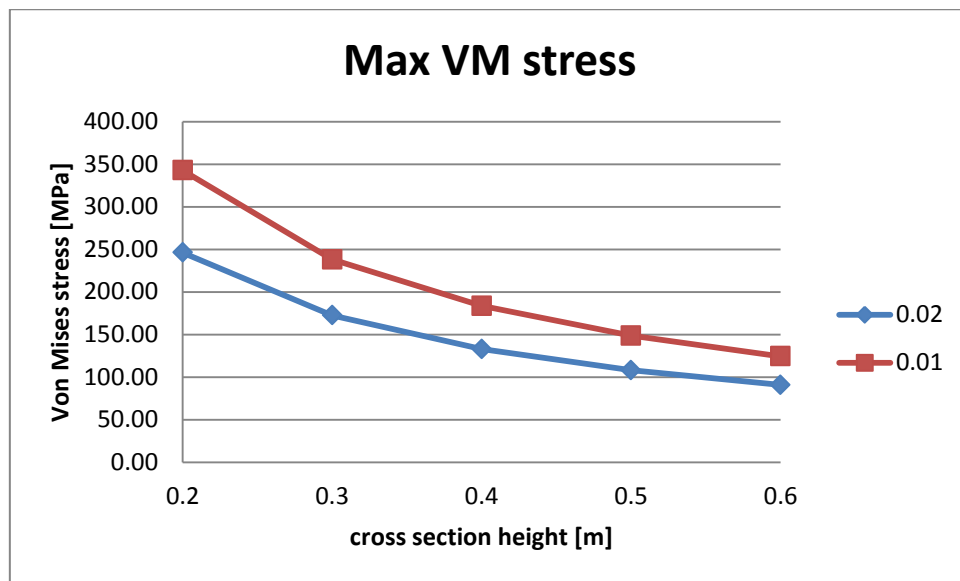


Figure 58. Maximum Von Mises stress present in the structure when a range of cross sections is assigned

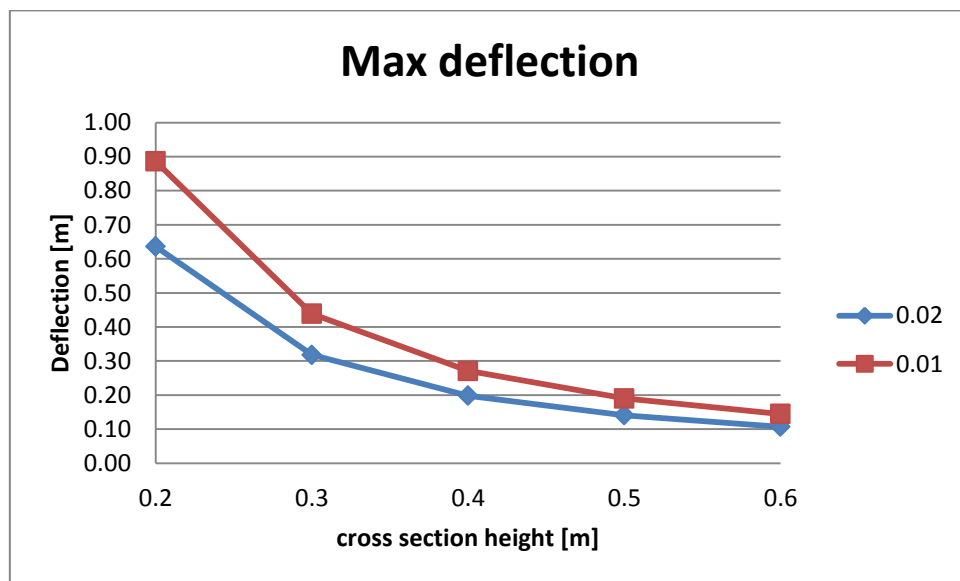


Figure 59. Maximum deflection present in the structure when a range of cross sections is assigned

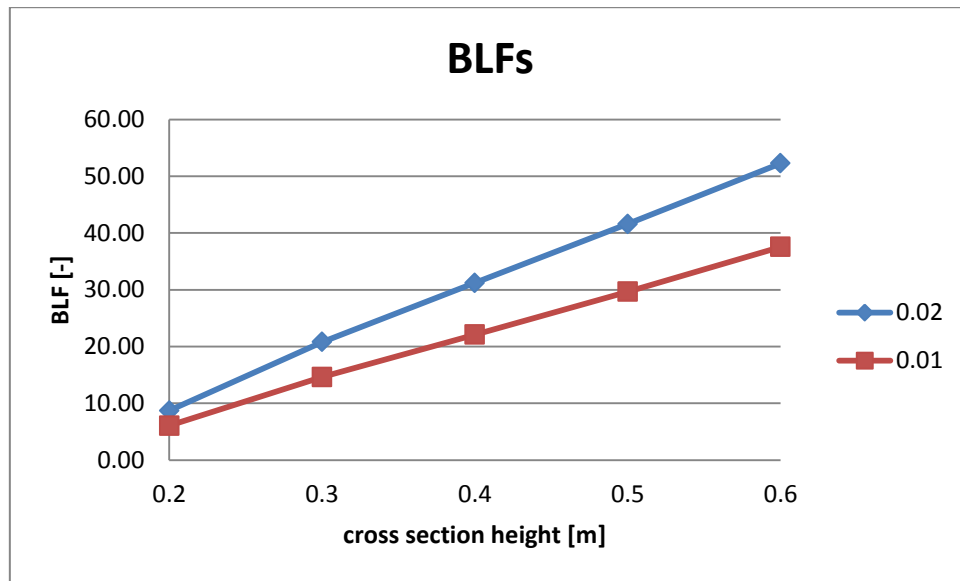


Figure 60. Critical Buckling Load Factor of the structure when a range of cross sections is assigned

It can be noted that the deflection is critical in this design. Even the smallest cross section assigned, doesn't show higher stress or smaller buckling load factor than the allowed.

In the figure of the deflection when different cross sections are assigned (Figure 59) can be seen that the smallest cross section that fulfills this requirement has 40cm height and 20mm flange thickness. In order not to limit the starting cross section of the cross section list, a loop has been decided to be included in the script, which assures that the deflection of the structure is not higher than the accepted value. In order to achieve that, this loop assigns iteratively more material on the structure until the deflection is limited to the maximum allowed. It has been noted that slenderer structures can be explored when this approach is being implemented.

6.2.1 Grouping

In the base tool every element of the finite element mesh is checked based on its stress. When an element is found to be overstressed, a higher cross section is assigned to it and a recalculation is performed. This approach might lead to big differences in the cross section of the adjacent elements. In theory this is a good approach because it will assign as less material as possible to the least number of elements. On the other hand, when a structure is to be constructed, a great variety of cross sections in one structure is not desirable. The cross sections assigned should be limited to a small number. Furthermore, the distribution of the different cross sections in the structure should follow certain logic. In order to achieve this goal, grouping of the elements is performed based on their stress. As a first step, the first cross section of the list of cross sections is assigned to the whole roof structure and the stresses are computed. The elements with similar stress are grouped together.

Two different approaches for the grouping of the elements have been explored. The first includes computing the range of VM stresses and dividing this to equal parts according to the number of groups chosen from the user. All the elements that have a value of VM stress between the boundaries of a stress range are grouped together as shown in Figure 61. When this approach is implemented, it can be noted that the lower stressed groups include significantly higher amount of

elements than the higher stressed groups. This is an indication of the fact that only small parts of the surface present high VM stresses. The highest stressed areas are located at the connection of the roof with the triangular like covers. Contact forces are introduced in these elements and stress concentrations are spotted.

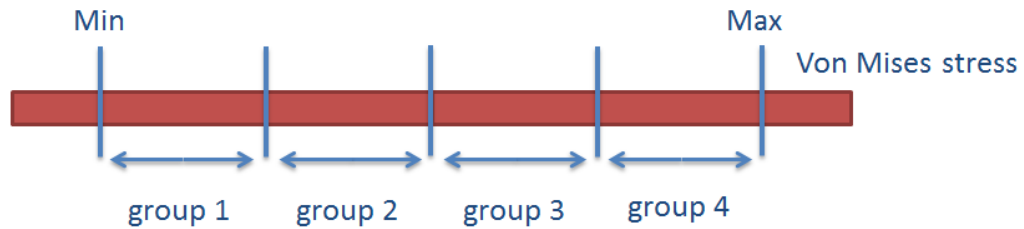


Figure 61. Grouping of the elements in equal stress ranges

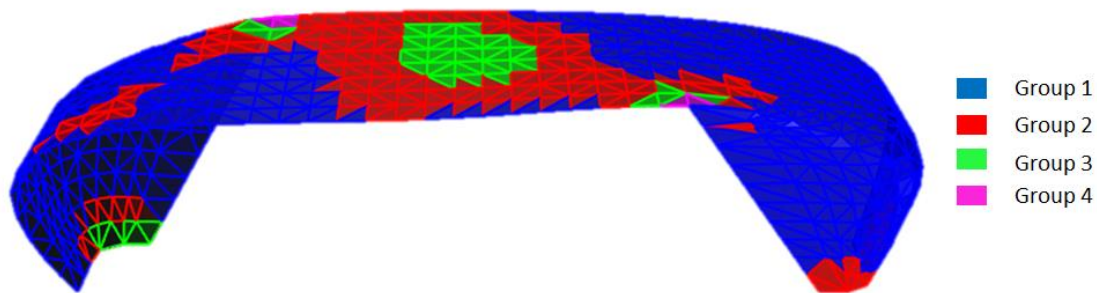


Figure 62. Visualization of the grouping in 4 equal stress ranges

A second approach that has been implemented and explored is to group the elements based on the mean VM stress of the structure. In this case the minimum, maximum and mean VM stresses of the structure are computed. The stress range between the minimum and mean VM stress is divided in equal parts as well as the stress range between the mean and maximum VM stress present in the structure. The total number of divisions is equal to the number of groups assigned from the user. The amount of elements present in most of the groups is of the same order of magnitude. The higher stressed group, though, contains a very small number of elements. Stress concentration due to the introduction of contact forces is possibly the reason for the significant excess of stress in these elements; consequently it is considered reasonable that not many elements exist in the higher stressed group.

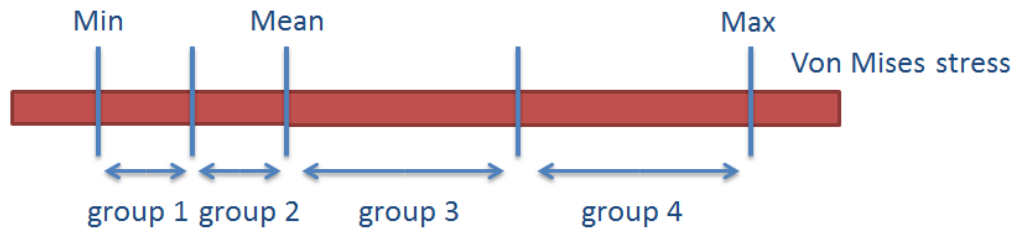


Figure 63. Grouping of the elements based on the mean stress of the structure

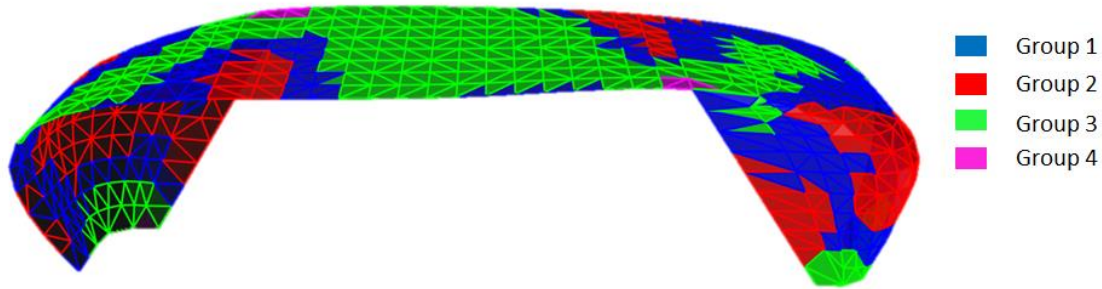


Figure 64. Visualization of the grouping based on the mean stress

Based on the visualization of the two approaches can be seen that in the first approach the least stressed group contains the higher amount of elements, whereas in the grouping based on the second approach the distribution of the elements in the groups is more even. When the two grouping approaches are implemented in the tool, differences are noted on the number of iterations necessary for concluding on the adequate cross section of each group as well as in the total amount of material assigned in the structure. The second grouping approach requires less iterations and material than the first grouping approach, consequently this is the one applied in the design tool.

6.2.2 Deflection loop

An additional loop has been decided to be implemented in the design tool that will be used for the analysis of the Post Rotterdam case study. The final workflow of the Python script as well as the required user input is presented in Figure 65. It becomes obvious that 2 loops are integrated in one process. Since the shape is further manipulated from an external loop, in the end 3 loops are necessary for the optimisation of the shape and the distribution of material of the Vertical Foyer.

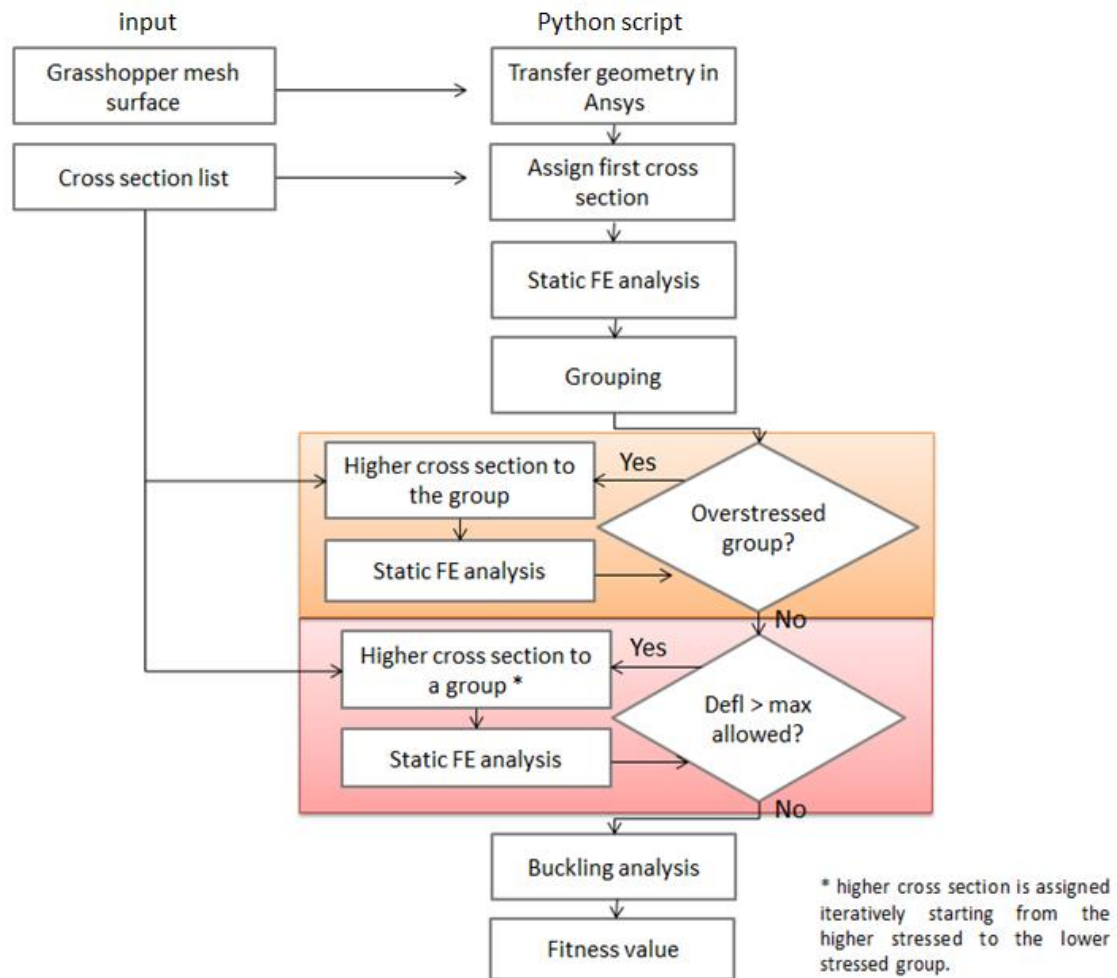


Figure 65. Workflow of the Python script and the required user input

In order to size the elements having as a target the restriction of the deflection, different methods can be applied, such as the one of Olsson (2012). He proposes a method based on virtual work for assigning material to elements depending on their contribution to stiffness in the critical for deflection degree of freedom. In this research, the stress based grouping that has already been performed will be also used for the loop designed for making sure that the analysed structure does not deflect more than the allowed.

The loop is assigning higher cross section iteratively starting from the higher stressed group to the lower stressed group. It has been noted that when the deflection of the structure concluded from the stress based loop is more than 20cm higher than the allowed deflection, the deflection loop is assigning higher cross section to all the groups and starts iterating again from the higher stressed group. In order to reduce the number of iterations of the deflection loop and consequently to reduce the computing time of the loop, an additional feature has been included in the tool. A higher cross section is assigned to all the groups when the difference in the deflection of the last analysed structure before the start of the deflection loop and the target deflection is higher than 20cm. If the target deflection is not achieved in this iteration, then higher cross section is assigned starting from the most stressed group to the least stressed group.

6.2.3 Validation of the functionality of the tool

In order to validate that the tool is accurately performing the tasks assigned to it, an analysis has been performed using the starting shape shown in Figure 27. In every iteration of the tool, the cross section of each group, the maximum Von Mises stress as well as the maximum deflection present in the structure are reported in Table 9.

| Iteration number | Stress loop | | | | Deflection loop | | |
|---------------------|-------------|-------|-------|-------|-----------------|-------|-------|
| | 1 | 2 | 3 | 4 | 5 | 6 | 7 |
| Group 1 | 1 | 1 | 1 | 1 | 2 | 2 | 2 |
| Group 2 | 1 | 1 | 1 | 1 | 2 | 2 | 2 |
| Group 3 | 1 | 1 | 1 | 2 | 3 | 3 | 4 |
| Group 4 | 1 | 2 | 3 | 4 | 5 | 6 | 6 |
| Max VM stress [Mpa] | 514 | 530 | 451 | 346 | 231 | 223 | 195 |
| Max deflection [m] | 1.002 | 0.929 | 0.853 | 0.524 | 0.289 | 0.281 | 0.221 |

Table 9. Control of the functionality of the scripted Python component

It can be observed that the stress loop terminates when the maximum Von Mises stress present in the structure is lower than the yield strength (355MPa). Furthermore, the deflection of the structure in the last iteration of the stress based material distribution loop is 0.524m which is more than 20cm higher than the acceptable deflection limit ($0.24+0.20=0.44\text{m}$). Consequently, in the first iteration of the deflection loop higher cross section is assigned to all the groups. The deflection loop, finally, stops when the maximum deflection of the structure is smaller than the maximum acceptable (0.24m). It has to be noted that the maximum Von Mises stress present in the structure after the execution of both loops is significantly smaller than the limit of 355MPa, which validates the choice not to include a safety factor in the yield strength limit.

As a consequence, it can be validated that the Python script has the functionality that is required for the analysis of the case study roof structure.

6.3 Validation of the analysis

In order to validate that the finite element analysis is producing accurate results, a comparison between the deflection of the analysed model and hand calculations will be performed. The forces computed in the finite element software depend on the stiffness of the structure and the deflection of the structure. In a linear structure this relation takes the form:

$$[F]=[K]*[u] \quad (6.2)$$

Where $[F]$ is the matrix of the forces

$[K]$ is the stiffness matrix and

$[u]$ is the displacement matrix

The stiffness matrix is a user input and the validation of the one used in this analysis has been performed in Section 5.4.2. Consequently, if the accuracy of the computed deflection of the FE software can be validated, it is an indication that also the computed element forces will be accurate.

The shape of the vertical foyer can be approximated as a double clamped beam, the deflection of which can be calculated analytically as has already been shown in Figure 39. The clamps in the structure can be estimated to be located at the triangular covers. Consequently, the length to be taken into account in the equation is the length of the diagonal that connects the 2 triangular covers. The analysis in Ansys has been performed assigning to the whole structure the 4th cross section of the cross section list (Table 6) being loaded only by the self-weight. The contour of the deformed shape calculated in Ansys is visible in Figure 66.

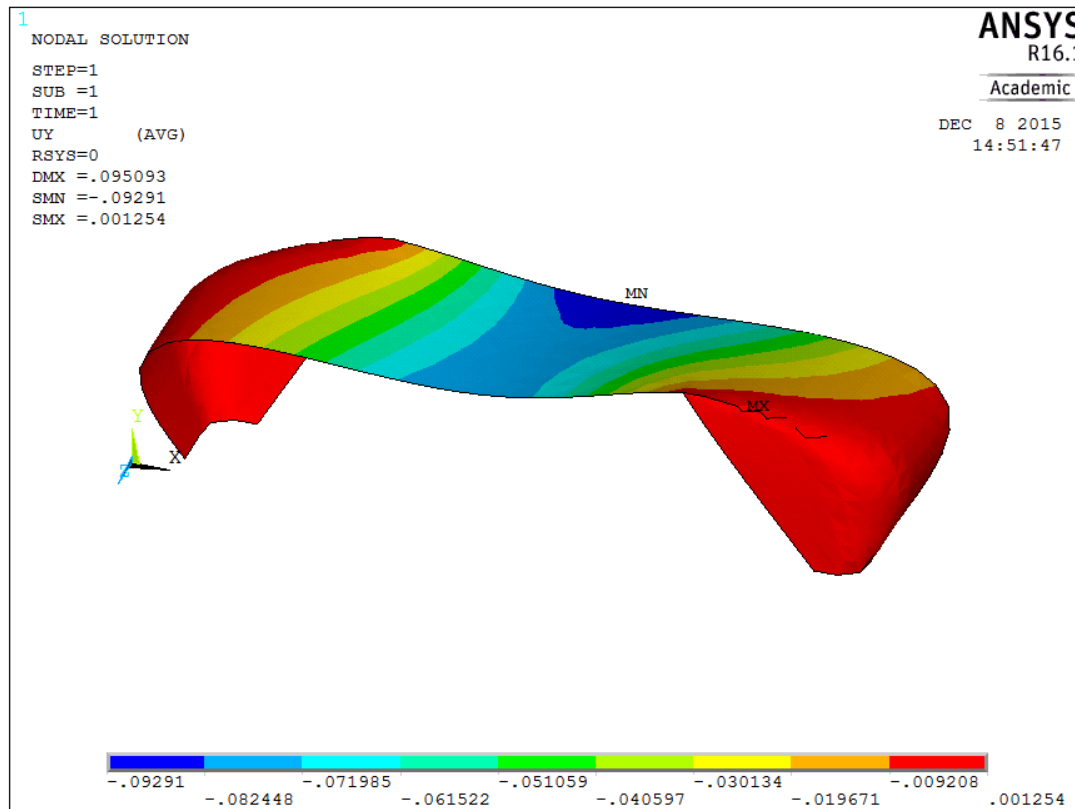


Figure 66. Vertical deflection of the roof structure under self-weight

The input of the equation presented in Figure 39 for the analytical calculation of the deflection is visible in Table 10 and the comparison between the computed deflections of the two methods in Table 11.

| | | | |
|------------------------------|---|----------|------------------|
| distributed load | q | 1925 | N/m |
| length of the beam | l | 47.43 | m |
| modulus of elasticity | E | 2.1E+11 | N/m ² |
| moment of inertia | I | 1.25E-03 | m ⁴ |

Table 10. Input of the formula to compute the deflection of a double clamped beam (Figure 39)

| | analytical solution | FE solution | difference |
|--------------------------------|----------------------------|--------------------|-------------------|
| maximum deflection [mm] | 96.6 | 92.9 | 4% |

Table 11. Comparison between the results of the analytical and the FE analysis

It can be noted that the difference between the two methods is small, consequently the accuracy of the results computed in Ansys is validated.

6.4 Analyses and results

Having implemented in the design tool all relevant users' input presented in paragraph 6.1, the optimisation analysis of the vertical foyer of the Post Rotterdam case study can be performed. Every analysis is initiated with the same starting structure which is assumed to be the geometry closer to the original design of the architectural firm UNStudio and is shown in Figure 67. The design space that the tool can search is defined from the variables that will be selected to be the genomes of the genetic algorithm. For this analysis 13 variables have been selected. The variables as well as the range of values that each variable can assume are presented in Figure 68.

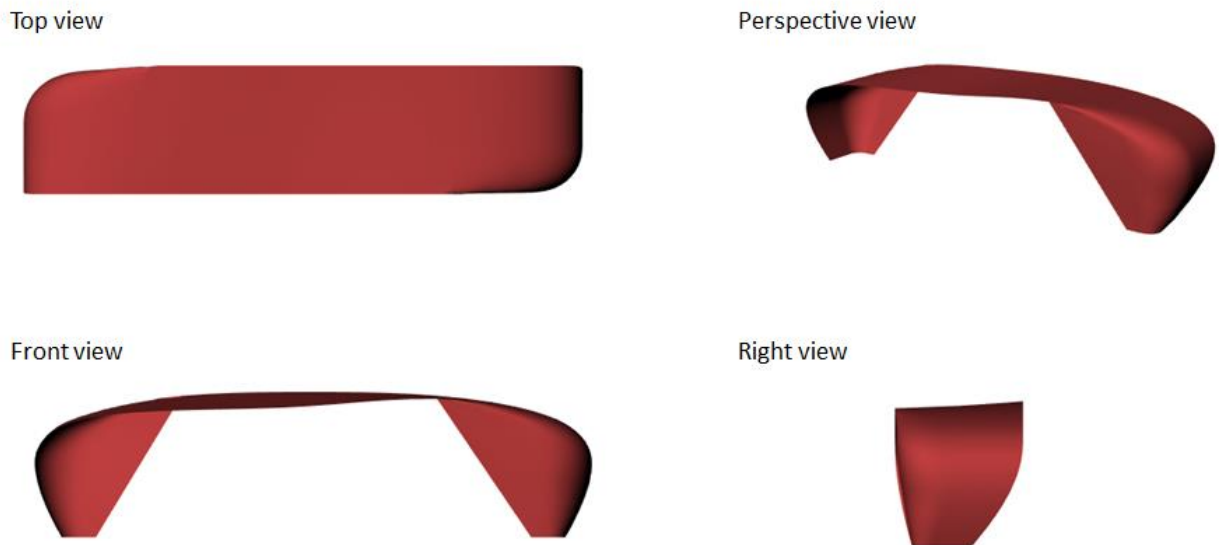


Figure 67. Geometry of the starting structure

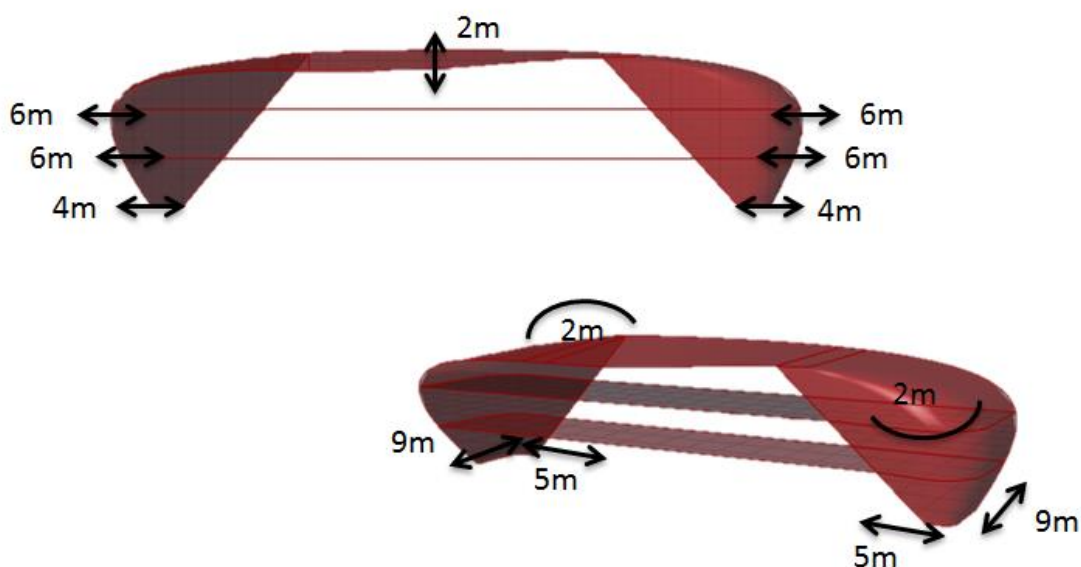


Figure 68. Value ranges of the variables of the parametric model

It has been deemed important to optimize the roof structure based on the amount of material necessary for its construction, the material per unit area and the mean Von Mises stress of the structure. The results of these analyses will be presented in this section. The detailed analysis as well as the geometrical characteristics of the optimum shapes can be found in Appendix 5 – Analyses results.

6.4.1 Analysis No 1

The first analysis to be performed has as fitness value the total weight of the structure. When the amount of material is being reduced, the cost of the structure reduces as well. The geometry of the structure that the algorithm concludes that can be constructed with the least possible material is shown in Figure 69.

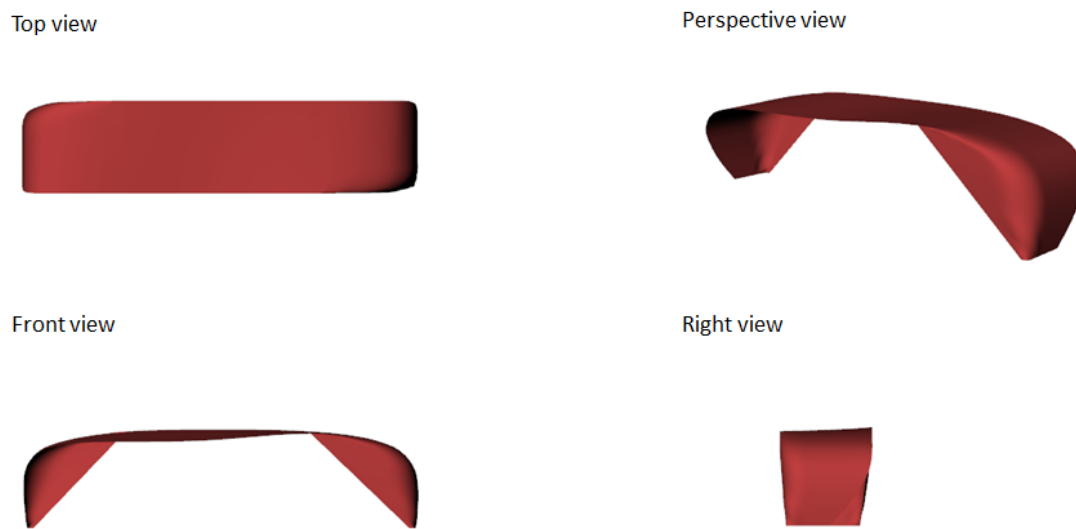


Figure 69. Geometry that presents the least total weight

It can be noted that the genetic algorithm is reducing the material usage mainly by reducing the area of the surface to be constructed. Consequently, not a lot of information can be retrieved regarding the structural performance of the shape under the assumed loading.

6.4.2 Analysis No 2

A better evaluation of the structural performance of the geometry of the roof structure can be achieved when the weight per unit area is set as a fitness value. For computing this value, the total weight of the structure which is an output of the design tool is divided by the total mesh area calculated in Grasshopper. The shape that requires the least weight per unit area is presented in Figure 70.

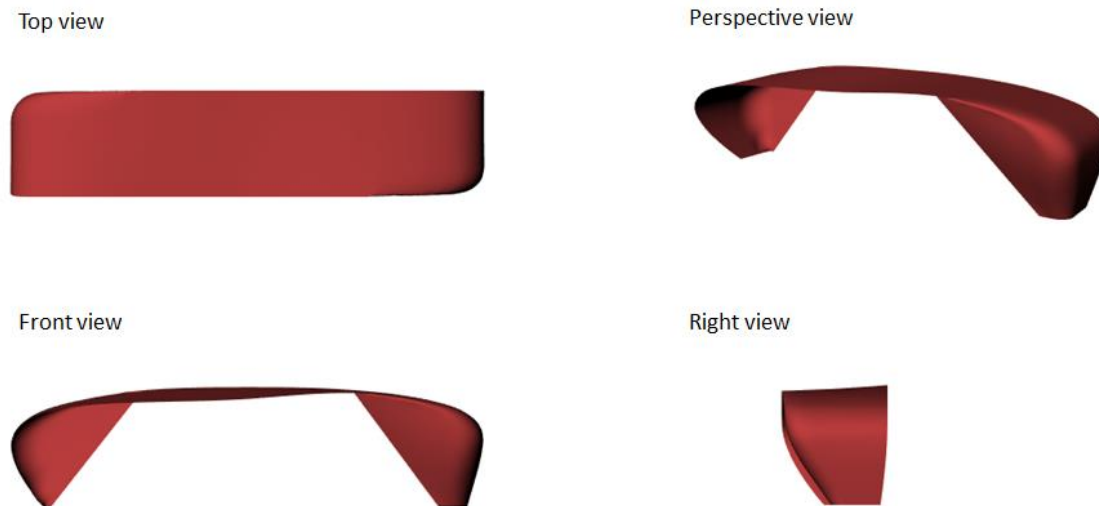


Figure 70. Geometry that presents the least weight per unit area

The geometry concluded from the genetic algorithm presents different characteristics in the left and right part. The differences include the length of the base, the inclination of the triangular cover relatively to the ground and the curvature of the roof side. The existence of the different characteristics is considered logical due to the non-symmetric structure in combination with the non-symmetric loading due to wind. The geometry under consideration requires small cross sections in order to be constructed. The biggest part of the structure can be constructed with the first cross section of Table 6 whereas the 3rd and 4th groups require cross sections number 4 and 6 respectively. The goal that is achieved with this shape is that the geometry presents the highest mesh area that can be constructed with the least amount of material.

It can be noted that the triangular covering of the left side is almost perpendicular to the ground. That way, a smaller area of the triangular cover is projected and is loaded from the wind. On the other hand, the front free edge is inclined which is not favorable for transferring the vertical loads to the foundation-base. From the analysis of this design, becomes obvious that minimizing the load introduced in the structure is relatively more important than the way the loads are transferred to the foundation.

Since the wind is blowing from left to right in the analysis, a tendency of more material in the right part of the structure is noted in order to resist the horizontal loads. Furthermore, the way of transferring the loads to the foundation seems more important in this side than the minimization of the projected area. Possibly, this has to do also with the reduced load value of the wind in this side.

6.4.3 Analysis No 3

The mean Von Mises stress represents that a big part of the structure has a VM stress similar to the mean one. It would be beneficial to have a structure with as low mean VM stress value as possible. That way, a lower steel grade could be used for a big part of the structure, which leads to less cost. The structural system of the vertical foyer is composed out of several parts welded together as presented in Section 5.3. When low stress is present in the connections, they can be welded more economically. The geometry that has been concluded from the tool to be lower stressed is visible in Figure 71.

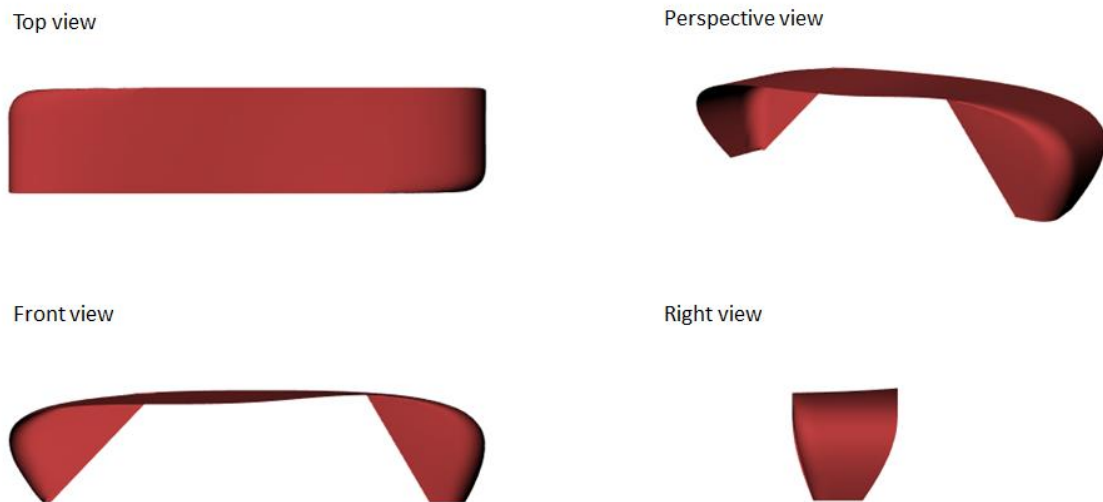


Figure 71. Geometry that presents the least mean VM stress

In the output report of the tool available in Appendix 5 – Analyses results, can be seen that higher cross sections are assigned to the groups compared to other structures analysed. Due to high local stresses and relatively high deflection in the starting structure, the algorithm that is responsible for fulfilling the stress and deflection constraints, assigns higher cross section even to the elements which are not presenting high VM stress reducing it even further. Consequently, the mean VM stress of the structure when the tool stops iterating is low. On the other hand, this does not mean that the shape of the concluded geometry is responsible for the minimization of the stress. If this would be the goal of the optimisation process, then the mean VM stress had to be computed and compared in the first analysis where a uniform cross section is assigned in the entire structure.

6.4.4 Comparison between analyses

The values of the results of the analysis as well as the optimized geometry according to each specific goal are presented in Table 12. A detailed elaboration on the differences between the various geometries is available in Appendix 5 – Analyses results. The reduction in percentage between the performance of the starting structure and the optimized one after the use of the design tool can be seen in Table 13.





| Analysis | Geometry | Weight [Kg] | Weight/area [Kg/m ²] | Mean VM stress [MPa] |
|----------------------|---|----------------|-------------------------------------|----------------------------|
| Starting shape |  | 250860 | 165 | 54.2 |
| Total weight |  | 229275 | 164 | 62.2 |
| Weight per unit area |  | 251037 | 159 | 58.4 |
| Mean VM stress |  | 288857 | 182 | 48.3 |

Table 12. Geometry and performance results of the design tool analyses

| | Total weight | Weight per unit area | Mean stress |
|-----------------|--------------|----------------------|-------------|
| | [Kg] | [Kg/m ²] | [MPa] |
| Starting value | 250860 | 165 | 54.2 |
| Optimised value | 229275 | 159 | 48.3 |
| Reduction | -9% | -4% | -12% |

Table 13. Reduction achieved in each goal from the implementation of the design tool

It can be observed that even small differences in the geometry lead to significant differences in the computed by the tool performance of the structure.

6.4.5 Analysis No 4

The usability of the tool can be further extended. When a structure is concluded from the tool that is not satisfactory for the user, then the boundaries of the design variables can be iterated in order to make it impossible for the previously optimized structure to be analyzed again. Further design constraints can be also placed through the design variables. Such an analysis has been performed, having as a fitness value the weight per unit area of the structure. The iterations to the design variables include:

- A variation in the possible height range. Instead of 14-16m the new range is 15-17m.
- The curvature of the upper part of the roof sides is now controlled by 2 sliders instead of 4 that allow only symmetrical variation in the two sides and
- The inclination of the triangular covers relative to the floor is constrained to be equal in both covers.

The optimum concluded shape of this analysis is presented in Figure 72.

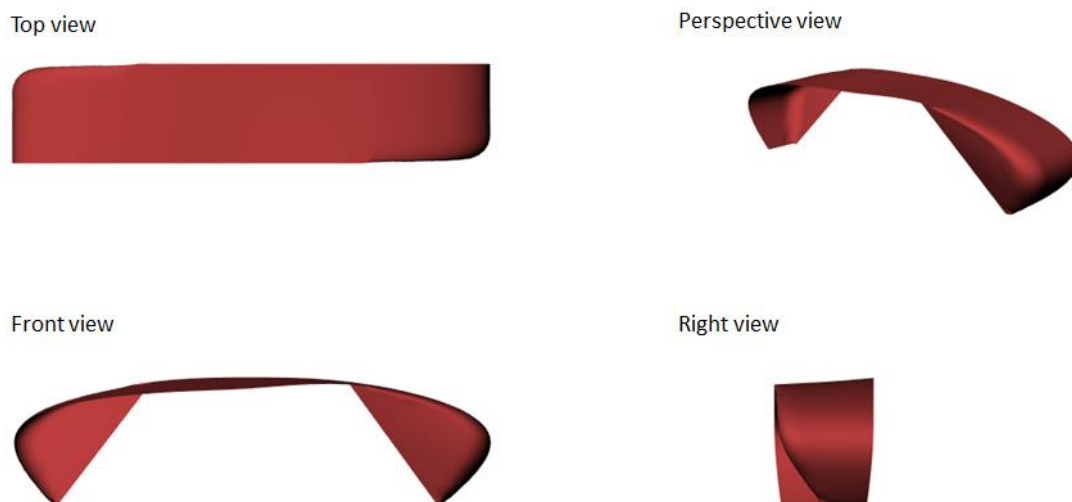


Figure 72. Geometry that presents the least weight per unit area when new constraints apply

When comparing the output of the 2nd and 4th analysis can be noted that with the new constraints implemented, a further reduction of the weight per unit area could be achieved. The weight per unit area of the optimized geometry of the 2nd analysis is 159 Kg/m² as presented in Table 12, whereas the geometry after the iteration of the constraints shows a further reduction of 2 Kg/m².

Based on the results of the presented analyses, can be seen that by iterating the fitness value or the set-up of the optimisation problem the optimized geometry of the structure changes. Even though the differences are small and is in most cases difficult to be spotted if the geometries under comparison are not overlaid on each other, only one of them has to be chosen in order to be further analyzed and constructed. This choice will be made by the architect in collaboration with the structural engineer.

6.4.6 Translating the FE model to a structure

The output of the design tool is a meshed surface where every mesh element has a specific cross section assigned to it. Consequently, adjacent elements exist with different cross sections assigned to them. If the structure would be realized following exactly the mesh model, a non-smooth surface would have to be constructed as presented in Figure 73. This way of construction would create difficulties in its realization and is also not aesthetically desirable. A smooth transition between the adjacent mesh elements that present different cross sections should be applied.

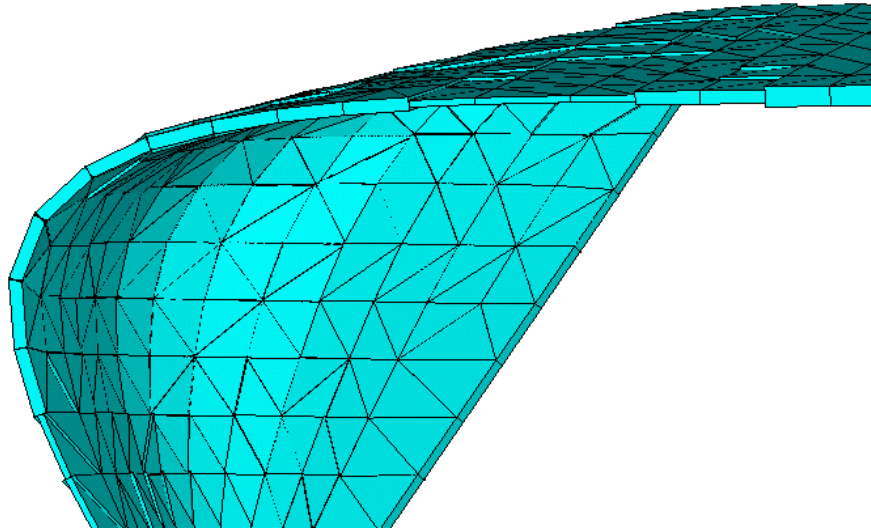


Figure 73. Realization of the structure following exactly the meshed surface model

The analysis has been conducted assuming that the surface under consideration represents a “surface of symmetry” of the real structure. Consequently, the 2 plates should be placed in equal distances from the analyzed surface. As a result, if adjacent elements present a height difference of 20cm, the upper plate should be placed 10cm higher and the bottom plate 10cm lower. It can become obvious that the visible outer shell of the structure will no longer present exactly the geometry of the analyzed surface, since small “hills” will be visible in the areas where bigger cross sections are required (Figure 74). In order to avoid this disturbance of smoothness, there is the possibility to lower only the inner shell surface which will most probably be covered from a layer for the accommodation of the installations.

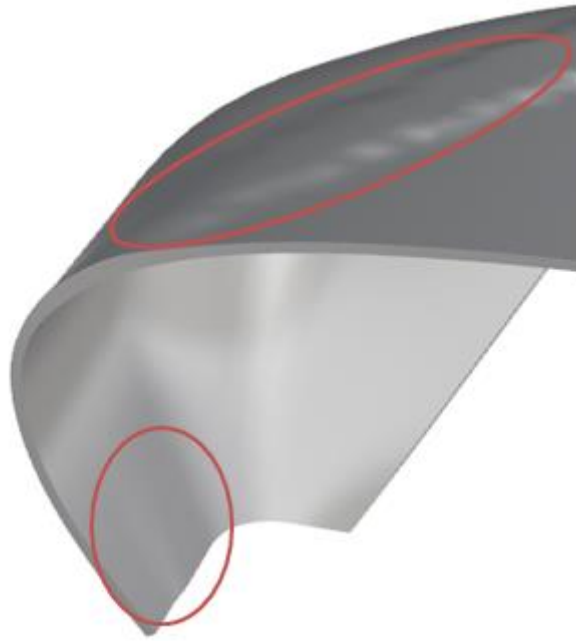


Figure 74. Detail of the non-smoothness of the surface due to the bigger cross sections required.

The structural behavior of this second option is not expected to be exactly the same as the one of the structure analyzed, since the “surface of symmetry” of the structure will not have the same shape as the one analyzed. The difference in the structural behavior, though, is expected to be very small. If this method of construction is chosen, this difference has to be taken into account in the detailed analysis.



Figure 75. Front view of the structure of the starting geometry

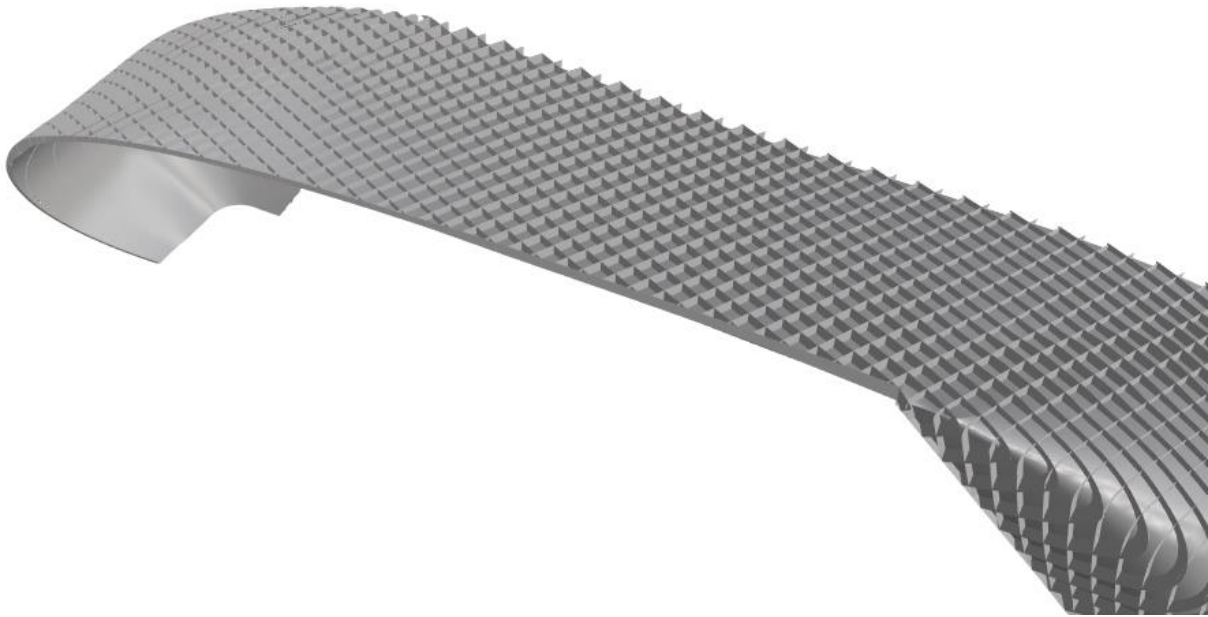


Figure 76. Lower shell, ribs and stiffeners of the structure

6.4.7 Comparison between the design tool and the preliminary analysis

The preliminary analysis which was conducted with an orthogonal representation of the geometry presented in Figure 11, has shown that the required total amount of steel for the construction of the vertical foyer is around 1000 tons. The analysis has been executed with 15mm thick upper and lower plates and 12mm thick ribs and stiffeners and includes the realization of the roof structure as well as the 2 floors. The surface area of the two floors is approximately the same as the area of the roof structure. Consequently, it can be estimated that half of the material of the preliminary analysis is addressed for the construction of the roof structure. From the analysis performed with the help of the design tool became obvious that the estimation of the amount of material for the construction of the roof structure is around half of the one of the preliminary analysis. It has to be noted that since the floors were included in the preliminary analysis and were supported by the roof structure, higher amount of material is expected to be necessary compared to the tool analysis that does not include the loads introduced from the floors. On the other hand, the addition of the floor loads is not expected to double the required amount of material of the roof structure. Consequently, it can be seen that with the implementation of the design tool, the estimated amount of material is less than the estimation of the conventional preliminary analysis. It presents a reduction of around 30%. A fact that shows that the analysis of the exact shape of the free form structure can prevent from over dimensioning the structure in the early design phase and from concluding to a higher expected cost than necessary.

7. Discussion

In the previous chapters of the thesis, the steps for the development of a design tool for the automatic manipulation of the geometry of a free form structure based on performance information have been presented. These steps were carried out and the base tool was created. The base tool and its capabilities have been tested through an implementation in the Post Rotterdam case study, where special requirements of the project showed the necessity of adding functionality to it.

The discussion driven from this research will be presented in this chapter. It is divided in two groups based on its relevance to the design tool or the case study analysis.

Design tool

The initial idea of the current research was to develop a design tool that could perform complete structural optimisation of free form structures in a short amount of time. This type of design tool would be very interactive since the user would be able to explore various set-ups of the optimisation problem and quickly receive information regarding the optimum shape given the boundary conditions and the set goal. It would also be used in collaboration with the architect during the early design phase, to be able to directly see which shapes perform better and if these shapes are desirable from the architect. This interactivity could not be achieved by using one single machine for performing the optimisation. The large amount of analysis required from the genetic algorithm before concluding on the optimum result in combination with the time necessary for one analysis, are restricting the interactivity. The option of using a cluster of computers was soon rejected, since there was no availability of multiple software licenses. The capabilities of the software used, inserted further restrictions that shaped the outcome of this research project.

The base tool presents a method for the analysis of free-form shell like structures and is oriented to be applicable to many structures. Each project to be analysed, though, shows special requirements which are yielding necessary iterations to be implemented in the tool. The implementation of the tool to a new project is not possible to be performed by every structural engineer, since knowledge of specific software is required. The structural engineer should have knowledge of Python programming language, Rhino-Grasshopper software and Ansys Parametric Design Language (APDL). The reason is that the surface structure of the project has to be created in Rhino-Grasshopper in order to be given as an input of the tool. Following, the command listing has to be checked if it is appropriate for the specific design. Mainly, the loading is expected to require significant modifications for every project. Finally, if additions have to be included in the tool, these have to be implemented through the Python script. Only when the tool is ready and tested by the structural engineer, it can be further used by the architect.

Furthermore, the applicability of the design tool is dual. Firstly, when connected to an optimisation algorithm, the optimum geometry according to a set goal will be discovered. Secondly, it can be used as a standalone component that connects Rhino-Grasshopper with Ansys in order to analyse the structural performance of a surface-geometry. The aim of the standalone component is to be used during the early design phase of a project in order to explore the effect of the geometry manipulation to the performance of the structure. Structural engineers and architects can perform manually iterations in the geometry by triggering the shape parameters and the effect of them in the structural performance can be detected. The shape exploration with the help of the standalone component will accommodate the gathering of information regarding the desire of the architect and the set-up of

the optimisation problem. The optimisation analysis will be performed in a later stage of the early design phase when more time is available.

Additionally, the structural performance, meaning the total amount of material required and the mean VM stress of the structure, is an output of the scripted component. Consequently, the output of the tool is a certain number of values which do not give a full insight on the performance of the structure and also on the effect of each loop iteration on the performance of the structure. An initial work towards the usability of the tool in terms of visualisation of the results in an easy and understandable way for both architects and engineers has been conducted in the current research, but the algorithm still performs like a “black box”.

Case study

The required time for one analysis depends on the number of iterations necessary before the tool concludes to a design with no overstressed elements and no excess of deflection. It has been noted that in the case study implementation, due to the grouping of the elements, in most geometries the number of iterations does not exceed the value 10. Consequently, every geometry is being analysed in less than one minute. Furthermore, the required time for the analysis of one generation of the genetic algorithm is approximately 30 minutes. Since, the maximum stagnant limit used in this research is 50 generations, the minimum duration of an optimisation analysis is 25 hours. The maximum duration detected is approximately 4 days (100 hours). As it becomes obvious, time is a limitation for the usability of the design tool in the first steps of the early design phase, but it is not a limitation in the last steps when more time is available.

The current development of the design tool includes a linear static and a linear buckling analysis. It is not proven, though, if these analysis types are adequate for the accurate analysis of free form shell like structures and consequently, if the analysis of the case study leads to accurate results. The performance of non-linear analysis might prove the necessity of its inclusion in the design tool.

8. Conclusions and recommendations

The conclusions of the current research as well as the recommendations for further research regarding the case study and the expansion of the functionality of the tool are elaborated in this chapter.

8.1 Conclusions

- The applicability of the design tool is not restricted to a specific geometry, material or cross section type. This can be concluded due to the fact that the geometry of the free form structure to be analysed is given as an input of the design tool. Furthermore, the choice of material of the structure as well as the cross section type are assigned through a computed stiffness matrix.
- The method used in the base tool can be the basis for developing custom-made design tools for the optimisation of various projects. This became obvious from the implementation to the Post Rotterdam case study, in which the base tool was customised for serving the special requirements of the project.
- The time required for the analysis of one geometry is less than one minute. Consequently, it can be concluded that the usability of the tool as a standalone component is achieved.
- Based on the required time for convergence of the external optimisation algorithm (at least 25 hours), can be noted that the current development of the tool can be used as a design method at the end of the early design phase. All the information regarding the set-up of the optimisation problem is already defined at that stage and the necessary time for the analysis is available.
- Through the analysis of the Post Rotterdam case study can be concluded, that the use of the design tool in the early design phase can lead to the estimation of less required material for a free form roof structure compared to a simplified analysis. As a consequence, it leads to lower estimated costs for the project in that phase.
- From the analysis results presented in Table 13 becomes obvious that with the help of the design tool, a reduction of the specified goal can be achieved. The percentage of the reduction depends on the specified goal and on the set up of the optimisation problem.
- The execution of the Analysis No 4 has shown that the set-up of the optimisation problem, meaning the design space for search and the design constraints, influences notably the result of the optimisation algorithm.
- In Table 12 the optimised geometry of every optimisation analysis as well as its performance is presented. It can be concluded that the shape plays a significant role in the performance of a structure and in the amount of material required for its construction. It has been shown that even small geometric iterations can lead to significant differences in the performance.

8.2 Recommendations

Design tool

- The current development of the design tool analyses only surface structures, consequently only shell elements are incorporated. The tool can be expanded to be used also for grid shell structures, which require beam elements to be defined.
- In order to reduce the computing time, a division of the required computing power in a cluster of computers would be deemed necessary. In this way the computing time would be approximately divided in the number of computers that would be part of the cluster.
- One more option for reducing the computed time for convergence is to use an optimisation algorithm that requires less amount of computation than evolutionary algorithms.
- The constructability of the free form structures is an important aspect, which would be beneficial to be implemented in the design tool. It could be implemented in terms of constraints on the shapes analysed.
- Visualisation in an easy and understandable way for both architects and engineers, of every step of the analysis would lead to better understanding of the design process and improvement of the usability of the tool.
- In order to research further the usability of the design tool, structural engineers and architects which are not familiar with it should use it for an already set-up optimisation problem or for the implementation in a new project.

Case study

- For the Post Rotterdam case study, different grouping methods could be researched that would lead to less iterations and less material assigned to the structure. A grouping method based on the virtual work (Olsson, 2012) could be an option.
- The research of the sensitivity of the vertical foyer to non-linear effects is deemed important in order to validate the accuracy of the choice of analysing the structure with linear analysis.
- The inclusion in the analysis of other parts of the structure such as the floors is deemed an important further analysis step for the case study.
- Lastly, a research on the weight difference between the early design phase analysis and the detailed final analysis would be considered useful. The detailed analysis of the structure would define the density as well as the thickness of the ribs and stiffeners. Consequently, these values could be compared to the assumed ones in the design tool and an indication of the material difference in percentage between the estimation of the early design phase and the final one could be concluded.

Bibliography

AKOS G. and PARSONS R. (2014). Foundations - The Grasshopper Primer Third Edition. Available from: < <http://modelab.is/grasshopper-primer> > [10/05/2015].

ANSYS (2015). Help Documentation.

ARGYRIS J.H., PAPADRAKAKIS M., APOSTOLOPOULOU C., KOUTSOURELAKIS S. (2000). The TRIC shell element: theoretical and numerical investigation. *Computer Methods in Applied Mechanics and Engineering*, vol.182, 217–245.

ARORA J. (2012). Introduction to optimum design. *Elsevier*, 3rd edition.

BLETZINGER K., BISCHOFF M., RAMM E. (2000). A unified approach for shear-locking free triangular and rectangular shell finite elements. *Computers and Structures*, vol.75, Issue 3, 321-334.

BRITISH STANDARDS INSTITUTION (2005). *Eurocode 3: Design of steel structures*. London, BSI.

BUELOW P., FALK A., TURRIN M. (2010). Optimisation of structural form using a genetic algorithm to search associative parametric geometry. In *Proceedings of the First International Conference on Structures and Architecture (ICSA)*, Guimarães, Portugal.

CHRISTENSEN P.W. and KLARBRING A. (2009). An Introduction to Structural Optimisation. *Springer*, vol.153.

COENDERS J.L. (2008). Reader for the course CT5251: *Structural Design - Special Structures of Delft University of Technology*.

COENDERS J.L. (2011). Networked Design. Next generation infrastructure for computational design. *Phd Dissertation Delft University of Technology*.

DELLA PUPPA G. and TRAUTZ M. (2015). Multi-objective shape optimization of shell structures based on buckling forms. In *Proceedings of the IASS Symposium, Amsterdam*.

FOURIE P.C. and GROENWOLD A.A. (2002). The particle swarm optimization algorithm in size and shape optimization. *Structural and Multidisciplinary Optimization*, vol. 23, 259-267.

GALAPAGOS, computer software (2015). Available from: <<http://www.grasshopper3d.com/group/galapagos>> [20/06/2015].

GEYER P. and RUECKERT K. (2005). Conceptions for MDO in Structural Design of Buildings. 6th *World Congresses of Structural and Multidisciplinary Optimization*, Rio de Janeiro, Brazil. Figure 1, p. 2.

HAMBLETON D., HOWES C., HENDRICKS J., KOOYMANS J. (2009). Study of Panelization Techniques to Inform Freeform Architecture. In *Proceedings of the 11th International Conference on Glass Performance Days (GPD)*, Finland.

HOLLAND J.H. (1975/1992). Adaptation in Natural and Artificial Systems. *Cambridge, MA: MIT Press*, Second edition (First edition, 1975).

- HOLLAND J.H. (1992). Genetic Algorithms. *Scientific American*, July 1992, 66-72.
- HOOGENBOOM P.C.J. (2015). Shell Analysis, Theory and Application, CIE4143. *Delft University of Technology*, Delft.
- HOOGENBOOM P.C.J. (2005). Analysis of hollow-core slab floors. *HERON*, vol.50, No 3.
- KABIR H.R.H. (1992). A shear locking free isoparametric three-node triangular finite element for moderately thick and thin plates. *International journal for numerical methods in engineering*, vol.35, 503-519.
- KEGL M. and BRANK B. (2006). Shape optimization of truss-stiffened shell structures with variable thickness. *Computer methods in applied mechanics and engineering*, vol. 195, 2611-2634.
- LAGAROS N.D., FRAGIADAKIS M., PAPADRAKAKIS M. (2004). Optimum Design of Shell Structures with Stiffening Beams. *AIAA Journal*, vol. 42, No 1, 175-184.
- MOAVENI S. (1999). Finite element analysis, Theory and Application with ANSYS. *Prentice-Hall*, New Jersey.
- MITCHELL M. (1995). Genetic algorithms: An overview. *Complexity*, vol.1, p. 31-39, New Mexico, USA.
- OLSSON, J. (2012). Form finding and size optimization. *Master's thesis Chalmers University of Technology*.
- PASTERNAK H. and KRAUSCHE T. (2013). The Porsche Pavilion in the Autostadt Wolfsburg, Germany. *Procedia Engineering*, vol.57, 63-69.
- PRUSZKOWSKI W. (2015). Steel grid shells, Stress-based sizing optimisation. *Master's thesis Delft University of Technology*.
- PYTHON.org (2015). Available from: < <https://www.python.org/> > [29/09/2015].
- RHINO (2015). Available from: <<https://www.rhino3d.com/nurbs>> [07/10/2015].
- RUBEN A., CANALES J., TARRAGO J., RASMUSSEN J. (2002). An integrated approach for shape and topology optimisation of shell structures. *Computers & Structures*, vol.80, 449-458.
- RUTTEN D. (2010). Evolutionary Principles applied to Problem Solving. *Blog Post based on the lecture given at the AAG10 conference, Vienna. Available from:*
<<http://www.grasshopper3d.com/profiles/blogs/evolutionary-principles>> [07/10/2015]
- SCHEIBLE F. and DIMCIC M. (2011). Parametric Engineering-Everything is Possible. *In Proceedings of the IABSE-IASS Symposium, London*.
- TOMAS A. and MARTI P. (2010). Shape and size optimisation of concrete shells. *Engineering Structures*, vol. 32, 1650-1658.
- TURRIN M., BUELOW P., STOUFFS R. (2011). Design explorations of performance driven geometry in architectural design using parametric modeling and genetic algorithms. *Advanced Engineering Informatics*, vol.25, 656-675.

- VAN DIJK W., STERKEN R., FALGER M. (2015). Complex shapes ask for drastic measures. *In Proceedings of the IASS Symposium, Amsterdam.*
- VELTKAMP M. (2007). Free Form Structural Design. Schemes, Systems and Prototypes of Structures for Irregular Shaped Buildings. *Phd Dissertation Delft University of Technology.*
- VERMEIJ P.TH. (2006). Parametric associative design for free form architecture. *Master's thesis Delft University of Technology.*
- WOODBURY R., BURROW A.L. (2006). Whither design space? *Artificial Intelligence for Engineering Design, Analysis and Manufacturing, vol.20 (Issue 2, Special Issue: Design Spaces: The Explicit Representation of Spaces of Alternatives), 63–82.*
- WU Y., XIA Y., LI Q. (2015). Structural morphogenesis of free form shells by adjusting the shape and thickness. *In Proceedings of the IASS Symposium, Amsterdam.*
- YENIAY O. (2005). Penalty function methods for constrained optimization with genetic algorithms. *Mathematical and Computational Applications, vol.10, No 1, 45-56.*

Appendix 1 - Loading

In this appendix the calculation of the loading is presented.

- Self-weight:

The self-weight of the steel structure is calculated directly in Ansys. The user inputs in this calculation are the gravitational acceleration and the density of the material. Since the modelled structure consists of only one shell layer, the density of the steel imported has to be modified to take into account the weight of the original structure. For the definition of the self-weight, when pre-integrated shell elements are used, Ansys takes into account a unit thickness of the shell element (Ansys 2015). Based on the height difference (h) between the 2 steel plates and the thickness of the steel plates (t) and stiffening ribs (t/2), the density is calculated as:

$$\gamma = \gamma_{\text{steel}} * V_{\text{origstr}} / V_{\text{modstr}} = \gamma_{\text{steel}} * (2 * t * 1 + 2 * t / 2 * h) / 1 \quad (1)$$

The gravitational acceleration used is:

$$g = 9.81 \text{ m/s}^2$$

- Dead weight

In order to take into account the dead weight of the ceiling, installations and pipelines, an additional dead load of 0.5 kN/m² is used.

- Snow load

The snow load is being calculated according to the Eurocode (EN 1991-1-3:2003) and the Dutch National Annex.

Snow load on roofs is determined based on the Equation 5.1 of the Eurocode:

$$s = \mu_i * C_e * C_t * s_k \quad (2)$$

where:

C_e is the exposure coefficient taking the value of $C_e=1$ for normal topography

C_t is the thermal coefficient taking the value of $C_t=1$ for roofs with low thermal transmittance ($<1 \text{ W/m}^2\text{K}$)

s_k is the characteristic value of snow load on the ground which is $s_k=0.7$ for the Netherlands.

μ_i is the shape coefficient which is calculated according to the special characteristics of each roof.

In the case of the vertical foyer, the roof is attached to a higher structure which will cause snow accumulation. Consequently, the snow load will be higher close to the adjacent building and lower when moving away from the Post Rotterdam building. The distribution of the snow load is shown in Figure 77.

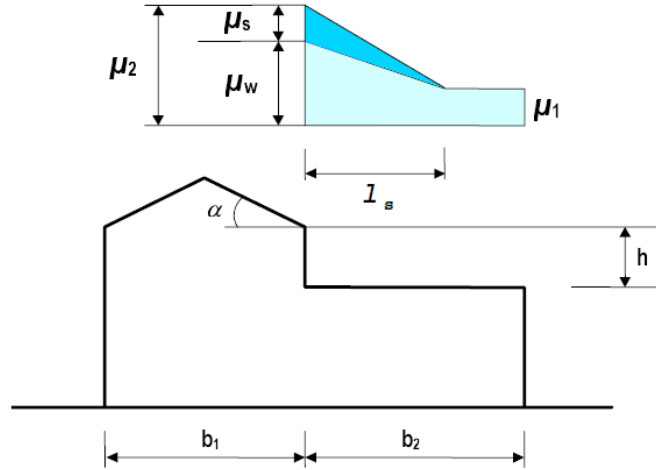


Figure 77 Snow load shape coefficients for roofs abutting to taller construction works (Figure 5.7 from EN 1991-1-3:2003)

$\mu_1=0.8$ since it is assumed that the roof of the vertical foyer is flat.

$$\mu_2 = \mu_s + \mu_w \quad (3)$$

where:

μ_s is the snow load shape coefficient due to sliding of snow from the roof of the Post Rotterdam building. In this case the value of snow load due to sliding is considered $\mu_s=0$ since protection exists not to let the snow slide from the adjacent building.

μ_w is the snow load shape coefficient due to wind and it can be defined based on the following expression:

$$\mu_w = (b_1 + b_2)/(2 \cdot h) \leq \gamma \cdot h/s_k \quad (4)$$

$$\mu_w = (60+15)/(2 \cdot 8) = 4.7 \leq 2 \cdot 8/0.7 = 22.9$$

But, the range for μ_w is defined in the Dutch National Annex as $0.8 \leq \mu_w \leq 4$, consequently

$$\mu_2 = 4$$

The drift length l_s needs to be defined. According to EN 1991-1-3:2003 equation 5.9, the drift length is:

$$l_s = 2 \cdot h = 2 \cdot 8 = 16\text{m}$$

But, the Dutch National Annex determines a restriction for the drift length equal to $5\text{m} \leq l_s \leq 15\text{m}$.

Consequently, the drift length of the vertical foyer is the whole width of the roof structure.

For simplification reasons a uniformly distributed mean load is applied to the projected area of the roof structure under consideration. The mean value of the snow load is:

$$s = (\mu_1 + \mu_2)/2 \cdot s_k = (0.8 + 4)/2 \cdot 0.7 = 1.68 \text{ kN/m}^2$$

- Wind load

The wind load is defined according to the Eurocode (EN 1991-1-4:2005) and the Dutch National Annex.

The wind force (F_w) acting on a structure can be calculated based on Equation (5.3) of the EN 1991-1-4:2005.

$$F_w = c_s * c_d * c_f * q_p(z_e) * A_{ref} \quad (5)$$

Where:

$c_s * c_d$ is the structural factor which is used in order to take into account the effect on wind actions from the non-simultaneous occurrence of peak wind pressures on the surface (c_s) together with the effect of the vibrations of the structure due to turbulence (c_d). For low rise buildings ($h \leq 15m$) the structural factor is equal to $c_s * c_d = 1$.

$q_p(z_e)$ is the peak velocity pressure at reference height z_e . The vertical foyer will be constructed in the center of Rotterdam (urban area) which is in the second wind region of the Netherlands as depicted in Figure 78. The reference height is $z_e = 15m$. Based on these information the peak velocity can be defined from the Dutch National Annex as $q_p(z_e) = 0.80 kN/m^2$.

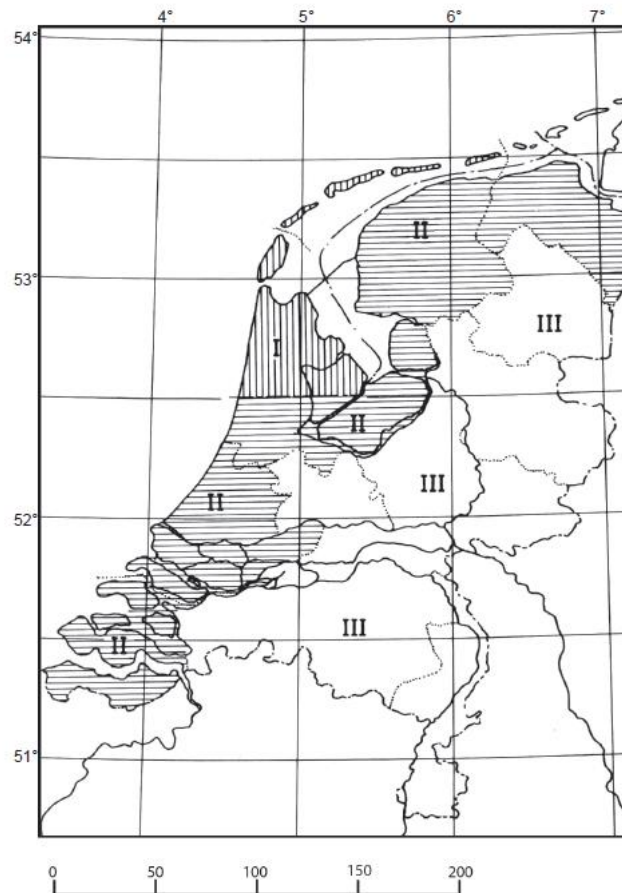


Figure 78. Wind regions of the Netherlands (NEN 6702 Loadings and deformations TGB 1990)

C_f is force coefficient which varies the wind force based on where is the location of the part of the structure under consideration respectively to the wind direction.

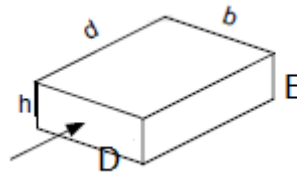


Figure 79. Side of wind application for the determination of the wind forces

In the case of the vertical foyer, the following values are valid.

$$h=15\text{m}$$

$$b=15\text{m}$$

$$d=65\text{m}$$

The values of the coefficients for the inclined parts depend on the ratio $h/d=0.23<0.25$. Consequently, $C_f=+0.7$ for the part facing the wind and $C_f=-0.3$ for the other part of the structure.

The upper part of the roof structure, will be subjected to wind load also due to friction. The covering material is steel which is considered a smooth material, consequently the friction coefficient is $c_f=0.01$ for the upper part.

| side | C_f | $q_p(z_e)$ | A_{ref} | wind load |
|-------|-------|----------------------|-------------------|-------------------|
| | [-] | [KN/m ²] | [m ²] | [KN] |
| D | +0.7 | 0.8 | projected area | 0.56 * A_{ref} |
| E | -0.3 | 0.8 | projected area | -0.24 * A_{ref} |
| upper | 0.01 | 0.8 | total area | 0.008 * A_{ref} |

Table 14. Input for the calculation of the wind load based on Equation 5

- Variable load

The roof structure will be accessible only for maintenance and repair works and not to the public. Consequently, the roof can be categorized in the H loaded area according to the Table 6.9 of EN 1991-1-1:2002. For this category the imposed load is provided in the Table 6.10 of the National Annex as:

$$q_k = 1\text{KN/m}^2 \text{ distributed loads over an area of } 10\text{m}^2 \text{ and}$$

$$Q_k = 1,5\text{KN concentrated load on a surface of } 0.1 \times 0.1\text{m}$$

- Load combinations

The load combinations that have been taken into account are based on the Eurocode 0 and the Dutch National Annex.

| ULS | | | | |
|-------------|-----------|-----------|-----------|--------------|
| Combination | Dead load | Snow load | Wind load | Imposed load |
| 1 | 1.35 | | | |
| 2 | 1.2 | 1.5 | | |
| 3 | 1.2 | | 1.5 | |
| 4 | 1.2 | | -1.5 | |
| 5 | 1.2 | | | 1.5 |

Table 15. Ultimate Limit State combinations

| SLS | | | | |
|-------------|-----------|-----------|-----------|--------------|
| Combination | Dead load | Snow load | Wind load | Imposed load |
| 1 | 1 | 1 | | |
| 2 | 1 | | 1 | |
| 3 | 1 | | -1 | |
| 4 | 1 | | | 1 |

Table 16. Serviceability Limit State combinations

The imposed load for maintenance and repair works is lower than the snow load and applied in the same direction. Consequently, the imposed load will not be used in the load combinations as it is considered not to be critical.

The load combinations that have been analyzed are for the Ultimate Limit State, combinations 1 to 3 and for the Serviceability Limit State, combinations 1 to 2.

Appendix 2 - Geometry transfer

In this appendix the options that were explored regarding the transfer-generation of the geometry in Ansys are presented.

A) Import geometry in Ansys

Ansys Mechanical gives to the user the option to import a geometry that has been generated in other software, such as Rhino. The importing file types that are supported by Ansys Mechanical are: IGES, CATIA, CATIA V5, Creo Parametric, NX, ACIS, PARA. From these file types Rhino is able to export geometry only in IGES (Initial Graphics Exchange Specification) format. As a consequence, the option to export the generated geometry from Rhino-Grasshopper in IGES format and then import it in Ansys has been further investigated.

In the parametric model the geometry has been generated as a surface-brep (boundary representation). The surface-brep has been exported from Rhino and imported in Ansys as an area. The properties of the surface remain as well as any discontinuities created by the Rhino-Grasshopper modeling. As presented in Section 4.1, the surface of the roof structure is not possible to be modeled as one surface or one open Brep. Different surfaces are generated and then merged. The merge command, however, does not prevent from discontinuities between the adjacent surfaces. When importing the .iges file a warning for discontinuity appears. With a more careful-zoomed in look, the discontinuities are obvious between the different areas and are presented in Figure 80.

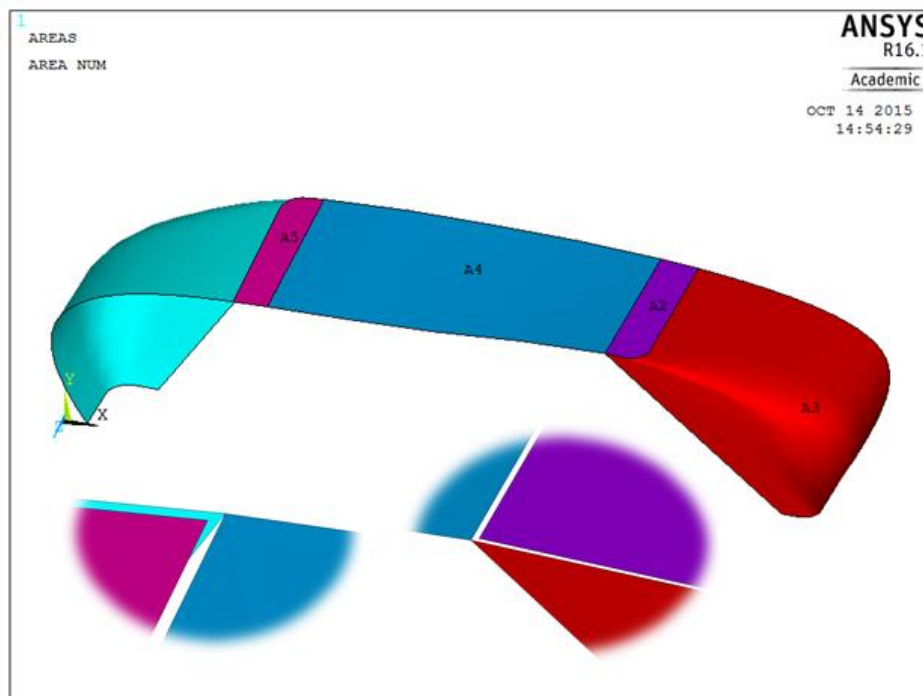


Figure 80. Import the areas in Ansys- discontinuities

Even though discontinuities exist, Ansys is able to mesh the areas and perform a structural analysis. When meshing the areas the discontinuities seem to disappear.

The approach that has been chosen for the modeling of the structure, has led to the use of pre-integrated shell elements. These elements, as has been already presented, have no cross sectional properties or material properties. This indicates that the thickness of the elements is non-defined. In this approach of importing the areas which are further on meshed in Ansys, the mesh elements are presenting curvature. Ansys before analysing a structure computes some tests for the adequacy of the elements to be analysed. A first check is related to the shape of the element. An aspect ratio of 20 is the limit for accurate results. Another check is the ratio of the radius of curvature divided by the thickness of the elements. As can be anticipated, when the curved elements are modeled with pre-integrated shell elements, warning messages are produced for all the curved elements and the analysis is not possible to be completed. Consequently, the approach of importing the surface created in Grasshopper is possible when there is no need of using pre-integrated elements.

B) Create geometry in Ansys

One other option is to create the geometry directly in Ansys. In this way the discontinuities generated in Rhino-Grasshopper modelling will be prevented. From the parametric model, only the control points are necessary to be imported in this case. The surface will be generated based on them. The process to be followed for generating the geometry in Ansys is visible in Figure 81 to Figure 84. A first step is to model the lines that go through these control points. The options available in Ansys for line creation are: lines, arcs and splines. Consequently, instead of NURBs curves, splines are being used for the modeling of the free form roof structure and lines are used for the triangle-like coverings as well as the base of the roof. After having created all the lines, arbitrary areas are generated based on them. For a closer to the original representation of the vertical foyer, the double curvature of the diagonal angles has to be modeled. The only option in Ansys is to perform an area fillet between the roof surface and the triangular-like covers. The result of this fillet command is shown in Figure 84. It can be noted that some parts of the roof surface are being cut. A possible solution is to reduce the width of the middle part of the roof surface by almost the radius of the fillet (Figure 85). In this case, the radius of the fillet is not defined from the parametric model and cannot be a parameter for the optimisation algorithm.



Figure 81. Import the control points generated in Rhino-Grasshopper

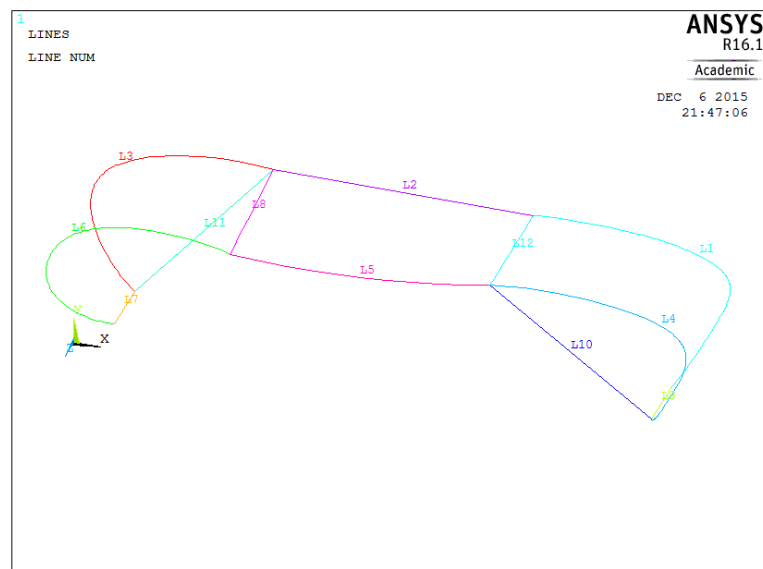


Figure 82. Model with Splines the roof structure and with straight lines the triangular covers and the base

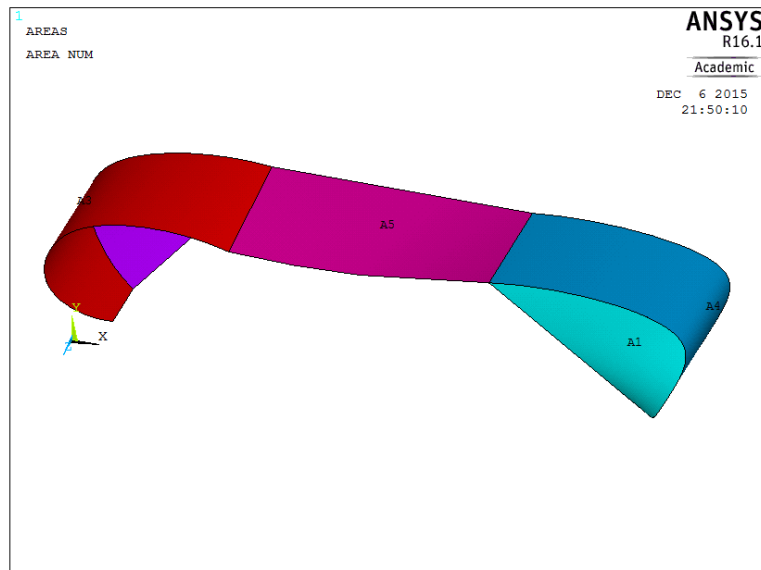


Figure 83. Create surfaces from the boundary lines

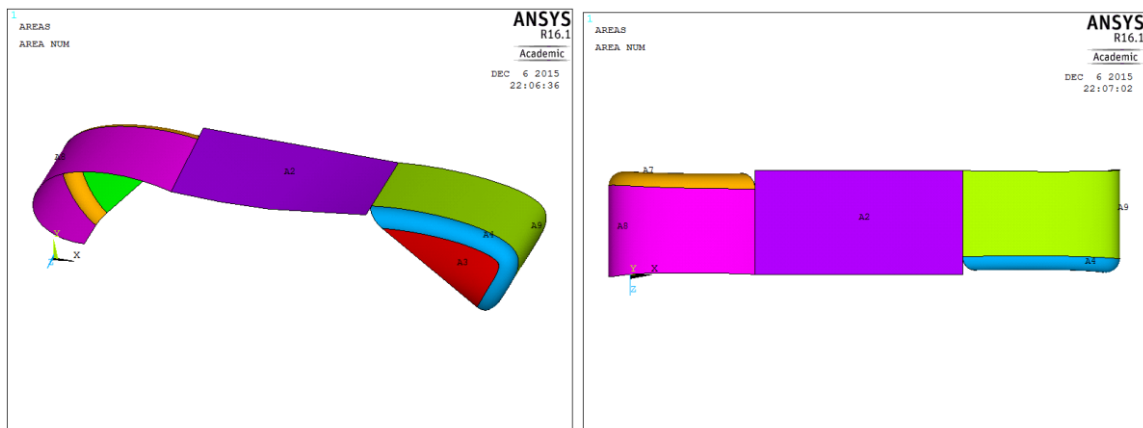


Figure 84. Final geometry after filleting the edges- Parts of the roof are cut. Left: perspective view/Right: top view

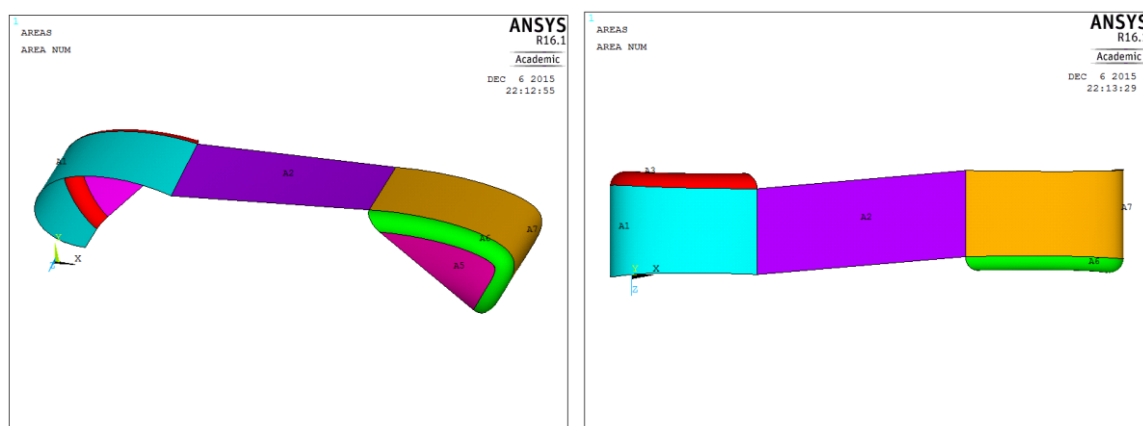


Figure 85. Final geometry after filleting the edges- No parts of the roof are cut. Left-perspective view/Right-top view

It can be noted from the outcome of the shape generation, that the shape is not as fluent as it is when generated in Rhino-Grasshopper. Ansys has limited capabilities regarding free-form shape generation. Consequently, it is not a preferred method for this tool. Furthermore, with the previous

presented methods completely different free form shapes can be transferred in Ansys and analyzed with small further manipulation. Whereas, if this method would be chosen, the tool would be applicable only in this specific case.

Appendix 3 - Equivalent structure

The reasons why an equivalent structure has to be modeled have been analysed in Section 4.3. In this appendix, the process that has been carried out for deciding the most appropriate approach will be presented.

Instead of modeling all the structural elements, it has been decided to model just one surface and to further mesh this surface for the finite element analysis. Consequently, the two plates as well as the ribs and stiffeners will be modeled as one plate-shell with equivalent properties.

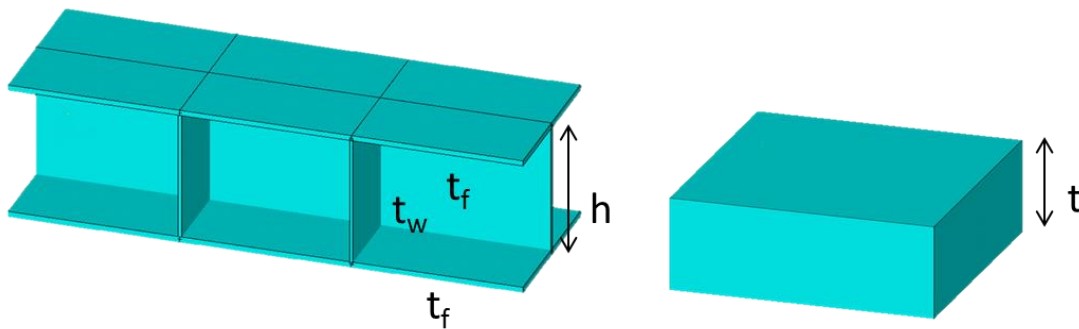


Figure 86. Modeling of the original structure (left) with one plate-shell (right)

In order to achieve a perfect equivalency between the two cross sections, the bending stiffness (EI), the membrane stiffness (EA), the shear stiffness (GA_s) and the torsional stiffness (GI_t) have to be equivalent. Based on these properties the internal forces will be computed.

Where:

E : Young's modulus (depends on the material)

G : Shear modulus (depends on the material). It can be calculated as $G = E / (2 * (1 + \nu))$ where ν is the Poisson ratio.

A : The area of the cross section

A_s : The area of the cross section that is going to take up the shear forces

I : Moment of inertia (depends on the shape of the cross section)

I_t : Torsion constant (depends on the thickness of each part of the cross section as well as if the cross section is open or closed)

The element type that has been chosen to be used for the structural analysis is Ansys' element SHELL281. The cross section of this element is a solid cross section and the user has to define the thickness as well as the material properties. When not pre-integrated shell section is used, it is not possible to assign directly the different stiffness values of the element. The only stiffness value that can be assigned when defining a cross section in this way is the shear stiffness of the cross section, so this will not be a constraint for the equivalency calculation. As a consequence, the variables that have to be defined are the thickness of the shell element (t), the modulus of elasticity of the material (E) as

well as the density of the material (d). The density of the material is important so that the self-weight of the equivalent structure is the same as the original one, but it has no effect on the stiffness of the structure.

Since the value of shear stiffness can be a user input for the cross section, there is a need to define an equivalency for bending, membrane and torsional stiffness. The variables that have to be defined based on this equivalency, are the modulus of elasticity of the material and the thickness of the cross section. As a consequence, there are 2 unknown variables and 3 equations depending on them that need to be fulfilled. This is not possible to be solved. Only two out of the three equations can be fulfilled.

The shape of the vertical foyer implies that the loads will be carried mainly by bending. The roof has a large span with low curvature and the double curved angles even though they present high curvature, they are not well supported. As proved by an experiment when the shell is not well supported, the applied loads will cause in-extensional deformations and will be carried mainly by bending (Hoogenboom, 2015). Consequently, it is considered adequate to fulfill the bending and torsion equations and accept to have a small error because of the non-equivalent membrane stiffness.

The bending stiffness and the torsion stiffness of the original structure can be calculated. Based on these values the properties of the equivalent cross section will be defined. Both bending and torsion stiffness of the equivalent cross section depend on the entity $E \cdot t^3$ and in each case this has a different value. As a consequence the system of equations is inconsistent and bending and torsion stiffness cannot be equivalent for these two structures.

Following has been analysed the case in which only bending equivalency is achieved, as well as the case in which bending and membrane equivalency are achieved.

| Cross section properties | | Original structure | Equivalent structure | | |
|---------------------------------|----------|--------------------|----------------------|-------------------|----------------------------------|
| plate width | s | 1 | 1 | m | |
| height: distance between plates | h | 1 | - | m | |
| thickness of the upper plate | t_{f1} | 0,04 | - | m | |
| thickness of the lower plate | t_{f2} | 0,04 | - | m | |
| thickness of the web | t_w | 0,02 | - | m | |
| equivalent shell thickness | t_{eq} | - | 0,636 | m | |
| area | A | 0,099 | 0,636 | m ² | |
| volume | V | 0,118 | 0,636 | m ³ | |
| moment of inertia | I | 0,021 | 0,021 | m ⁴ | |
| torsion constant | I_t | 0,016 | 0,086 | m ⁴ | |
| | | | | | |
| Material properties | | | | | |
| modulus of elasticity | E | 2,10E+11 | 2,10E+11 | N/m ² | |
| shear modulus | G | 8,75E+10 | 8,75E+10 | N/m ² | |
| density | γ | 7850 | 1460 | Kg/m ³ | |
| | | | | | |
| Stiffness properties | | | | | Ratio equivalent/original |
| bending stiffness | EI | 4,51E+09 | 4,51E+09 | N*m ² | 1,00 |
| shear stiffness | GA_s | 8,68E+09 | 5,57E+10 | N | 6,42 |
| membrane stiffness | EA | 2,08E+10 | 1,34E+11 | N | 6,42 |
| torsional stiffness | GI_t | 1,40E+09 | 7,52E+09 | N*m ² | 5,37 |

Table 17. Equivalent structure properties based on bending equivalency

| Cross section properties | | Original structure | Equivalent structure | | |
|---------------------------------|----------|--------------------|----------------------|-------------------|----------------------------------|
| plate width | s | 1 | 1 | m | |
| height: distance between plates | h | 1 | - | m | |
| thickness of the upper plate | t_{f1} | 0,04 | - | m | |
| thickness of the lower plate | t_{f2} | 0,04 | - | m | |
| thickness of the web | t_w | 0,02 | - | m | |
| equivalent shell thickness | t_{eq} | - | 1,612 | m | |
| area | A | 0,099 | 1,612 | m ² | |
| volume | V | 0,118 | 1,612 | m ³ | |
| moment of inertia | I | 0,0215 | 0,349 | m ⁴ | |
| torsion constant | I_t | 0,016 | 1,397 | m ⁴ | |
| | | | | | |
| Material properties | | | | | |
| modulus of elasticity | E | 2,1E+11 | 1,29E+10 | N/m ² | |
| shear modulus | G | 8,75E+10 | 5,38E+09 | N/m ² | |
| density | γ | 7850 | 577 | Kg/m ³ | |
| | | | | | |
| Stiffness properties | | | | | Ratio equivalent/original |
| bending stiffness | EI | 4,51E+09 | 4,51E+09 | N*m ² | 1,00 |
| shear stiffness | GA_s | 8,68E+09 | 8,68E+09 | N | 1,00 |
| membrane stiffness | EA | 2,08E+10 | 2,08E+10 | N | 1,00 |
| torsional stiffness | GI_t | 1,40E+09 | 7,52E+09 | N*m ² | 5,37 |

Table 18. Equivalent structure properties based on bending and membrane equivalency

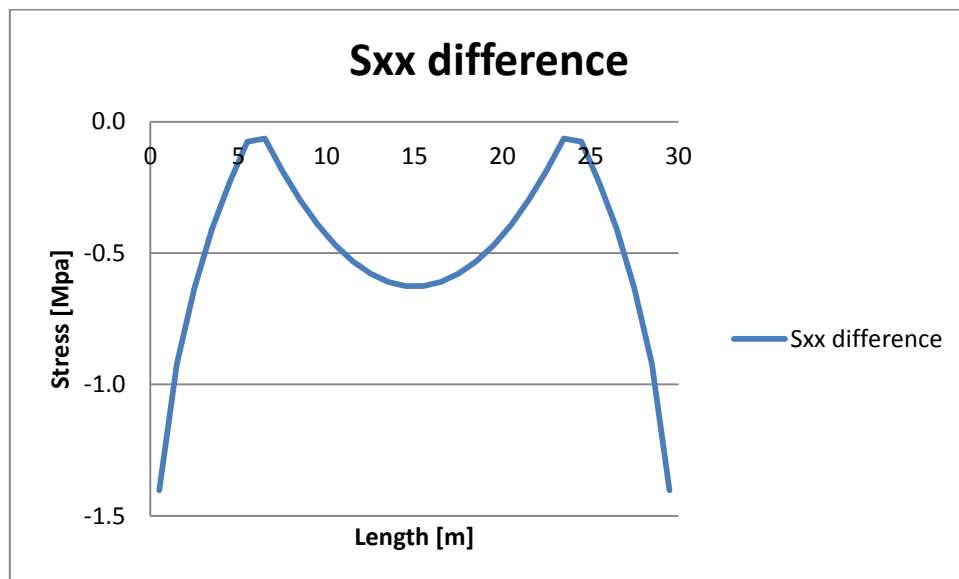
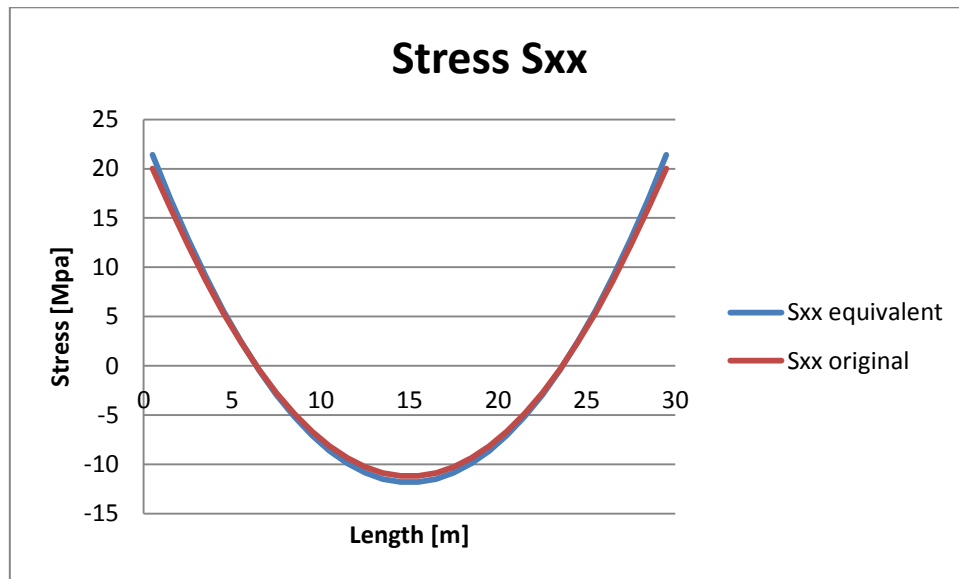
It can be noted that in the first case the required thickness of the shell elements is around 600mm whereas in the second case, the required thickness of the shell elements is around 1600mm. Furthermore, in the case where only the bending stiffness is the same, the equivalent structure presents 5 to 6 times stiffer behaviour in membrane and torsion, whereas in the second case, the equivalent structure is 5 times stiffer only in torsion. Consequently, the second equivalency would be considered to be more adequate for this analysis.

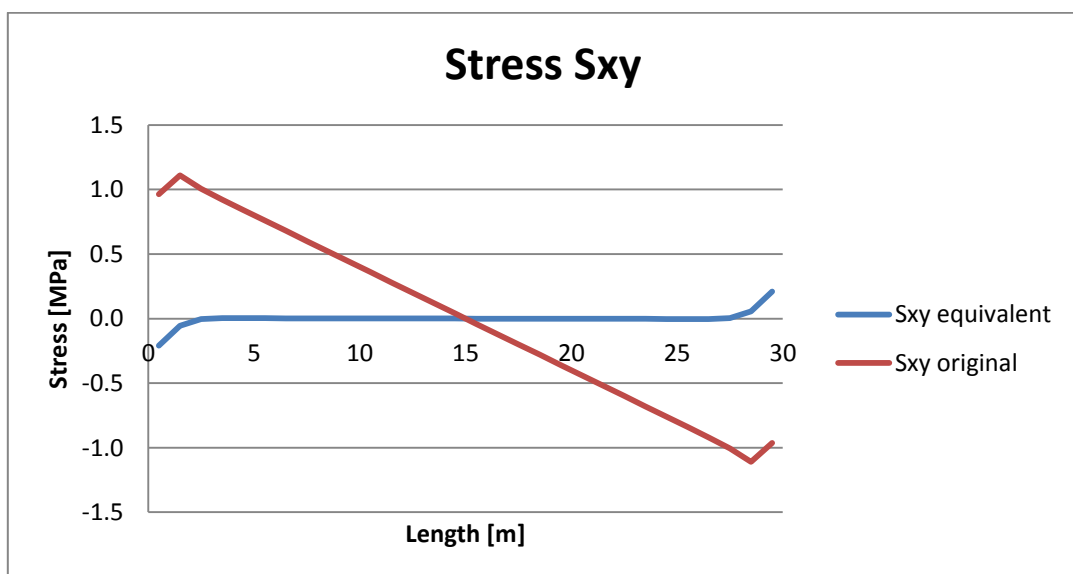
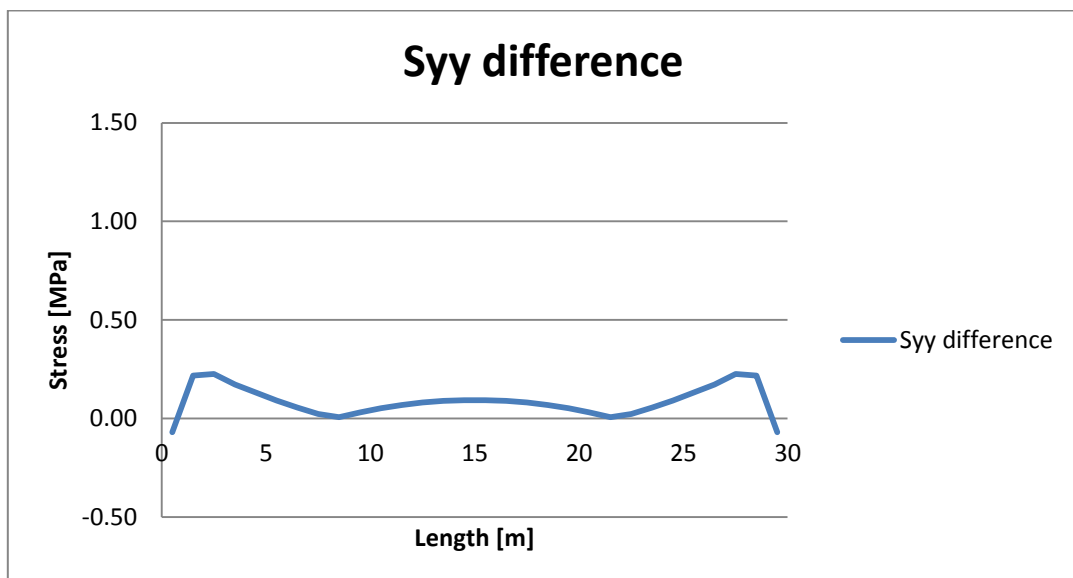
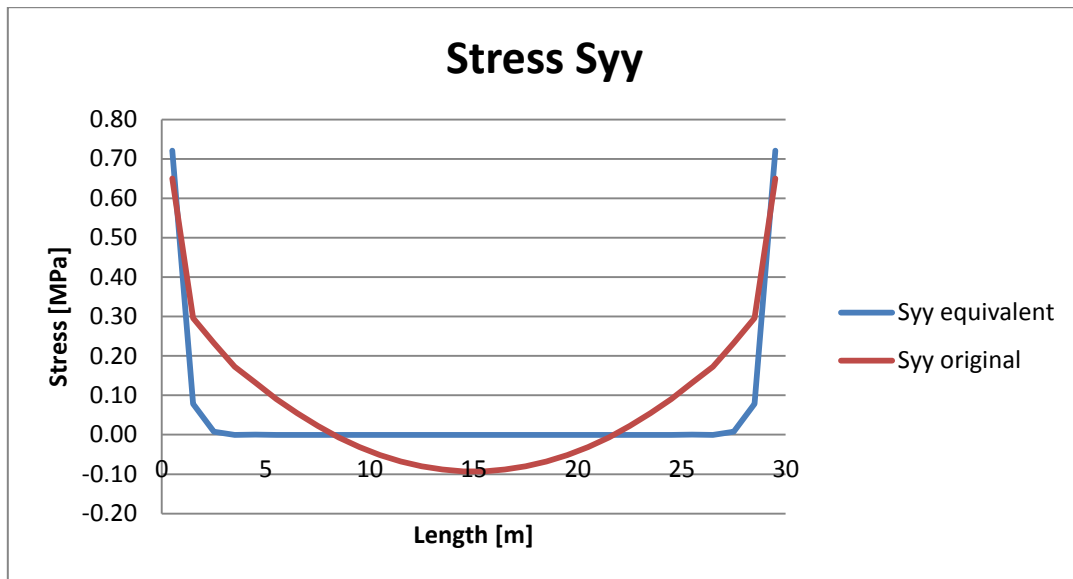
The chosen element in Ansys (SHELL281) is able to calculate thin to moderately thick shell elements. Before analysing a structure though, a check is performed regarding the ratio thickness to radius of curvature. When the thickness of 600mm is imported, a warning is generated regarding this ratio. Ansys is warning for excess thickness of the shell elements and is advising reconsideration of the input thickness. The same occurs when the thickness of 1600mm is imported.

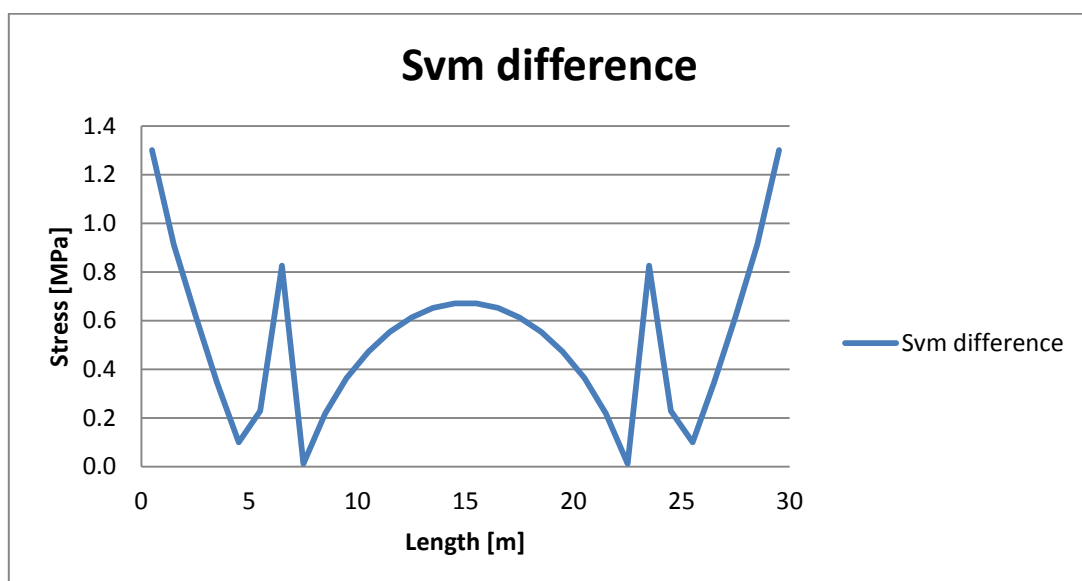
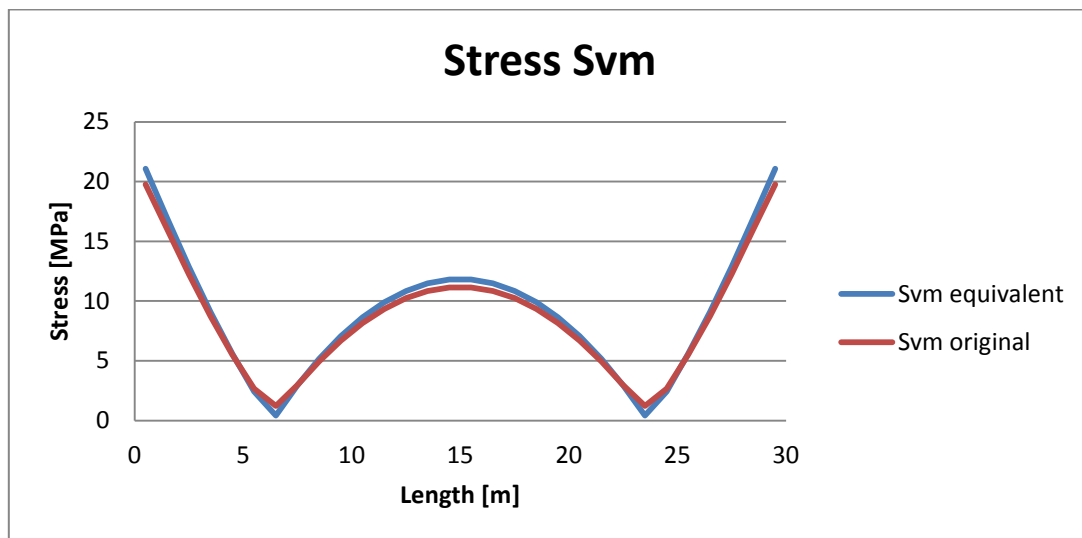
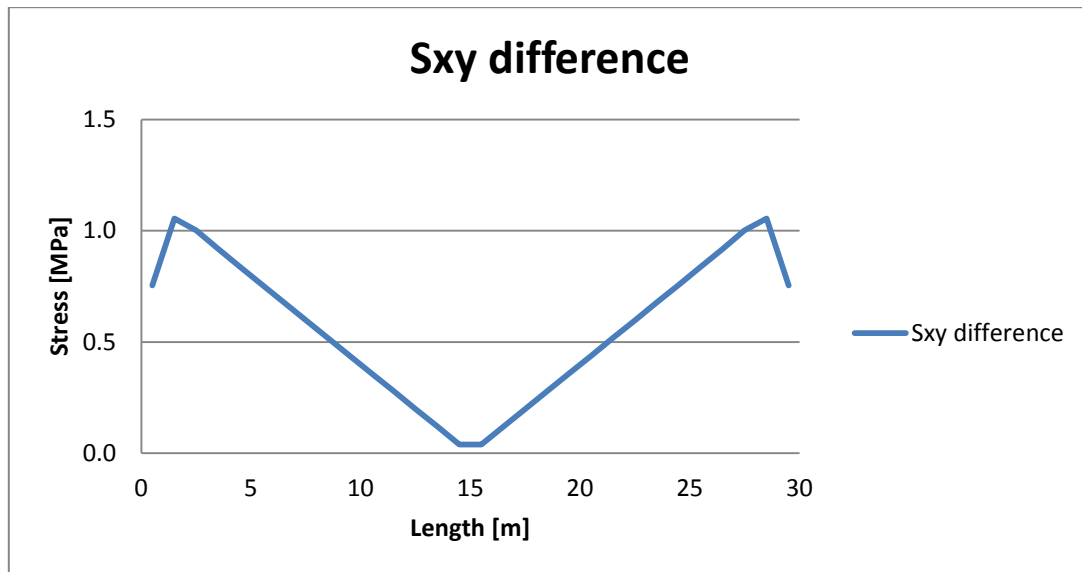
As a consequence, none of the above approaches can be used in order to model an equivalent structure. The chosen approach is to use pre-integrated shell elements in which the stiffness matrix is user input as has been presented in Section 5.4.

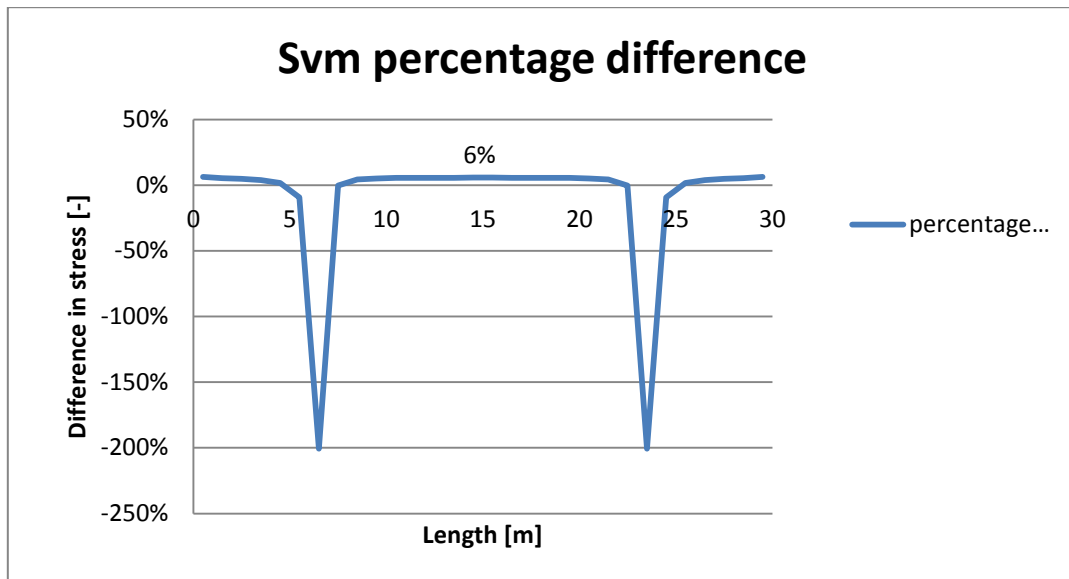
Appendix 4 - Stress equivalency comparison

Upper flange:



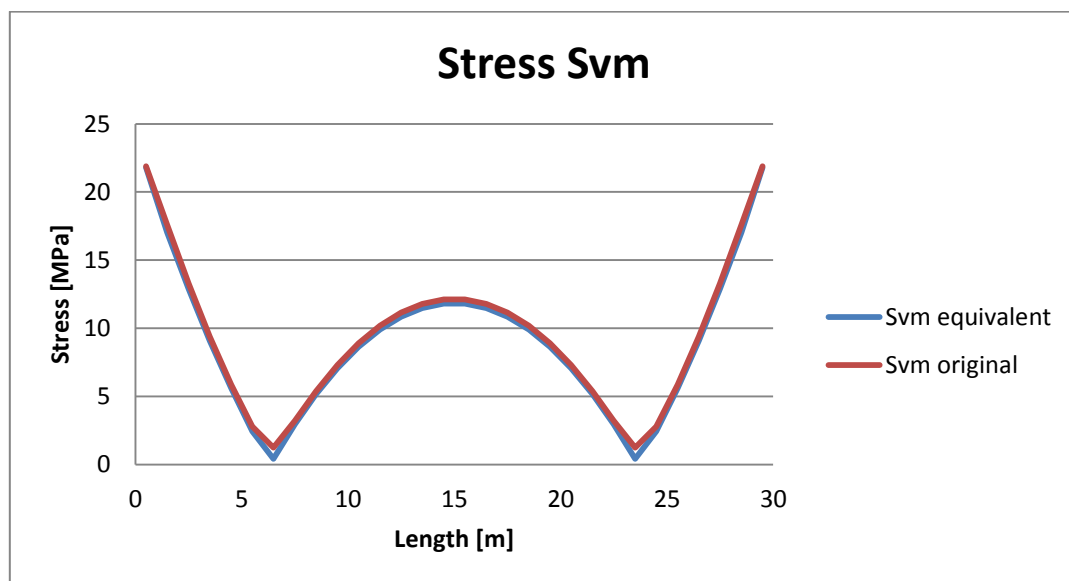


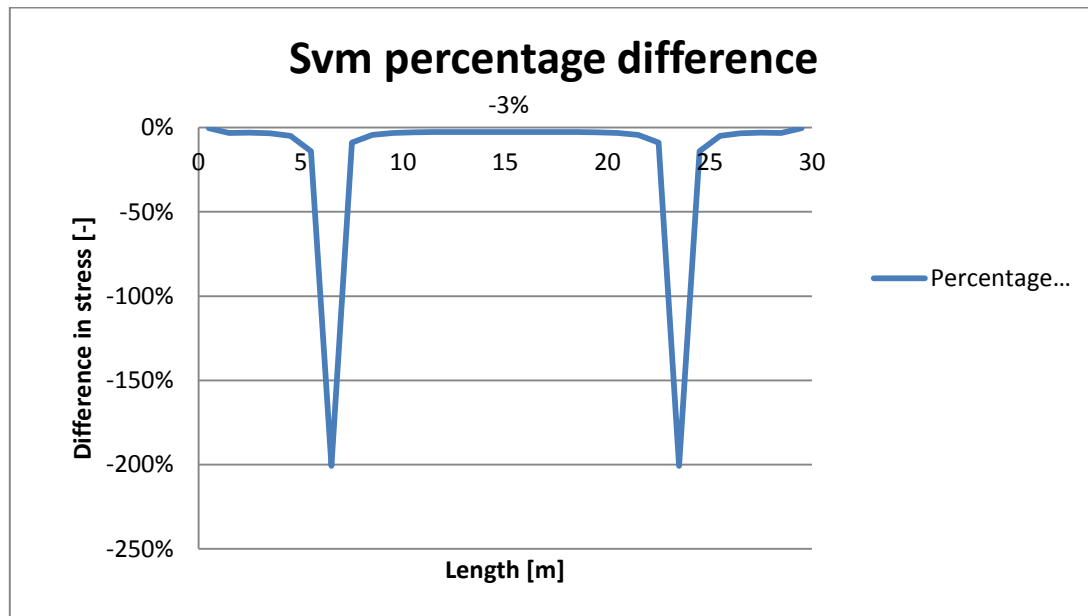
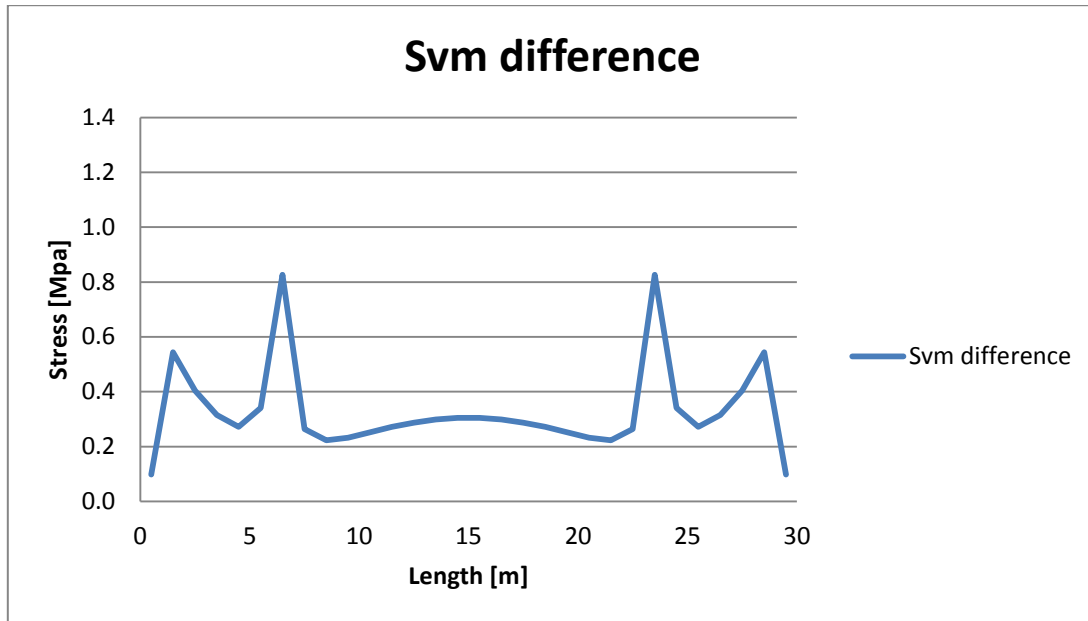




Lower flange:

In the case where the stresses at the lower flange are compared to the ones of the equivalent structure the form of the graphs remain the same. Consequently, only the graphs of the Von Mises stress will be presented as well as the percentage of the difference of the Von Mises stress.





Appendix 5 - Analyses results

The geometry of the starting structure and the optimised shapes will be presented in this Appendix as well as the reports generated from the analysis with the design tool. In the figures of the geometries, the control points responsible for the iteration of the shape are visible. These are the design variables of the optimisation problem. In the starting shape the values of the shape characteristics are visible whereas in the optimised geometries the new location of the points is presented compared to the starting shape.

Starting shape

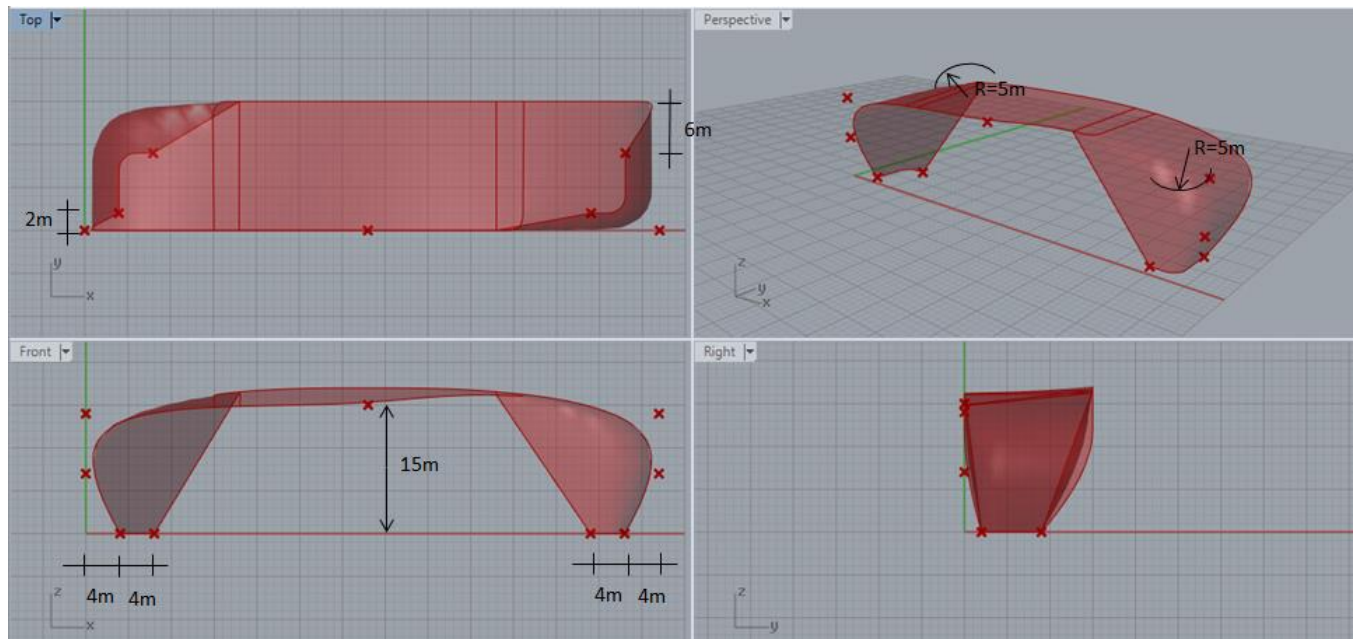


Figure 87. Geometrical characteristics of the starting shape

1. **Start of the analysis**
2. **Number of mesh elements in each group**
3. Group1: 221
4. Group2: 349
5. Group3: 354
6. Group4: 8
7. **Start of stress based material distribution**
8. Iteration number: 0
9. Maximum deflection: 1.0024
10. Maximum VM stress: 514.0MPa
11. 5 elements need modification
12. Group 4 has been modified
13. Iteration number: 1
14. Maximum deflection: 0.92925
15. Maximum VM stress: 530.0MPa
16. 6 elements need modification
17. Group 4 has been modified
18. Iteration number: 2
19. Maximum deflection: 0.85282
20. Maximum VM stress: 451.0MPa

21. 6 elements need modification
22. Group 3 has been modified
23. Group 4 has been modified
24. Iteration number: 3
25. Maximum deflection: 0.52397
26. Maximum VM stress: 346.0MPa
27. 0 elements need modification
28. **Start of the deflection based material distribution**
29. Iteration number: 4
30. For deflection group 1 has changed
31. For deflection group 2 has changed
32. For deflection group 3 has changed
33. For deflection group 4 has changed
34. Max deflection= 0.2886
35. Maximum VM stress: 231.0MPa
36. Iteration number: 5
37. For deflection group 4 has changed
38. Max deflection= 0.28139
39. Maximum VM stress: 223.0MPa
40. Iteration number: 6
41. For deflection group 3 has changed
42. Max deflection= 0.22097
43. Maximum VM stress: 195.0MPa
44. **Final cross section that is assigned in every group**
45. Group 1: cross section number 2
46. Group 2: cross section number 2
47. Group 3: cross section number 4
48. Group 4: cross section number 6
49. **Performance of the final design**
50. Maximum deflection: 0.22097m
51. Critical BLF: 18.217
52. Mean stress: 54.2 MPa
53. Total weight: 250860.0Kg
54. Weight per unit area: 165 Kg/m²

Analysis 1 – Minimise total weight

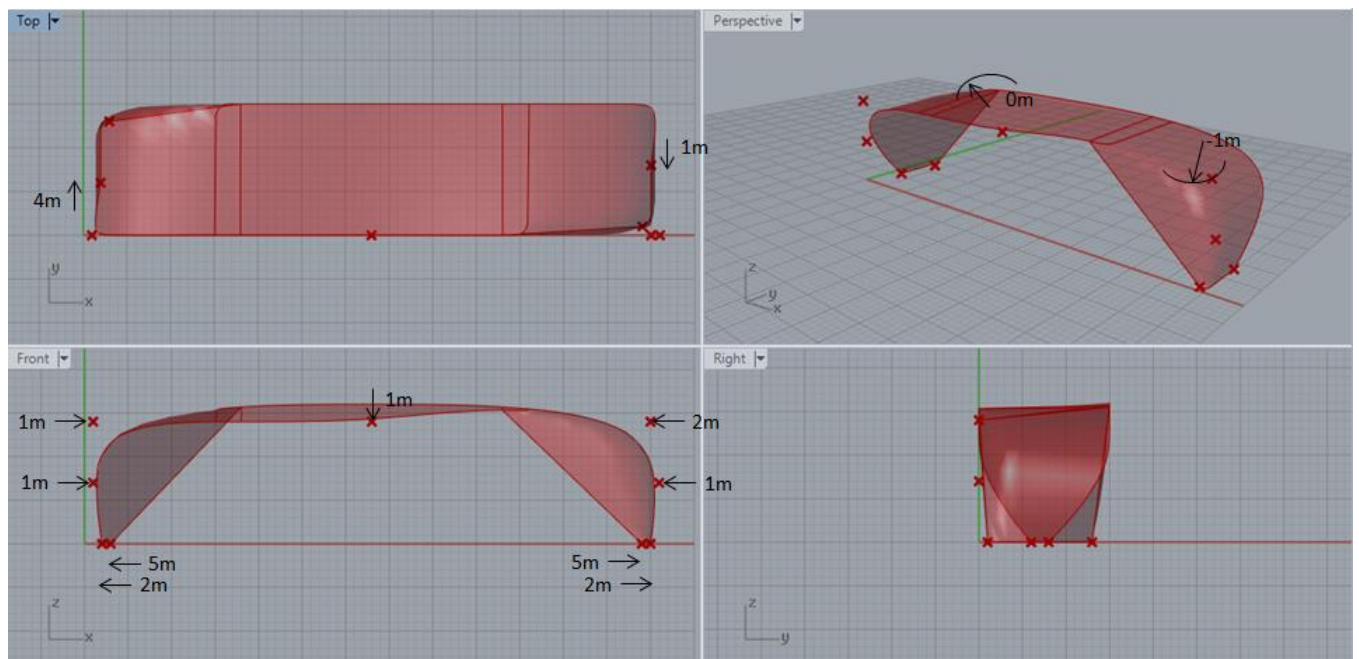


Figure 88. Characteristics of the optimised geometry for the minimization of the total weight compared to the starting shape

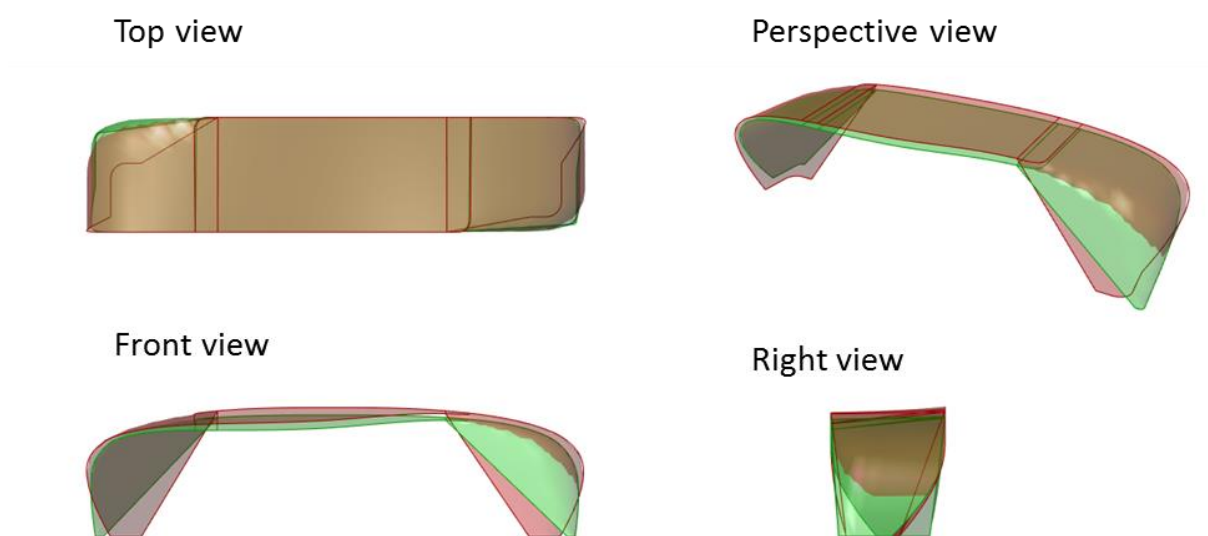


Figure 89. Geometry of minimum weight (green) overlaid on the starting geometry (red)

1. Start of the analysis
2. Number of mesh elements in each group
3. Group1: 214
4. Group2: 305
5. Group3: 278
6. Group4: 7
7. Start of stress based material distribution
8. Iteration number: 0

9. Maximum deflection: 1.0997
10. Maximum VM stress: 570.0MPa
11. 7 elements need modification
12. Group 4 has been modified
13. Iteration number: 1
14. Maximum deflection: 1.0161
15. Maximum VM stress: 558.0MPa
16. 8 elements need modification
17. Group 3 has been modified
18. Group 4 has been modified
19. Iteration number: 2
20. Maximum deflection: 0.59303
21. Maximum VM stress: 357.0MPa
22. 1 elements need modification
23. Group 4 has been modified
24. Iteration number: 3
25. Maximum deflection: 0.56967
26. Maximum VM stress: 339.0MPa
27. 0 elements need modification
28. **Start of the deflection based material distribution**
29. Iteration number: 4
30. For deflection group 1 has changed
31. For deflection group 2 has changed
32. For deflection group 3 has changed
33. For deflection group 4 has changed
34. Max deflection= 0.31117
35. Maximum VM stress: 212.0MPa
36. Iteration number: 5
37. For deflection group 4 has changed
38. Max deflection= 0.30429
39. Maximum VM stress: 202.0MPa
40. Iteration number: 6
41. For deflection group 3 has changed
42. Max deflection= 0.23852
43. Maximum VM stress: 174.0MPa
44. **Final cross section that is assigned in every group**
45. Group 1: cross section number 2
46. Group 2: cross section number 2
47. Group 3: cross section number 4
48. Group 4: cross section number 6
49. **Performance of the final design**
50. Maximum deflection: 0.23852m
51. Critical BLF: 15.514
52. Mean stress: 62.2 MPa
53. Total weight: 229275.0Kg
54. Weight per unit area: 164 Kg/m²

Analysis 2 – Minimise weight per unit area

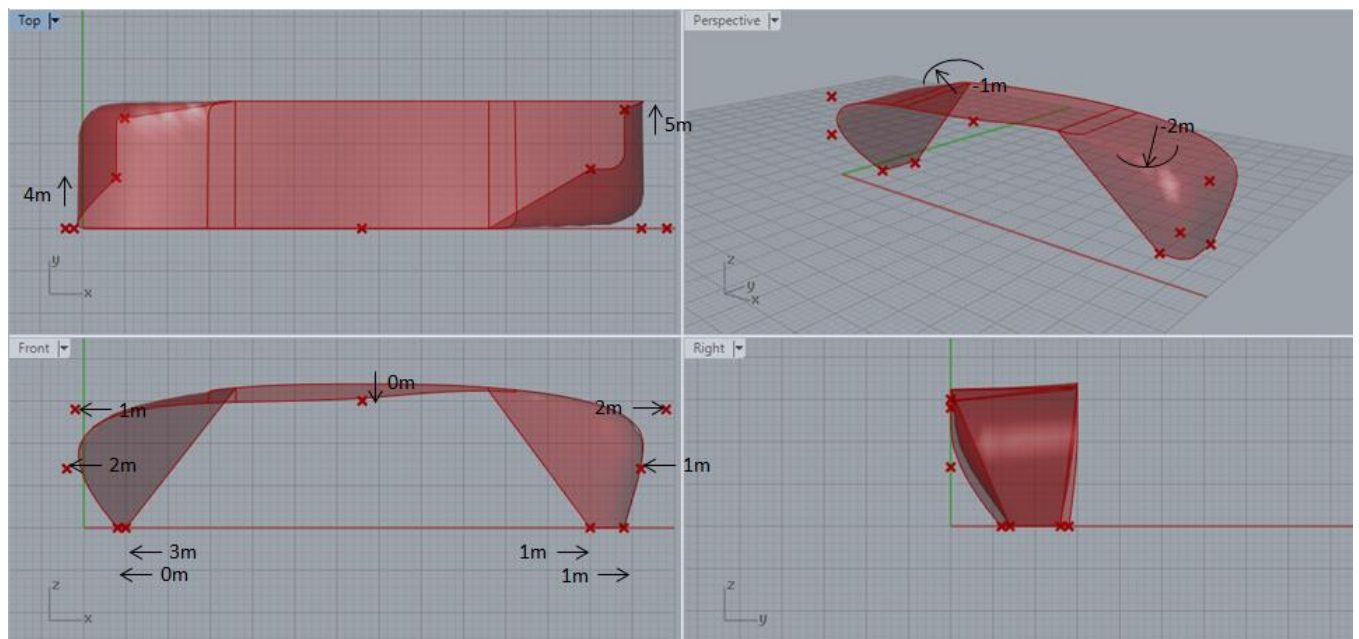


Figure 90. Characteristics of the optimised geometry for the minimization of the weight per unit area compared to the starting shape

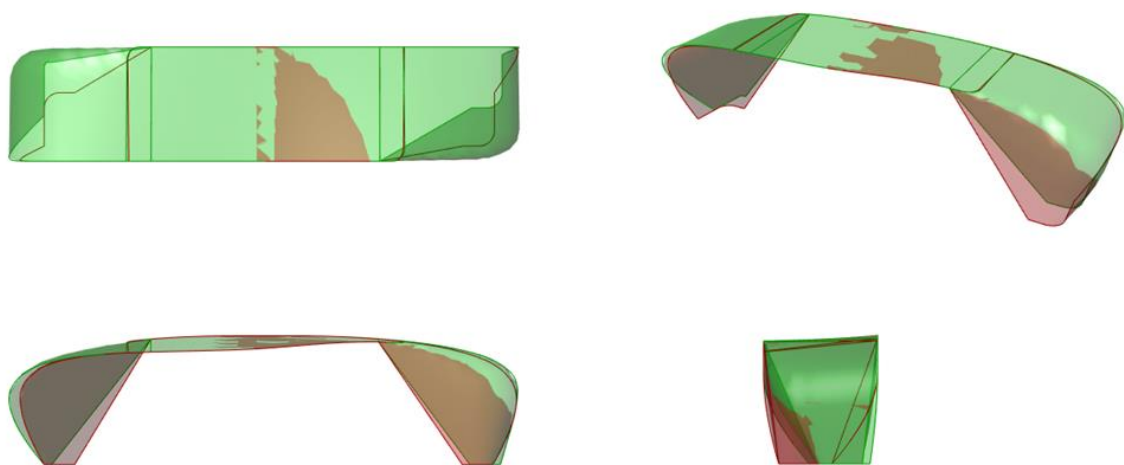


Figure 91. Geometry of minimum weight per unit area (green) overlaid on the starting geometry (red)

1. Start of the analysis
2. Number of mesh elements in each group
3. Group1: 246
4. Group2: 403
5. Group3: 333
6. Group4: 6
7. Start of stress based material distribution
8. Iteration number: 0

9. Maximum deflection: 1.0272
10. Maximum VM stress: 629.0MPa
11. 7 elements need modification
12. Group 3 has been modified
13. Group 4 has been modified
14. Iteration number: 1
15. Maximum deflection: 0.58046
16. Maximum VM stress: 448.0MPa
17. 3 elements need modification
18. Group 4 has been modified
19. Iteration number: 2
20. Maximum deflection: 0.54604
21. Maximum VM stress: 383.0MPa
22. 2 elements need modification
23. Group 4 has been modified
24. Iteration number: 3
25. Maximum deflection: 0.53018
26. Maximum VM stress: 357.0MPa
27. 2 elements need modification
28. Group 4 has been modified
29. Iteration number: 4
30. Maximum deflection: 0.51063
31. Maximum VM stress: 359.0MPa
32. 1 elements need modification
33. Group 3 has been modified
34. Iteration number: 5
35. Maximum deflection: 0.31928
36. Maximum VM stress: 249.0MPa
37. 0 elements need modification
38. **Start of the deflection based material distribution**
39. Iteration number: 6
40. For deflection group 4 has changed
41. Max deflection= 0.31378
42. Maximum VM stress: 240.0MPa
43. Iteration number: 7
44. For deflection group 3 has changed
45. Max deflection= 0.23754
46. Maximum VM stress: 209.0MPa
47. **Final cross section that is assigned in every group**
48. Group 1: cross section number 1
49. Group 2: cross section number 1
50. Group 3: cross section number 4
51. Group 4: cross section number 6
52. **Performance of the final design**
53. Maximum deflection: 0.23754m
54. Critical BLF: 9.374
55. Mean stress: 58.4 MPa
56. Total weight: 251037.0Kg
57. Weight per unit area: 159 Kg/m²

Analysis 3 – Minimise mean VM stress

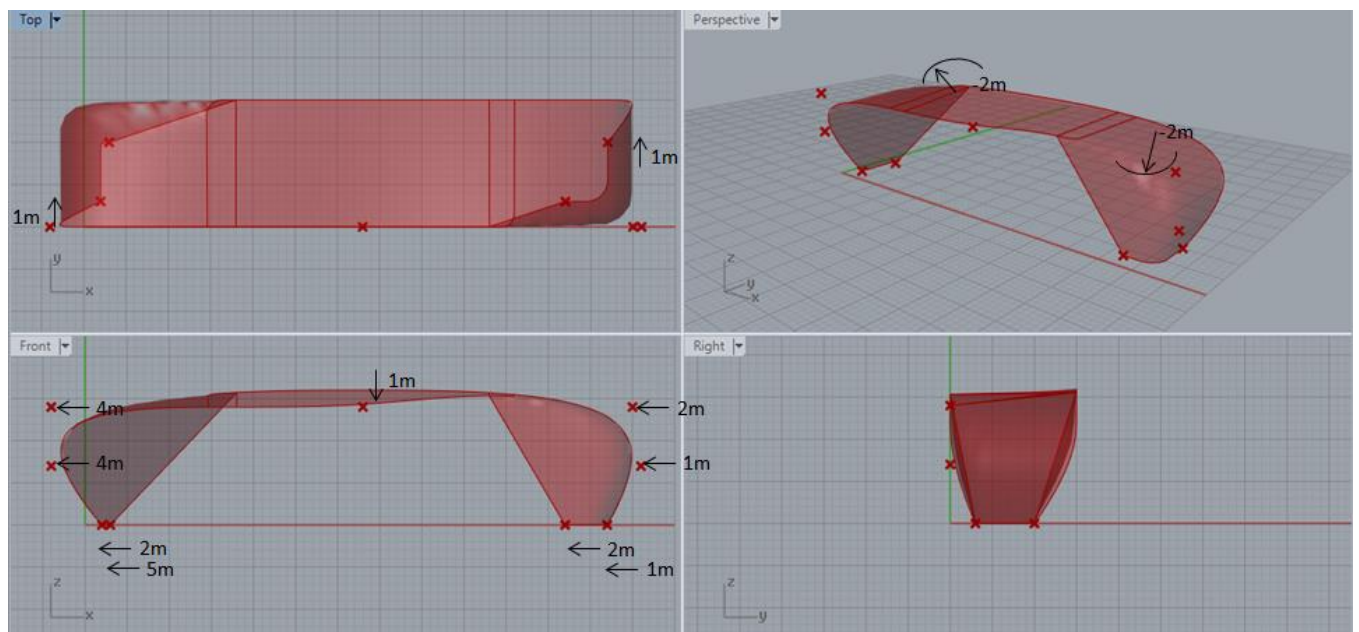


Figure 92. Characteristics of the optimised geometry for the minimization of the mean VM stress compared to the starting shape

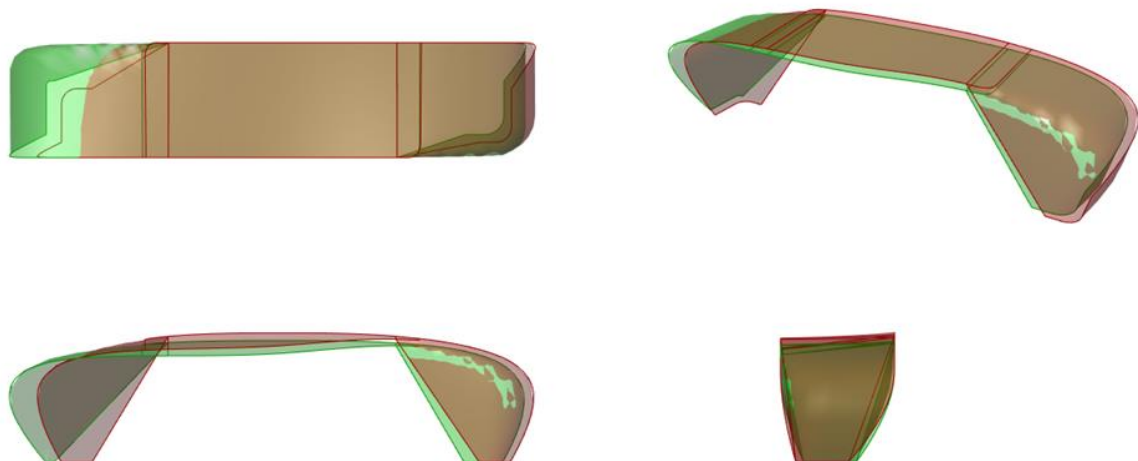


Figure 93. Geometry of minimum mean VM stress (green) overlaid on the starting geometry (red)

| |
|---|
| 1. Start of the analysis |
| 2. Number of mesh elements in each group |
| 3. Group1: 246 |
| 4. Group2: 427 |
| 5. Group3: 348 |
| 6. Group4: 7 |
| 7. Start of stress based material distribution |
| 8. Iteration number: 0 |
| 9. Maximum deflection: 1.1232 |
| 10. Maximum VM stress: 630.0MPa |

11. 7 elements need modification
12. Group 4 has been modified
13. Iteration number: 1
14. Maximum deflection: 1.049
15. Maximum VM stress: 606.0MPa
16. 8 elements need modification
17. Group 3 has been modified
18. Group 4 has been modified
19. Iteration number: 2
20. Maximum deflection: 0.60406
21. Maximum VM stress: 385.0MPa
22. 1 elements need modification
23. Group 4 has been modified
24. Iteration number: 3
25. Maximum deflection: 0.58512
26. Maximum VM stress: 357.0MPa
27. 1 elements need modification
28. Group 4 has been modified
29. Iteration number: 4
30. Maximum deflection: 0.56194
31. Maximum VM stress: 363.0MPa
32. 1 elements need modification
33. Group 3 has been modified
34. Iteration number: 5
35. Maximum deflection: 0.36199
36. Maximum VM stress: 255.0MPa
37. 0 elements need modification
38. **Start of the deflection based material distribution**
39. Iteration number: 6
40. For deflection group 4 has changed
41. Max deflection= 0.35594
42. Maximum VM stress: 239.0MPa
43. Iteration number: 7
44. For deflection group 3 has changed
45. Max deflection= 0.2728
46. Maximum VM stress: 226.0MPa
47. Iteration number: 8
48. For deflection group 2 has changed
49. Max deflection= 0.25152
50. Maximum VM stress: 215.0MPa
51. Iteration number: 9
52. For deflection group 1 has changed
53. Max deflection= 0.24753
54. Maximum VM stress: 210.0MPa
55. Iteration number: 10
56. For deflection group 4 has changed
57. Max deflection= 0.2401
58. Maximum VM stress: 210.0MPa
59. Iteration number: 11
60. For deflection group 3 has changed
61. Max deflection= 0.18165
62. Maximum VM stress: 190.0MPa

63. Final cross section that is assigned in every group

64. Group 1: cross section number 2

65. Group 2: cross section number 2

66. Group 3: cross section number 5

67. Group 4: cross section number 7

68. Performance of the final design

69. Maximum deflection: 0.18165m

70. Critical BLF: 15.875

71. Mean stress: 48.3 MPa

72. Total weight: 288857.0 Kg

73. Weight per unit area: 182 Kg/m²

Appendix 6 - Tool manual

The required files for the design tool are: designtool_GhANSYS.gh, edit_areas.py, edit_text1.py and designtool_visualisation.3dm

In order to use the design tool, the user should have Rhino and Grasshopper installed as well as the plug-ins: GhPython, Karamba, MeshEdit and (optionally) gHowl_r50.

It is advised to use the Rhino file which comes with the design tool, so that the visualisation component can be executed.

Design tool

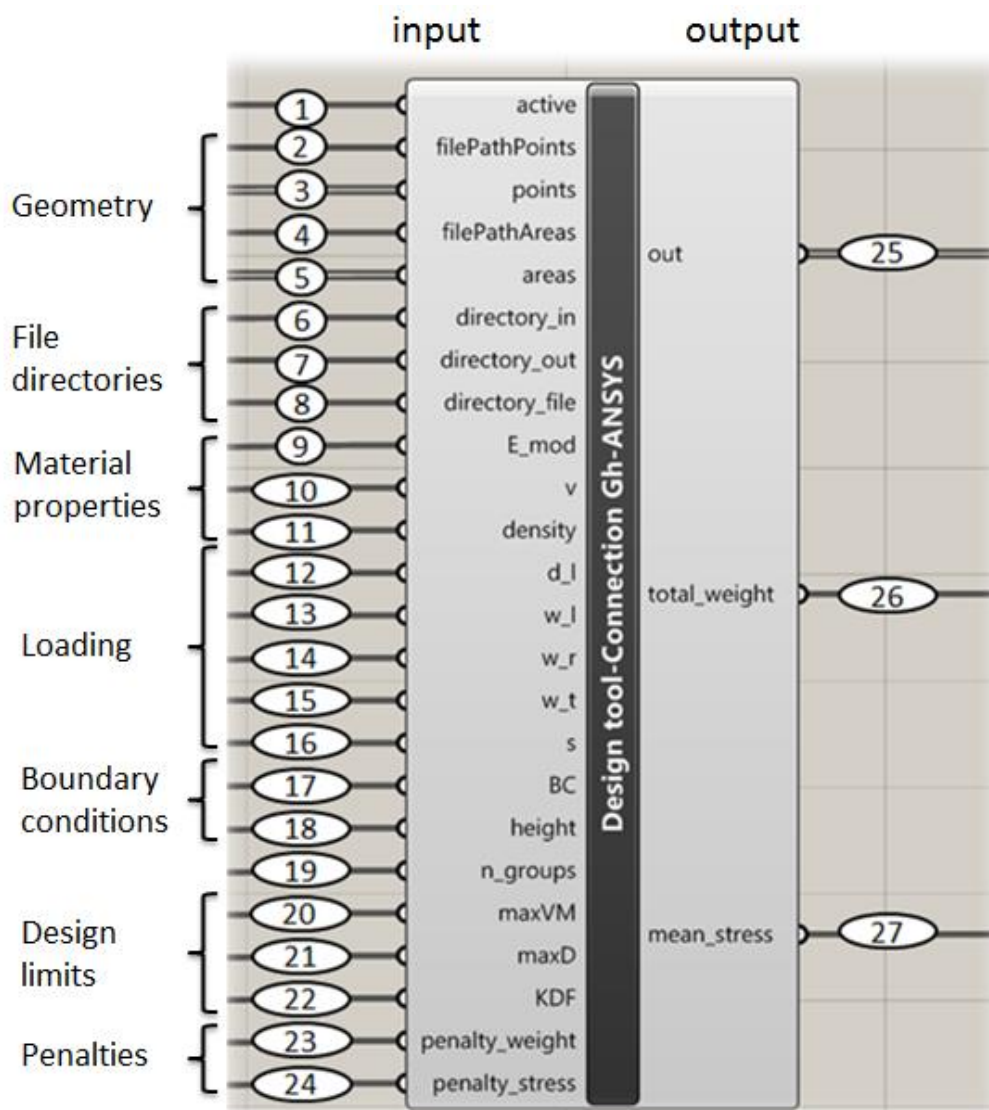


Figure 94. Component of the design tool with numbering for the input and output explanation

| Number | Explanation | Type of input-output |
|--------|---|----------------------|
| 1 | Boolean used to control the execution or not of the script. Possible user inputs: "true" & "false" from a Boolean Toggle component | boolean operation |
| 2 | The file path where the txt. file containing the points of the mesh will be generated for further manipulation | string |
| 3 | The coordinates of the mesh vertices that is an output of the Deconstruct Mesh component | string |
| 4 | The file path where the txt. file containing the areas of the mesh will be generated for further manipulation | string |
| 5 | The information for generating the mesh faces that is an output of the Deconstruct Mesh component | string |
| 6 | The directory where the APDL, batch and out files will be saved | string |
| 7 | The directory where the files containing the information retrieved from ANSYS will be saved | string |
| 8 | The directory where the files "edit_text1.py" and "edit_areas.py" are located | string |
| 9 | Modulus of elasticity of the material | float |
| 10 | Poisson ratio of the material | float |
| 11 | Density of the material | float |
| 12 | Dead load applied on the structure (not including the self-weight) | float |
| 13 | Wind load applying pressure on the structure | float |
| 14 | Wind load applying suction on the structure | float |
| 15 | Wind load due to friction | float |
| 16 | Snow load | float |
| 17 | Boundary conditions of the structure. Possible user inputs: "clamp" and "hinge" | string |
| 18 | Height of the structure where the boundary conditions should be applied | float |
| 19 | Number of groups to be created based on the stress of the elements | integer |
| 20 | Maximum Von Mises stress allowed on the elements | float |
| 21 | Maximum acceptable deflection of the structure in the Serviceability Limit State | float |
| 22 | Knock down factor to be used in the buckling analysis | float |
| 23 | Penalty to be applied in the total weight of the structure | float |
| 24 | Penalty to be applied in the mean VM stress of the structure | float |
| 25 | Report produced from the script when executed | string |
| 26 | Penalized total weight of the structure - to be used as an input for the optimisation algorithm | float |
| 27 | Penalized mean stress of the structure - to be used as an input for the optimisation algorithm | float |

Notes:

- (Applicable to n. 5) In order to let the tool generate the correct input for the modeling of the areas in Ansys, the input of the component in number 5 should not be directly the output of the Deconstruct Mesh component. A panel has to be used as an in-between component connecting the output of the Deconstruct Mesh component and the input of the Design Tool component, as presented in Figure 95.

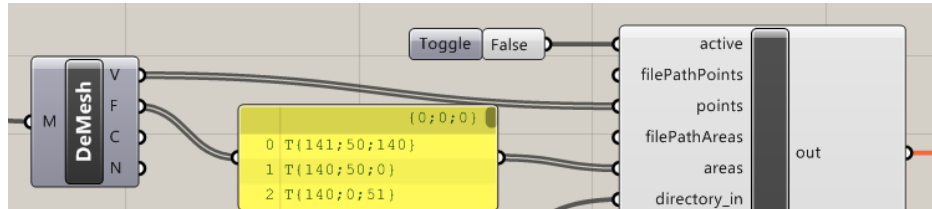


Figure 95. Panel used as input for the generation of the mesh faces-areas in Ansys

- (Applicable to n. 2,4,6,7,8) The file path provided by the user should have instead of one backslash \ two backslashes \\ to separate the folders.
- (Applicable to n. 2-5) The geometry that will be used as input of the design tool should have the y axis parallel to the height of the structure. The default coordinate system in Rhino-Grasshopper has the z axis parallel to the height, consequently the geometry should be rotated 90°.
- (Applicable to n. 9-16, 18, 20-24) The units of the input values should be consistent in order to assure the accuracy of the results computed in Ansys and in the Design Tool component. Possible consistent value units are: Newton (N), meter (m), second (s), pascal (P), kilogram (kg)
- In order to give the input cross section list, the values have to be assigned in the script. When double clicking the component there are 3 variables named h, w and t_f for the height of the cross section, the estimated density of the ribs and stiffeners and the thickness of the web respectively. It has to be noted that the values inserted should be floats and all three lists should include the same amount of values as presented in Figure 96.

```

1  if active:
2      #cross section values-user defined
3      h = [0.2,0.3,0.4,0.5,0.6,0.7,0.8,0.9,1.0,1.1,1.2]
4      w = [1.0,1.0,1.0,1.0,1.0,1.0,1.0,1.0,1.0,1.0,1.0]
5      t_f = [0.008,0.008,0.01,0.01,0.012,0.012,0.015,0.015,0.02,0.02,0.02]

```

Figure 96. Cross section list defined in the Python script

- External optimisation algorithms, like Galapagos, do not save the results of all iterations performed. If it is desirable to keep track of all the analysis, gHowl_r50 plug-in should be installed. Through this plug-in the chosen data can be written in a spreadsheet file.

Von Mises stress visualisation

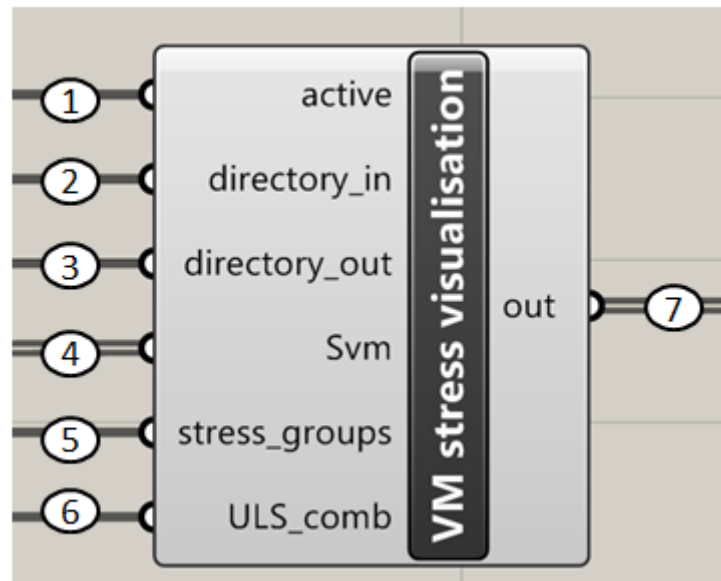


Figure 97. Component of the VM stress visualisation with numbering for the input and output explanation

| Number | Explanation | Type of input-output |
|--------|--|----------------------|
| 1 | Boolean used to control the execution or not of the script. Possible user inputs: "true" & "false" from a Boolean Toggle component | boolean operation |
| 2 | The file path where the files of the geometry generated by the design tool are saved | string |
| 3 | The file path where the files of the analysis generated by the design tool are saved | string |
| 4 | The list generated by the design tool that contains values of the Von Mises stress of all the elements for all load cases | list |
| 5 | The number of similarly stressed groups that the script will be asked to generate for the visualization | integer |
| 6 | The number of the ULS combination to be visualised | integer |
| 7 | Report produced from the script when executed | string |

Material distribution visualisation

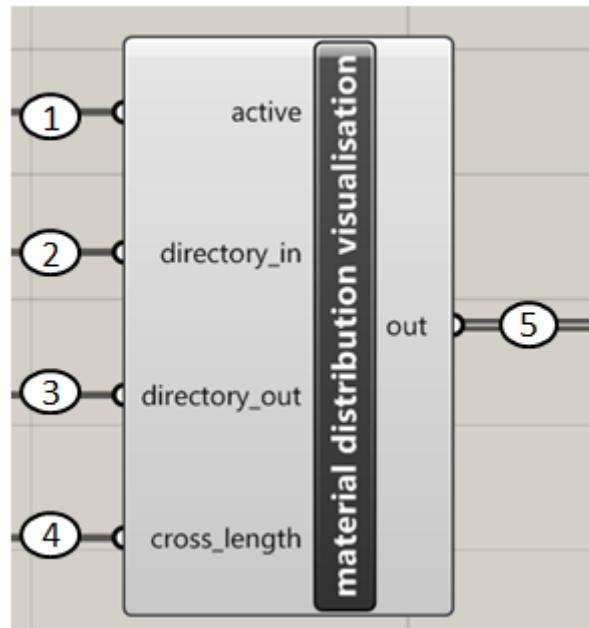


Figure 98. Component of the material distribution visualisation with numbering for the input and output explanation

| Number | Explanation | Type of input-output |
|--------|--|----------------------|
| 1 | Boolean used to control the execution or not of the script. Possible user inputs: "true" & "false" from a Boolean Toggle component | boolean operation |
| 2 | The file path where the files of the geometry generated by the design tool are saved | string |
| 3 | The file path where the files of the analysis generated by the design tool are saved | string |
| 4 | The length of the cross section list | integer |
| 5 | Report produced from the script when executed | string |

Table of Figures

| | |
|---|----|
| Figure 1. Arnhem station roof structure. Design by UNStudio (http://www.unstudio.com/projects/arnhem-central-transfer-hall) | 1 |
| Figure 2. Porsche pavilion in Wolfsburg, Germany. Design by HENN Architects (http://www.henn.com/de/projects/culture/porsche-pavilion) | 2 |
| Figure 3. Objectives in building design (Geyer and Rueckert, 2005, p.2)..... | 3 |
| Figure 4. Cross over of two genomes with four genes each | 6 |
| Figure 5. Blending of two genomes with four genes each | 6 |
| Figure 6. Mutation of a genome by iterating one gene | 6 |
| Figure 7. Strategy of the base tool | 11 |
| Figure 8. Grasshopper parametric model basics | 12 |
| Figure 9. Post Rotterdam building before redevelopment (http://www.skyscrapercity.com/) | 15 |
| Figure 10. Design of the redevelopment of Post Rotterdam. Design by UNStudio (http://www.unstudio.com/projects/post-rotterdam) | 16 |
| Figure 11. Original design of the vertical foyer from UNStudio | 17 |
| Figure 12. Dimensions (in mm) of the original design from UNStudio | 18 |
| Figure 13. Modeling of the roof structure with two NURBS curves of 9 control points each..... | 19 |
| Figure 14. Modeling of the base and the triangular covers | 19 |
| Figure 15. Modeling of horizontal lines connecting the 2 Nurbs curves and the triangular cover | 20 |
| Figure 16. Fillet of the horizontal lines | 20 |
| Figure 17. Curves-lines defining the shape of the vertical foyer..... | 21 |
| Figure 18. Options for modeling a free form surface in Grasshopper | 21 |
| Figure 19. Left and right part of surface..... | 22 |
| Figure 20. Left, right and top part of surface | 22 |
| Figure 21. Merged surface defining the shape of the vertical foyer | 22 |
| Figure 22. Floors are connected to the roof structure through the mesh | 23 |
| Figure 23. Detail of the connection between the floor and the roof structure | 24 |
| Figure 24. Comparison of meshing components..... | 24 |
| Figure 25. Topology extraction of the mesh | 25 |
| Figure 26. Meshing of the surface in Grasshopper | 25 |
| Figure 27. Geometry generation in Ansys based on the mesh of the parametric model | 26 |
| Figure 28. Meshing of the geometry in Ansys by dividing each line in 2 | 26 |
| Figure 29. Structure of the Porsche pavilion [http://www.archiscene.net/hospitality-retail/porsche-pavilion-henn-architekten] | 26 |
| Figure 30. Details of the Porsche pavilion structure [http://www.archiscene.net/hospitality-retail/porsche-pavilion-henn-architekten]..... | 27 |
| Figure 31. Parts of the structure of the vertical foyer | 27 |
| Figure 32. Deviations in the connections of the areas when ribs are modeled in Grasshopper and imported in Ansys..... | 28 |
| Figure 33. 8-node SHELL281 element (Ansys, 2015) | 29 |
| Figure 34. Approximated stress distributions of the presented section forces in the plates | 31 |
| Figure 35. Left: Point that the element forces are computed in Ansys. Right: Assumed point of application of the forces in the original structure..... | 32 |
| Figure 36. Part of the structure to be used for the equivalency validation | 33 |
| Figure 37. Double clamped surface for modeling the equivalent structure | 33 |

| | |
|--|----|
| Figure 38. Modeling of the original structure | 34 |
| Figure 39. Deflection of a double clamped beam under distributed load | 35 |
| Figure 40. Linear (eigenvalue) buckling curve (Ansys, 2015) | 37 |
| Figure 41. Thickness distribution algorithm | 39 |
| Figure 42. Plate modeled in Ansys, clamped boundary and pressure load | 39 |
| Figure 43. Meshing of the plate | 40 |
| Figure 44. Starting cross section height-Iteration 0 | 41 |
| Figure 45. Element's cross section height-Iteration 3 | 42 |
| Figure 46. Element's cross section height-Iteration 6 | 43 |
| Figure 47. Element's cross section height at convergence-Iteration 10 | 44 |
| Figure 48. Number of elements that require cross section modification in every iteration | 45 |
| Figure 49. Stress distribution of a free edge of the plate in every iteration | 45 |
| Figure 50. Galapagos component and the required input for the optimisation..... | 46 |
| Figure 51. Input used for the Galapagos evolutionary algorithm | 47 |
| Figure 52. Material distribution visualisation..... | 48 |
| Figure 53. Von Mises stress visualisation | 48 |
| Figure 54. Applied boundary conditions to the model..... | 50 |
| Figure 55. Loads that are applied on the structure..... | 51 |
| Figure 56. Element checked for stress convergence..... | 52 |
| Figure 57. Shape of the structure based on the mesh density | 53 |
| Figure 58. Maximum Von Mises stress present in the structure when a range of cross sections is assigned | 55 |
| Figure 59. Maximum deflection present in the structure when a range of cross sections is assigned | 55 |
| Figure 60. Critical Buckling Load Factor of the structure when a range of cross sections is assigned.. | 56 |
| Figure 61. Grouping of the elements in equal stress ranges..... | 57 |
| Figure 62. Visualization of the grouping in 4 equal stress ranges | 57 |
| Figure 63. Grouping of the elements based on the mean stress of the structure | 58 |
| Figure 64. Visualization of the grouping based on the mean stress | 58 |
| Figure 65. Workflow of the Python script and the required user input..... | 59 |
| Figure 66. Vertical deflection of the roof structure under self-weight..... | 61 |
| Figure 67. Geometry of the starting structure | 63 |
| Figure 68. Value ranges of the variables of the parametric model..... | 63 |
| Figure 69. Geometry that presents the least total weight | 64 |
| Figure 70. Geometry that presents the least weight per unit area..... | 65 |
| Figure 71. Geometry that presents the least mean VM stress | 66 |
| Figure 72. Geometry that presents the least weight per unit area when new constraints apply | 68 |
| Figure 73. Realization of the structure following exactly the meshed surface model..... | 69 |
| Figure 74. Detail of the non-smoothness of the surface due to the bigger cross sections required.... | 70 |
| Figure 75. Front view of the structure of the starting geometry | 70 |
| Figure 76. Lower shell, ribs and stiffeners of the structure | 71 |
| Figure 77. Snow load shape coefficients for roofs abutting to taller construction works (Figure 5.7 from EN 1991-1-3:2003) | 2 |
| Figure 78. Wind regions of the Netherlands (NEN 6702 Loadings and deformations TGB 1990) | 3 |
| Figure 79. Side of wind application for the determination of the wind forces..... | 4 |
| Figure 80. Import the areas in Ansys- discontinuities | 7 |

| | |
|--|----|
| Figure 81. Import the control points generated in Rhino-Grasshopper | 9 |
| Figure 82. Model with Splines the roof structure and with straight lines the triangular covers and the base | 9 |
| Figure 83. Create surfaces from the boundary lines | 10 |
| Figure 84. Final geometry after filleting the edges- Parts of the roof are cut. Left: perspective view/Right: top view..... | 10 |
| Figure 85. Final geometry after filleting the edges- No parts of the roof are cut. Left-perspective view/Right-top view | 10 |
| Figure 86. Modeling of the original structure (left) with one plate-shell (right)..... | 13 |
| Figure 87. Geometrical characteristics of the starting shape | 23 |
| Figure 88. Characteristics of the optimised geometry for the minimization of the total weight compared to the starting shape | 25 |
| Figure 89. Geometry of minimum weight (green) overlaid on the starting geometry (red) | 25 |
| Figure 90. Characteristics of the optimised geometry for the minimization of the weight per unit area compared to the starting shape | 27 |
| Figure 91. Geometry of minimum weight per unit area (green) overlaid on the starting geometry (red) | 27 |
| Figure 92. Characteristics of the optimised geometry for the minimization of the mean VM stress compared to the starting shape | 29 |
| Figure 93. Geometry of minimum mean VM stress (green) overlaid on the starting geometry (red) . | 29 |
| Figure 94. Component of the design tool with numbering for the input and output explanation..... | 33 |
| Figure 95. Panel used as input for the generation of the mesh faces-areas in Ansys..... | 35 |
| Figure 96. Cross section list defined in the Python script | 35 |
| Figure 97. Component of the VM stress visualisation with numbering for the input and output explanation..... | 36 |
| Figure 98. Component of the material distribution visualisation with numbering for the input and output explanation..... | 37 |